

UNIVERSITÀ DELLA CALABRIA



Dipartimento di Fisica

**Doctorate School of Science and Technique
“Bernardino Telesio”**

*A thesis submitted for the degree of Doctor of Philosophy in Science
and Technology of Mesophases and Molecular Materials*

XXVICycle
02/B3 - FIS/07

**“Properties of Biomolecules at the Interfaces:
Studies and Characterization of Chromonic Mesogens,
from the Basis to Applications”**

School Director

Prof. Roberto Bartolino

Curriculum Coordinator

Prof. Carlo C. Versace

Supervisor

Dr. Federica Ciuchi

Candidate

Caterina Maria Tone

December 2013

Abstract

The study of the interaction between molecules, in particular biological molecules and liquid crystals (LC), has experienced a huge growth in the recent years because of the development in devices engineering applied not only in photonics but also in the biomedical field. In order to design more efficient LC devices, it is first necessary to understand the behavior and properties of newly-synthesized liquid crystals and to garner a more in-depth understanding of currently-existing LCs in order to answer pending questions about them. The aim of this thesis work, is to better understand the interactions involved at the interface between liquid crystals and other materials, whatever is their nature, i.e. polymeric or biological. We started studying the effect of different confining surfaces on the alignment of a special class of lyotropic liquid crystals, called “chromonics”, which, in addition of LC properties, are biocompatible. Differently from the most common liquid crystals, i.e. thermotropic LC, the mesogens that constitute the chromonic LC phases are not amphiphilic, but they are “plan-like” aromatic compound. This class of molecules embraces not only dyes and drugs, but also DNA and its bases. Using the knowledge acquired with chromonic mesogen, we tried to understand a more complicate system, such as the phenomena involved at the biomolecules decorated-liquid crystals films interfaces. More specifically, it is possible to divide the work in two macro-parts. The first part concerns the alignment of a chromonic molecule, “disodium cromoglycate” (DSCG). The study of chromonic LC behaviour in confined geometries and its physical properties, could be a model for more complex biological assemblies. Hence, we demonstrated the role of alignment layer’s surface energy in the alignment of nematic phase of DSCG, achieving both alignments and for the first time, a stable-in-time homeotropic anchoring of this LC solution. With the knowledge acquired from DSCG, we were able to align also DNA bases liquid crystal solutions. In particular, guanosine monophosphate in pre-cholesteric and cholesteric liquid crystals phases were perfectly aligned homeotropically without means of external fields, as was done until now, and partially planar aligned. Moreover, we

observed that if ionic and/or silver doped solutions are added to the LC guanosine phases, it is possible to control the pitch of the cholesteric phase, modifying the helix structure. Instead, varying the nature of the confining surfaces, in such conditions, it is possible to obtain guanosine vesicles. Other studies have been carried out on new chromonic complexes, synthesized at Chemistry Department of UNICAL, with possible application as anticancer drugs. A complete characterization of these compounds were done (XRD, phase diagrams, etc) and also for these compounds, we developed a “route” to drive the alignment, particularly important for future application in biophotonic devices. The second part of the work is focused on LC based biosensors. From the biotechnological and biomedical applications point of view, the studies on interactions of proteins with lipids are an area of fundamental interest, due to enormous biological importance. In fact, studies on biosensor devices are tremendously increased in recent years, focusing the attention also on finding low cost raw materials with high efficiency: liquid crystals, thanks to their high sensitivity to the external conditions, represent the best candidate. It has been demonstrated that aqueous interface of LC has an instantaneous response when exposed to phospholipids. This is a good base to study the interaction between biomolecules using LC as probe. Starting from the results found in literature, we studied the effect of phospholipids on protein decorated-liquid crystal interfaces by means of optical microscopy and FT-IR measurements. The first technique allowed us to observe the response of decorated LC film when exposed to phospholipids vesicles, while the second, gave us insight on conformational changes involved in secondary structure of the protein in function of the time of interaction between protein and LC, and the pH of the surrounding environment. The results obtained show a new methods to report specific binding of vesicles on protein decorated interfaces.

Contents

1 Chromonic Liquid Crystals: A study on the role of surface energy in their alignment	1
1.1 Introduction	2
1.2 Brief history of Liquid Crystals	4
1.3 Thermotropic Liquid Crystals	5
1.3.1 Introduction to the structure and phase	5
1.4 Lyotropic Liquid Crystals	8
1.4.1 Introduction to the structure and phase	8
1.5 Chromonic Liquid Crystals	10
1.5.1 History, Structure, phase and aggregation	10
1.6 Alignment of Disodium Cromoglycate	13
1.6.1 Materials and methods	15
1.6.2 Results	16
1.7 Conclusion	22
2 Alignment of guanosine liquid crystal solutions: an intriguing scenario	24
2.1 Introduction	25
2.1.1 Stabilizing factors	26
2.2 Alignment of Guanosine LC phases	30
2.2.1 Materials and methods	32
2.2.2 Results	34
2.2.3 Discussion and conclusions	40
2.3 Atomic Force Microscopy studies on Langmuir-Blodgett film of guanosine derivatives	43
2.3.1 Breaf history of Langmuir-Blodgett films and applications	43

2.4	Brief introduction to “Atomic Force Microscopy”	45
2.5	Experiment	48
2.5.1	Intercalating materials	48
2.5.2	Materials and methods	49
2.5.3	Results	49
3	New synthesized chromonic molecules: non classical anticancer agents	52
3.1	Introduction	53
3.2	Structure of complex I, II and III	55
3.2.1	Materials and methods	56
3.2.2	Complex I: Phase diagram	57
3.2.3	Complex II: Phase diagram	58
3.3	Alignment	61
3.3.1	Materials and methods	62
3.3.2	High surface energy material: PMMA and PI	62
3.3.3	Low surface energy material: Cytop	64
3.4	Discussion and Conclusion	66
3.5	Use of complex I as intercalating agent in nematic phase of DSCG	70
3.5.1	Results	70
3.5.2	Discussion and conclusion	71
3.6	Atomic Force Microscopy investigation on dried LC film	73
3.6.1	Experimental section	73
3.6.2	Results	73
3.6.3	Conclusion	76
4	Liquid Crystal Based Biosensors: Study of the interactions between protein decorated LC interfaces and phospholipids	77
4.1	Introduction	78
4.2	Experimental Section	81
4.2.1	Materials	81
4.2.2	Methods	81
4.3	Results	84
4.3.1	Orientalional transitions in 5CB protein decorated interfaces	84
4.3.2	Effect of aged protein adsorbed at the LC interface	87
4.3.3	FT-IR measurements	90

4.3.4 Discussion and conclusion	97
5 Conclusion and Perspectives	100
Bibliography	104

Chapter 1

Chromonic Liquid Crystals: A study on the role of surface energy in their alignment

In this chapter we deal with the alignment of disodium chromoglycate (DSCG) liquid crystal phases. In particular we demonstrated the role of alignment layer's surface energy for achieving both planar and homeotropic orientation of nematic phase of DSCG, giving a general rule to follow for chromonic mesogens alignment. We show a detailed study of planar anchoring of DSCG and, for the first time in the literature, a stable-in-time homeotropic alignment [1], achieved using highly hydrophobic surfaces. We give an explanation of the behaviour observed for the molecules aligned in planar configuration, that with time, evolve into the so called "ribbon structures", a thermodynamically steady state. The results showed are very promising for future application in biosensors and optical devices, helping to shed light on the outstanding properties of this class of molecules.

1.1 Introduction

Research is an assignment that requires persistence, perseverance and strength of mind. The study of the interaction between biological molecules and liquid crystals (LC) has experienced huge growth in recent years due to the development of engineering devices applied not only in photonics but also in biomedical field. The liquid crystal phase of matter interests researchers for many reasons, mostly involving optical properties not seen in other fluids along with a sensitivity to external conditions. These properties have made liquid crystals a special candidate in production of display devices but during the last decades, they were also used in medicine as biosensors devices. In order to design more efficient liquid crystal devices, it is first necessary to understand the behavior and the properties of newly-synthesized liquid crystal materials. It is also important to garner a more in-depth understanding of currently-existing liquid crystals in order to answer pending questions about these materials. The aim of this thesis work, is to better understand the interactions involved at the interface between liquid crystals and other materials, whatever is their nature, i.e. polymeric or biological. In particular, using the knowledge acquired in thermotropic liquid crystals field, we tried to deeply understand the driving mechanism of a special class of liquid crystals, Lyotropic Chromonic Liquid Crystals (LCLCs), and to use the knowledge acquired for the future development in devices engineering applied not only in photonics but also in the biomedical field. The organization of the entire work is as follow. The *first chapter* relies on the alignment of a chromonic molecule, “disodium cromoglycate” (DSCG). Differently from the most common liquid crystals, i.e. thermotropic LC, the mesogens that constitute the chromonic LC phases are not amphiphilic, but they are “plan-like” aromatic compound. This class of molecules embraces not only dyes and drugs, but also DNA and its bases. The study of chromonic LC behaviour in confined geometries and its physical properties, could be a model for more complex biological assemblies. Starting from common procedures and methods largely employed in the alignment of thermotropic LC, we demonstrated the role of alignment layer’s surface energy in the alignment of nematic phase of DSCG, achieving both planar and homeotropic alignments, and obtaining for the first time, a stable-in-time homeotropic anchoring of this LC solution. We also tested unusual alignment layers and tested the effect of plasma etching on polymeric surfaces. The texture observed are quite interesting [1, 2]. With the knowledge acquired from DSCG, we were able to align also DNA bases liquid crystal solutions. This is the subject of the *second chapter*. We give firstly an introduction on guanosine

derivatives and its propensity to self assemble in organized structure. Then we focused on the alignment of guanosine monophosphate pre-cholesteric and cholesteric liquid crystals phases. We showed that, by means of surface energy of the confining surfaces, it is possible to perfectly align homeotropically these LC phases without means of external fields, as was done until now, but only partially in a planar configuration. Moreover, we demonstrated that the adding of a ionic and/or silver doped solution to the LC guanosine phases, allowed to tune the pitch of the cholesteric phase, modifying the helix structure. Finally, varying the nature of the confining surfaces, in such conditions, we obtained vesicles of guanosine, without starting from a modified bases, as was reported in literature until now [3, 4, 5]. *Chapter three* focuses on newly synthesized metal based chromonic compounds, produced at Chemistry Department of our University, with possible application as anticancer drugs. A complete characterization of these compounds is given, exploiting X-Ray Diffraction measurements, phase diagrams of their liquid crystal phases. Moreover, also for these compounds, we developed a “route” to drive the alignment, particularly important for future application in biophotonic devices. We used one of these complexes as intercalator of a well known chromonic system, for miscibility studies, important in biomedical field. Finally, using the knowledge acquired with chromonic mesogen, we tried to understand a more complicate system, such as the phenomena involved at the biomolecules decorated-liquid crystals films interfaces. *Chapter four* is focused on LC based biosensors. From the biotechnological and biomedical applications point of view, studies on interactions of proteins with lipids are the area of fundamental interest due to enormous biological importance. The interest in biosensor devices is tremendously increased in recent years and the research is always focused in finding low cost raw materials with high efficiency: liquid crystals, thanks to their high sensitivity to the external conditions, represent the best candidate. It has been demonstrated that aqueous interface of LC has an instantaneous response when exposed to phospholipids. This is a good base to study the interaction between biomolecules using LC as probe. Starting from the results found in literature, we studied the effect of phospholipids on protein decorated liquid crystal interfaces by means of optical microscopy and FT-IR measurements. The first technique allow us to observe the response of decorated LC film when exposed to phospholipids vesicles, while the second, give us insight on conformational changes involved in secondary structure of the protein in function of the time of interaction between protein and LC, and the pH of the surrounding environment. The results obtained show a new methods to report specific binding of vesicles on protein decorated interfaces.

1.2 Brief history of Liquid Crystals

The history of liquid crystals (LCs) began in the mid-nineteenth century, when several scientists observed unusual behaviour when polarized light impinged on liquid-like biological materials [6]. Rudolph Virchow, C. Mettenheimer, and G. Valentin were among the first that observed LC properties. They reported interesting anisotropic fluid behaviours in some biological materials; however, none of them realized that they were actually observing a different phase of matter [7]. The earliest, but still useful tools for the characterization of LCs, the polarizing microscope and heat stage, were first used by Otto Lehmann [7] to study these strange transitions. However, Friedrich Reinitzer is considered the “discoverer” of the liquid crystal phase, when he described two melting points and color phenomena in cholesteryl benzoate [8]. While this new phase of matter initially drew a lot of interest, liquid crystal research waned from the mid-1940s until the late 1950s when Glenn H. Brown published an article in Chemical Reviews. In general, the solid phase of a material exhibits more order than the liquid phase. In a solid crystal we can define for each particle a position and an orientation and its motion is generally confined to lattice vibrations. A liquid is *isotropic*, has no orientational order with no preferred direction; the particles’ motion is random. Some compounds do not lose their order completely at the melting temperature, but possess a *liquid crystal phase*, in which the material is a fluid, molecules possess a common orientation, but are (more or less) randomly distributed throughout the space. This means that it is possible to define an orientational order but not a positional ones. Fluidity allows the liquid crystal to easily change in response to a stimulus while orientational order gives liquid crystals interesting optical properties as compared to an isotropic liquid. Of course this simple picture of a liquid crystal needs to be refined and extended to take into account the tenths of different liquid crystalline phases that have been discovered during the twentieth century; all of them with different combinations of orientational and positional order [9]. The two main types of liquid crystals (LCs) are *thermotropic* LCs and *lyotropic* LCs. Thermotropic LCs show mesophases depending on temperature and pressure. Their basic building units are usually individual molecules which have a feature of pronounced shape anisotropy, such as rods, disk, etc. and they have been successfully used in display devices. Lyotropic LCs, instead, show mesophases according to the concentration of lyotropic LC molecules in a solvent. A general classification of liquid crystal phases is the following:

- **Thermotropic liquid crystals.** Pure compound forms the liquid crystalline phases,

due to a pronounced shape asymmetry. Based on this asymmetry a further division is often made in:

calamitic liquid crystals, whose molecule has a rod-like shape;

discotic liquid crystals, whose molecule has a disc-shape;

bent or banana shaped liquid crystals.

Apart from this mainly shape-based classification, another parameter is important for the liquid crystalline behaviour: some molecules do not have mirror symmetry, the mirror image cannot be translated or rotated onto the original molecule. This property, called chirality, gives in a number of liquid crystalline phases rise to supramolecular structures, for example helices.

- **Lyotropic liquid crystals.** The molecules are mixed with a solvent and LC phases appear varying the concentration and the temperature. A typical example is a surfactant mixed in a polar solvent like water. Such a surfactant has a polar head and an apolar tail (or more than one head or tail). The heads mix with the water, but the tails do not and stick together. This way micelles can be formed: droplets of surfactants with the polar heads directed outwards and the tails inside. At higher concentrations cylindrical or layered structures can be formed [6].

1.3 Thermotropic Liquid Crystals

1.3.1 Introduction to the structure and phase

The basic unit of liquid crystals is called “mesogen”. The amount of orientation, or lack thereof, that a group of mesogens has, determines the properties that a particular liquid crystal will have. Thermotropic liquid crystals are those liquid crystals whose phases are purely temperature-dependent. Generally mesogens consist of anisotropic organic molecules; the core consists of rigid aromatic rings to which flexible end groups are attached. Thermotropic phases exist in a certain temperature range. If the temperature rise is too high, thermal motion will destroy the delicate cooperative ordering of the LC phase, pushing the material into a conventional isotropic liquid phase. At too low temperature, most LC materials will form a conventional crystal. Many thermotropic LCs exhibit a variety of phases as temperature is changed. For instance, a particular type of mesogen

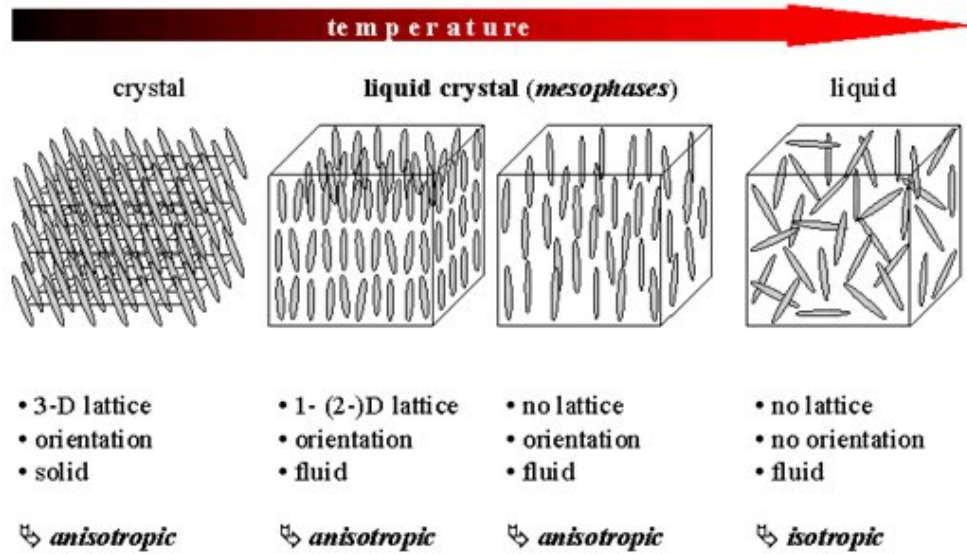


Figure 1.1: In thermotropic liquid crystals, a mesophase appears as a result of thermal effects. By either heating above the crystalline solid phase or cooling from the isotropic liquid phase a liquid crystal mesophase will appear.

may exhibit various smectic and nematic (and finally isotropic) phases as temperature is increased. Each of these phases is characterized by the type and amount of molecular ordering that the mesogens have. For this reason, a unit vector, called director \vec{n} , is introduced to represent the direction of preferred orientation of molecules in the neighborhood of any point.

Nematic Phase

The nematic phase (N) is about the most common liquid crystalline phase. This name derived from the Greek word $\nu\acute{\eta}\mu\alpha$ (nema), which means “thread”, as this particular phase can exhibit thread-like topological defects [9]. In this case, positional order is totally absent: the molecules are free to flow and their centers of mass are randomly distributed as in a liquid. The orientational ordering present in the nematic phase is long-range. The ordered structure of a liquid crystalline phase is described by an order parameter, the so-called “ S ”. For the nematic phase the choice is simple: the order can be quantified as the deviation of the molecules from the director. If θ is the angle between the director \vec{n} and the long axis of the molecule, the nematic order parameter S can be defined as:

$$S = \frac{1}{2} \langle 3\cos^2\theta - 1 \rangle \quad (1.1)$$

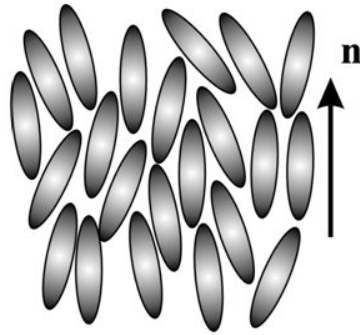


Figure 1.2: The nematic phase: an illustration of the orientation of the molecules.

where $\langle \rangle$ denotes an averaging over the ensemble of molecules [9].

Smectic Phase

The smectic phase is the generic term for a whole class of phases. Their common property is the presence of a layered structure. The differences are the structure inside the layers and the correlation between the layers. Smectic phases are distinguished by letters (A, B, C, ...) and until today 12 different variations have been identified. The smectic A phase consists of layers of liquid crystal molecules, but inside the layers there is only orientational order. One can look at the SmA phase as stacking of layers of a two dimensional oriented liquid or as the nematic phase with layered order. However the ordering is strong enough to give rise to Bragg reflections in X-rays. Since there are two types of order present, one-dimensional positional order and orientational order, the smectic order parameter should have two components: u that denotes the displacement of the layers from their equilibrium position and k_0 that indicates the wave number of the density wave[10]. The order parameter is then given by

$$\Psi = |\psi|e^{ik_0u} \quad (1.2)$$

The cholesteric or chiral nematic phase

The cholesteric phase is the equivalent of the nematic phase for chiral molecules, and it was first observed in the liquid crystalline derivatives of cholesterol. The local molecular ordering is that of the nematic structure, but the important difference is that the director is not a constant vector, it rotates in a direction perpendicular to the long axes of the molecules. This means that a helical structure is formed, whose pitch correspond to half

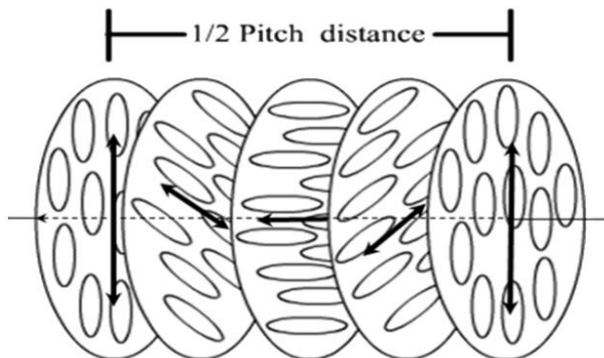


Figure 1.3: Schematic structure of a right-handed chiral nematic (cholesteric) phase. Black arrows represent the director, which rotates perpendicularly to an axis in a helical manner. Molecules (represented as ellipsoids) can take any orientation, but are preferentially aligned to the director.

helix length. It is half of the length because in a nematic, \vec{n} and $-\vec{n}$ are equivalent, i.e. it does not matter in which direction the director points out of two opposite ones. Thus after half a rotation of the helix, the situation is physically the same. Typical lengths of the pitches range from a few hundred nm to infinity for an ordinary nematic phase. The structure of this phase is depicted in figure 1.3. The main consequence of this helical structure is the strong influence on the polarization of the light that passes through it. A property that made this chiral nematic systems useful for display applications.

1.4 Lyotropic Liquid Crystals

1.4.1 Introduction to the structure and phase

As mentioned in the previous section, a liquid crystalline material is called *lyotropic* if phases having long-ranged orientational order are induced by the addition of a solvent. Historically the term was used to describe materials composed of amphiphilic molecules. Such molecules comprise a water-loving ‘hydrophilic’ head-group (which may be ionic or non-ionic) attached to a water-hating ‘hydrophobic’ group. Typical hydrophobic groups are saturated or unsaturated hydrocarbon chains. Examples of amphiphilic compounds are the salts of fatty acids, lipids and phospholipids. Amphiphilic molecules form aggregates through a self-assembly process that is driven by the ‘hydrophobic effect’ when they are mixed with a solvent, which is usually water. The aggregates formed by amphiphilic molecules are characterized by structures in which the hydrophilic head-groups shield the

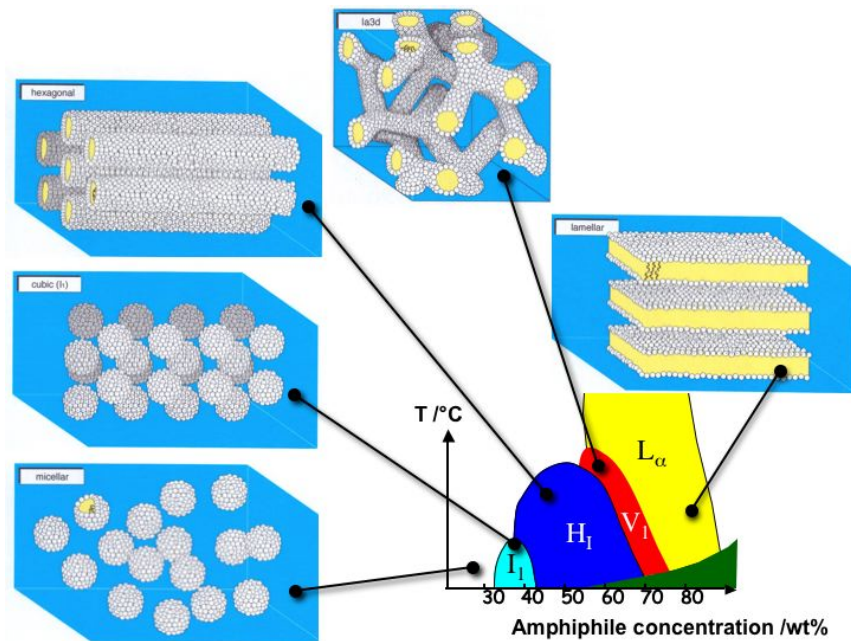


Figure 1.4: Schematic showing the aggregation of amphiphiles into micelles and then into lyotropic liquid crystalline phases as a function of amphiphile concentration and of temperature

hydrophobic chains from water contact. For most lyotropic systems aggregation occurs only when the concentration of the amphiphile exceeds a critical concentration (known as the “critical micelle concentration” (CMC)). The simplest liquid crystalline phase that is formed by spherical micelles is the “micellar cubic”, denoted by the symbol I_1 . This is a highly viscous, optically isotropic phase in which the micelles are arranged on a cubic lattice. At higher amphiphile concentrations the micelles fuse to form cylindrical aggregates of indefinite length, and these cylinders are arranged on a long-ranged hexagonal lattice. This lyotropic liquid crystalline phase is known as the “hexagonal phase”, or more specifically the “normal topology” hexagonal phase and is generally denoted by the symbol H_I . At higher concentrations of amphiphile the “lamellar phase” is formed. This phase is denoted by the symbol L_α . This phase consists of amphiphilic molecules arranged in bilayer sheets separated by layers of water. Each bilayer is a prototype of the arrangement of lipids in cell membranes. For most amphiphiles that consist of a single hydrocarbon chain, one or more phases having complex architectures are formed at concentrations that are intermediate between those required to form a hexagonal phase and those that lead to the formation of a lamellar phase. Often this intermediate phase is a bicontinuous cubic phase. In this chapter we concentrate on a special class of liquid crystal, a lyotropic liquid

crystal called “chromonics”. We will give a description of mesogen’s structure, phase and aggregation and present our studies on the alignment of these biocompatible molecules by varying the specificity of interactions between them and confining surfaces. We demonstrate how the surface energy of the alignment layers can play a fundamental role in both planar and homeotropic anchoring. More specifically, high surface energy materials are employed to obtain planar anchoring of the LC solutions, while low surface energy materials gives homeotropic configuration.

1.5 Chromonic Liquid Crystals

1.5.1 History, Structure, phase and aggregation

Liquid crystals have been known for more than 150 years but have entered the mainstream of the scientific and technical progress only during the last decades. Their optical properties proved to be convenient for the manufacture of simple and inexpensive indicating devices with a low power consumption. This led to a wide scale development of both chemical and physical and biological studies on liquid crystals. Over the last 10 years, since the early work of Attwood, Lydon, Tiddy and coworkers [11, 12, 13], the interest in a distinct family of lyotropic liquid crystals (LLCs), the so-called lyotropic chromonic liquid crystals (LCLCs) is grown. LCLCs represent a broad but not well-understood class of soft matter in which the reversible self-assembled aggregates formed by non-amphiphilic molecules, show liquid crystalline phases. The range of materials which forms chromonic LC phases includes drugs [12, 13, 14], dyes [15, 16], and DNA nucleotides, such as guanosine derivatives [17, 18]. Anisotropic optical properties of LCLCs, such as birefringence, can be used for enhancing optical images for biosensors. LCLCs are not toxic to many microbial species [19] and antibody-antigen binding is not altered by LCLCs [20], important conditions for using them in biological sensing. Because of all these characteristics, biocompatibility and features of liquid crystal mesogens, the interest on chromonic mesogens exponentially growth in last years. The existence of dye and medicinal drug mesophases has been known for a long time but they have not attracted the attention of chemists or physicists. As early at 1916, Gaubert [21] found that a series of substances capable of forming thermotropic mesophases on fusion when their solutions in ether, toluene, chloroform, carbon disulphide, etc. were evaporated. He later showed [22] that liquid crystals are formed also on evaporation of solutions of certain substances which do not give rise

to mesophases on fusion. The term chromonic was used for the first time in literature in 1915 when Sandquist described the unmistakable optical texture of a chromonic N phase in aqueous solutions of a phenanthrene sulfonic acid [23]. Later reports, mainly in the dye literature, by Balaban and King, Gaubert, Jelley and Scheibe, pictured molecules aggregated like *piles of pennies* or *stacks of cards*. So LCLCs were occasionally observed but they were a mystery until 1971, when the first basic observations and phase diagram of one LCLC were published. Most prior work in the area of chromonic liquid crystals has been focused on classifying the phases of chromonic liquid crystals, including the nematic (N), and hexagonal columnar (M) phases. Among the substances investigated, there were also a number of dyes but the structures of the mesophases of these compounds were not established and the above studies therefore remained unnoticed by specialists in the field of liquid crystals and had no influence on the further development of research into the physical chemistry of mesophases. Subsequently, in the 1940's - 1950's, studies on the lyotropic mesomorphism of these compounds became of current interest for some time in connection with the vigorous investigation of the influence of the aggregation process in aqueous solutions of dyes on their absorption spectra, but, owing to the lack of interest in liquid crystals in general, they did not receive due development. The study of the lyotropic mesomorphism of medicinal drugs began as early as the 1920's. The first drugs in which liquid crystal properties were discovered were apparently *salvarsan* (an organoarsenic molecule that was also the first modern chemotherapeutic agent) and *neosalvarsan* [24]. However, these features were studied independently of the study of the liquid crystal properties of dyes and did not find an apparent practical application. In recent years the situation has changed. The study of the structures of dye and drug mesophases showed that here there is a new type of mesomorphism. It was called chromonic mesomorphism, from the name of the antiasthmatic drug *sodium cromoglycate* a typical representative of this type of liquid crystal. It became clear in subsequent years that chromonic mesophases constitute one of the subgroups of lyotropic viscotic liquid crystals which are characterized by a column arrangement of planar molecules. Among them one can differentiate viscotic substances whose molecules have a symmetrical disc shape. On the other hand, chromonic mesophases form planar molecules with a low symmetry having the form of a plank (sanidic). They can therefore be referred to also as sanidic mesophases. Chromonic mesophases have found a practical application. Thus it has been discovered that their lyotropic mesomorphism has a direct bearing on the dyeing process and the therapeutic effect of preparations [24]. Other technical applications of these mesophases have also been

found, and consequently all these reasons have promoted the appearance of much interest in chromonic mesophases. It is now recognized that chromonics embrace not only dyes and drugs, but also nucleic acids [25] and recently Bellini et al. reported the polymorphism of very short oligomers [26]. One important application of LCLCs are biosensors: in literature a planar aligned chromonic liquid crystal can be distorted in presence of large particles by antigen-antibody interaction [27, 28]. The most extensively studied chromonic mesogens is disodium cromoglycate (DSCG), an antiasthmatic drug marketed under the trade name “INTAL”, examined initially in 1970s by Woodard and co-worker [14], which forms highly birefringent phases when dissolved in water. Cox et al. [29] observed the phases of the LCLC drug disodium chromoglycate (DSCG) and plotted a phase diagram in 1971 [23, 14], and soon thereafter, negative birefringence was observed in the nematic phase of DSCG [14]. The study of its behaviour in confined geometries and its physical properties could be a model for more complex biological assemblies. Lyotropic chromonic liquid crystals form a liquid crystal phase in the aggregate, which distinguishes them from thermotropic liquid crystals. In most of the liquid crystals that have been studied, including the lyotropic liquid crystal described above, the particles that form the liquid crystal phase are molecules. However, the particles in lyotropic chromonic liquid crystals, or LCLCs, are aggregates of molecules. Though these particles are formed from multiple molecules, they exhibit a nematic liquid crystal phase nonetheless. Chromonic phases can be considered to be the lyotropic counterparts of discotic phases. They are formed by a range of multiring aromatic compounds, including drugs, dyes and nucleic acids. The molecules aggregate in a face-to-face fashion into columns. This stacking occurs even in dilute solution and produces columns of increasing length as the solution is concentrated. Two mesophases are formed: at lower concentrations, the N phase, constituted by a nematic array of columns while at higher concentrations, the M phase, in which columns pack in a regular two-dimensional hexagonal lattice. The aggregation process is considered to be isodesmic, but they do not present a critical micelle concentration and the driving force for the aggregation is largely enthalpic rather than entropic. As a consequence of the progressive build-up of columns as the concentration is increased, the phase diagrams of chromonic systems have a characteristic multi-peritectic form. This is in contrast to those of conventional amphiphiles in which the sequence of different micelle types (spherical, cylindrical, planar, etc.) across the concentration range, leads to a multi-eutectic form [23]. Compared to other liquid crystals, very little is known about the molecular interactions or the phase of LCLCs, with the exception of DSCG. There is a great deal of data for

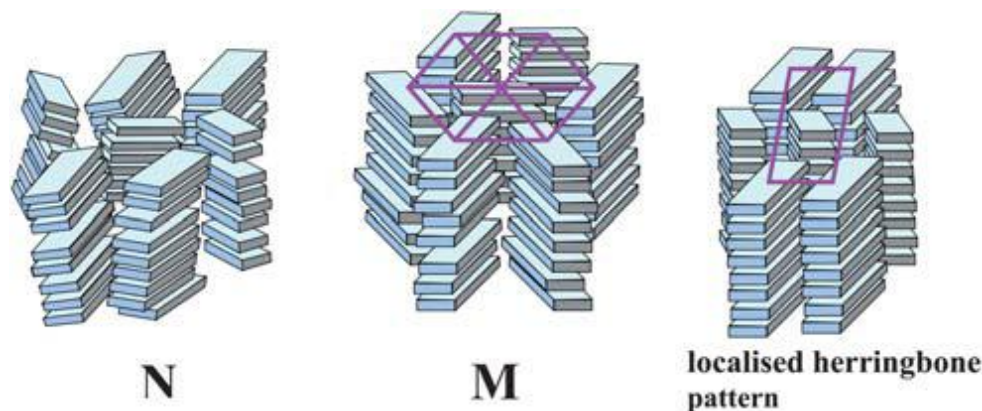


Figure 1.5: **The chromonic N and M phases.** In both mesophases the molecules are stacked in columns. In the N phase the columns lie in a nematic array with no positional ordering. In the M phase the column lie in a hexagonal array but it is thought that there are localized transient regions of rectangular, herringbone patterning, as shown on the right

DSCG, but only a general understanding of other LCLCs has been established. Clearly, there is plenty more to explore in this field.

1.6 Alignment of Disodium Cromoglycate

One of the most challenging goal for the application of chromonic liquid crystals in devices is represented by the possibility to obtain a good alignment, both planar and homeotropic of the LC solution. This goal is difficult to satisfy also because of the solvent of chromonic mesogens, i.e. water, whose evaporation is difficult to avoid in devices and inevitably causes a change in the phase of LCLCs. As previously said, the phase diagrams of chormonic mesogens is quite complex (an example is given in fig. 2.4).

The mesophases of this compound are formed for the same reason as the mesophases of the dyes; too water molecules play a major role. Like dyes, antiasthmatic drugs possess two main chromonic mesophases: nematic (N) and hexagonal (M). The phase diagram for the *DSCG* – *H₂O* system has been frequently investigated, being gradually refined and amplified. A common feature with dyes is the existence of a premesophase region where aggregates, usually dimers, are formed. At room temperature, aggregation begins when the DSCG concentration reaches approximately 5%wt. On the other hand, in the concentration range 5 – 25%wt, the aggregation of molecules is already manifested when the temperature of the system exceeds by 10 – 15°C the temperature of the region of the

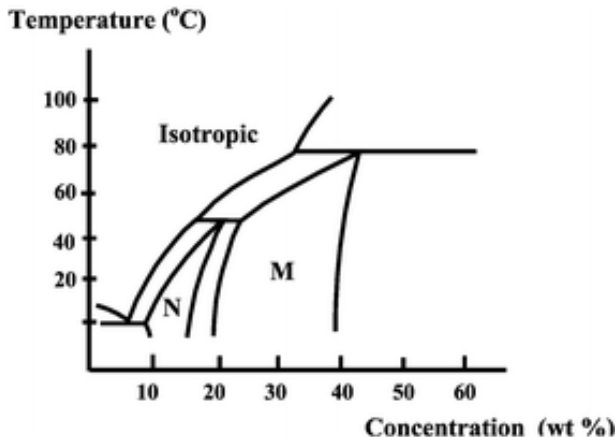


Figure 1.6: The phase diagram of the chromonic DSCG/water system. This was the first chromonic phase diagram to be recorded. Its multi-peritectic form later proved to be the standard classical pattern for chromonic systems.

mesophases.

The alignment of chromonics aggregates, like DSCG, in cells, has proven to be difficult: the molecules arrangement in cells parallel to the substrates has been achieved using standard procedure like SiO_x evaporation films, rubbed polymeric films [30], azobenzene-functionalized polymer or photopolymer [31]. Furthermore the control of azimuthal anchoring is documented using self assembled monolayers of functionalized alkanethiols on gold films that are anisotropic at the nanometer scale. The direction either parallel or perpendicular to the gold anisotropic features is reached by changing the number of methylene units in alkanethiols [32]. However, the homeotropic alignment remains a difficult task. Several groups tried to align DSCG perpendicular to the surface, but only Nazarenko describes the production of homeotropically aligned chromonic materials [33]. Nevertheless this state is metastable and after a while the director re-aligns becoming tangential to the surface. Finally, an important application of chromonic liquid crystals is the fabrication of thin liquid crystalline films which retain the mesogens structure under solvent evaporation and, owing to their anisotropic properties, found application as compensators, retarders, alignment layers and color filters. In this case it is quite easy to align LCLCs parallel to the substrate using technique like shear-induced orientation [34, 35], razor blade alignment [36] or polymeric channels [37]. On the other hand, no data are available for an homeotropic alignment of chromonic thin films.

In this work we report a detailed study of chromonics planar anchoring and of a stable-

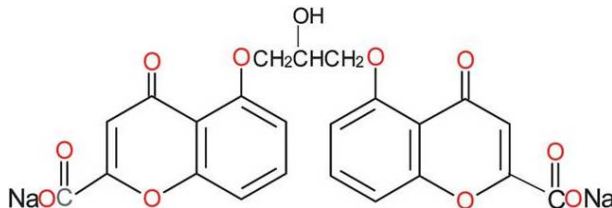


Figure 1.7: Molecular structure of Disodium Cromoglycate

in-time homeotropic anchoring of DSCG, using a surface property of the alignment layer, i.e. the hydrophobicity. In fact, in literature is well reported how the hydrophobicity of the alignment layer plays a fundamental role in the homeotropic alignment of several thermotropic liquid crystals [38]. Nevertheless usual surface treatment for thermotropic LC as homeotropic polyimides (NISSAN), mixtures of homeotropic and planar polyimides, silane derivatives do not work properly with chromonics. Scarce data are available for commercial polyimides, and the analysis of their electronic configuration is difficult; on the other hand the main problem with silane derivatives is to obtain homogeneous layers and avoid arrangements induced by steric interactions, i.e. avoid the molecules lying down on the surface. Hence we tried surfaces showing very low surface energy. Excellent candidates are pure polybutadiene (PB), polydimethylsiloxane (PDMS) and a fluoropolymer, Cytop. The first is a highly resilient synthetic rubber, optically transparent, used in several application. The second is employed in photonics due to its low-cost, high optical quality and compatibility with soft-lithography, and it has been used to realize channels for chromonic thin films [39]. All of them are characterized to be optically transparent, durable and hydrophobic. The surface energy of PB is around $33mN/m$ [40] and it is well known that, when it is a component of block polymer, tends to segregate into air due its low surface energy. The surface energy of PDMS and Cytop is even smaller ($19mN/m$) [41] and ($18mN/m$) respectively. Their use could confirm our strategy.

1.6.1 Materials and methods

Disodium cromoglycate (5'DSCG) was purchased from Sigma Aldrich (in fig. 1.7 the molecular structure is given). All solutions of liquid crystal were prepared with ultra-pure water with a resistivity of $18.2M\Omega cm$ (Millipore, Synergy). Glass microscope slides (PEARL) were cut and cleaned in a NaOH bath, at 40° degrees, sonicated and rinsed several times in distilled water. As alignment layers we used rubbed polymethylmetacry-

late (PMMA), SiO_x , polylysine, and rubbed polyimide for planar anchoring, while pure polybutadiene (PB), purchased from Sigma Aldrich, and Polydimethylsiloxane (PDMS) from Sylgard, silicone elastomer kit for homeotropic alignment. Cytop was purchased from Asahi Glass Co. Ltd., Japan. Polymeric thin films were prepared by spin coating technique, at 3000rpm, using a spin coater from Calctec (Italy) and an appropriate thermal treatment. A 5%wt solution of PB in toluene was prepared and used after an equilibration time of 24 hours, then spin coated and placed on a hot plate at 40°C for 3 hours. PDMS requires a more careful preparation. A solution of 1:10 w/w parts of catalyst (hardener) in pre-polymer was prepared at room temperature. The solution was degassed in a low vacuum for 30 minutes to avoid the presence of air bubble and in order to catalyze the reaction. Afterward, the solution was deposited by spin coating on glass plates and then baked at 130°C for 30 min. Cells were assembled using 12 μm mylar spacers and filled with DSCG (13%wt) in the isotropic phase and then sealed by epoxy glue. After allowing the glue to dry, the temperature was slowly decreased. This procedure allows to reduce the evaporation rate of the mixture contained in the cells. A wedge cell was also prepared similarly to the cell described above, by using a single mylar strip of 40 μm , placed at one end. Aligning layers and chromonic solutions were prepared in a temperature controlled clean room class 100. To check the uniform alignment of DSCG, optical observations were made by a Axioscope Zeiss polarized optical microscope (POM), equipped with a CCD color camera connected to a PC, at 25°C temperature. Other trials with mixtures of homeotropic/planar polyimides [42], homeotropic polyimides (NISSAN) and silane derivatives have been done, as previously discussed, but no particular alignment was observed.

1.6.2 Results

DSCG molecules are easily oriented planar to the substrate using surface treatments already known in literature to give a planar alignment. SiO_x evaporated thin films (fig. 1.8 (a-b))(evaporation angle 60°, thickness 300Å) and rubbed PMMA films (fig. 1.8 (c-d)) give good planar anchoring. The time stability for the planar anchoring depends on the used alignment layer. For SiO_x it is maintained for months.

PMMA cells show an initial planar alignment (fig. 1.8 (c-d)) that after c.a. 5 days evolves into ribbon structures in an isotropic matrix (fig. 1.9). In fact it is well known that alignments due to PMMA rubbing are affected by degradation over time [43]. Moreover,

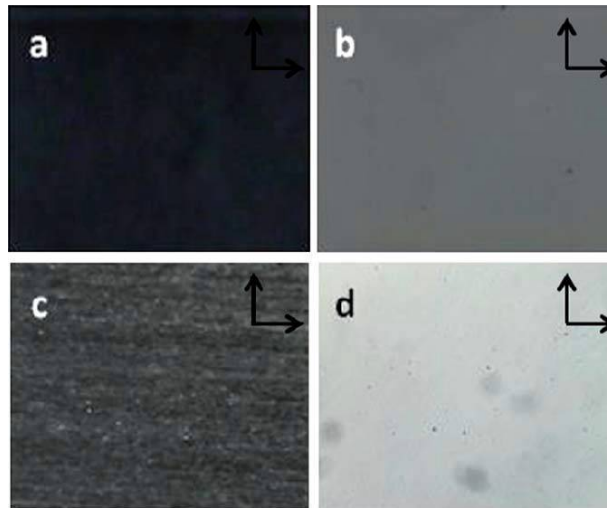


Figure 1.8: POM view of the cell filled with DSCG nematic phase using SiO_x (a and b) and PMMA (c and d) layers. Magnification $20\times$. In pictures (a and c) the alignment direction is parallel to the polarizer, in (b and d) the cell is rotated 45 degrees.

polylysine, a charged polymer usually used in biology to immobilize biological “structures” on mica surfaces, was also used since DSCG is a negatively charged molecule and it could be immobilized at the surface. The aim is to stretch the molecules, charged at the end, in the direction perpendicular to the confining surfaces via electrostatic interactions.

Unfortunately, polylysine cells initially show a degenerate planar alignment that evolves as well into ribbon structures, suggesting that this configuration corresponds to an energy minimum with respect to the starting alignment. Ribbons show the coexistence of an isotropic phase and M phase (i.e. the phase in which columns pack in a regular two-dimensional lattice) and were observed on cooling the DSCG from the isotropic phase into the M phase while we observe them starting from a degenerate alignment (fig. 1.10 (a)).

Homeotropic alignment is not straightforward as for planar alignment, and several attempts were carried out with the most commonly used treatments in the literature. The best results were obtained in cells prepared using glasses treated with Cytop, but also the employment of PB and PDMS deserve to be explained. Just after filling, the cell made up using Cytop as alignment layer show a perfect homeotropic anchoring that remains stable in time for months. Same results are observed on PDMS cells. On the contrary, even if the surface energy of the alignment layer is almost the same for pure PB, the homeotropic anchoring was reached after 24 hours. The alignment is confirmed by conoscopic images (fig. 1.11 e and f inset).

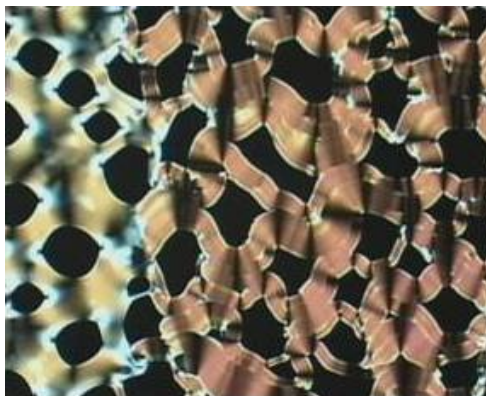


Figure 1.9: POM view, in crossed polarizers, of the cell filled with the DSCG nematic phase observed after 5 days at room temperature. Transition from planar anchoring achieved using PMMA, into ribbon texture. Magnification $5\times$

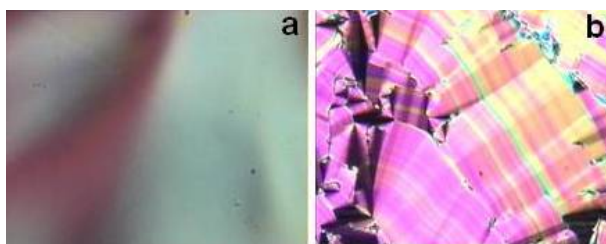


Figure 1.10: POM view (crossed polarizers) of the degenerate planar alignment achieved using polylysine (a) and evolution in ribbon texture after 5 days (b).

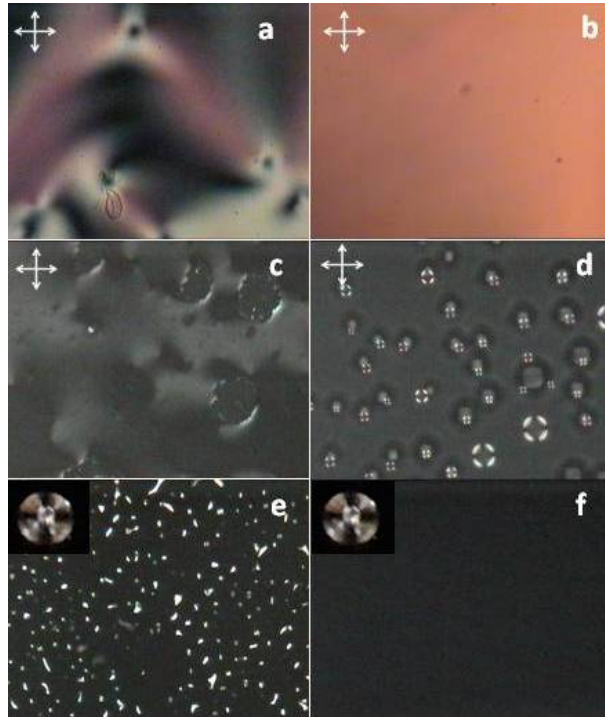


Figure 1.11: POM view under crossed polarizers of PB (a, c and e) and PDMS (b, d and f) alignment layer cells. (a and b) show the DSCG texture just after cell filling: in both case a degenerate planar alignment is the initial configuration. Pictures (c and e) and (d and f) show the evolution in time of the DSCG molecule until the homeotropic configuration is reached. For PB, the molecular reorientation takes place in 24 hours:(c) texture after 5 hrs, (e) after 24 hrs; while for PDMS this process is faster (d) after 2 hrs, (f)after 2.30 hrs. The characteristic cross of the homeotropic alignment in the conoscopic image is visible for both PB and PDMS.

In order to verify whether the homeotropic alignment persists at different thickness, wedge cells were prepared. The evolution in time of the wedge cells made up with PB and PDMS presents very interesting features. At the beginning, for both alignment layers, at large thicknesses, we observe a degenerate planar anchoring with some defects. After 24 hours a re-arrangement of the molecules begins and the homeotropic anchoring is reached. At small thicknesses the PB wedge cells are always homeotropic, suggesting that the confining surfaces induce this configuration. The evolution over time is more complicated, and ribbon textures appear for PB cells (fig. 1.12), while PDMS cells maintain the homeotropic anchoring once achieved. Long time evaporation effects cannot be excluded. Other experiments have been done on plasma treated Cytop and PDMS layers. It is well known that plasma treatment on these surfaces induce a decrease in surface energy giving



Figure 1.12: POM view (crossed polarizers, $20\times$ Magnification) of a wedge cell made up with PB treated glass ($40\mu\text{m}$ to 0), after 15 days from preparation, in which the thickness decreases from left to right as clearly visible from the picture, the colored ribbon textures change as optical retardation decreases.

to the layer an “hydrophilic character” [44]. Glass slides with depositions of both polymer were treated at plasma power of $50W$ for 5 minutes. Then two glasses with the same surface treatment were used to assemble the cell filled with DSCG in nematic phase. Below an example of the results obtained is shown. As alignment layer we tested also layers of Styrene-Butadiene-Styrene (SBS) 28% block copolymer (Sigma Aldrich) spin coated starting from a toluene solution and commercial mixed homeotropic and planar polyimides (V PI and H PI) purchased from Japan Synthetic Rubber Co., dissolved and diluted in the standard solvent provided by the company. The former is an elastomer used in asphalt, in particular SBS is a copolymer which self-organizes into microdomains, lamellar, sphere or columns, depending on the concentration of the minority block (styrene, in this case). This material does not align thermotropic LC and it is dissolved by cyanobiphenyls (data not shown), while the latter is used to control the surface pre-tilt angle of thermotropic LC. In this case the solution was spin coated on glass surface, pre-annealed at $90^\circ C$ for 5 min followed by hard baking at $230^\circ C$ for 90 min. Both polymers present a relatively low surface energy but they do not give a good homeotropic alignment. Nevertheless the results obtained are interesting [2]. The cells prepared using SBS as alignment layer and DSCG in nematic phase are shown in fig. 1.14 (a, b). No particular alignment is observed (fig. 1.14 (a)). After one week “bamboo” structures develop (Fig. 1.14 (b)) [24]. Otherwise, the cells filled with solution in hexagonal phase (fig. 1.14 (c, d)) exhibit a peculiar texture.

H PI and V PI mixtures, as reported in literature, allow to control thermotropic LC tilt angle varying the percentage of V PI in H PI; AFM analysis reveals the presence of nanostructures on the surfaces [45]. We chose H PI and V PI mixtures for their hydrophobicity and for the nanostructured surface in order to check if their presence could help in aligning homeotropically DSCG. Even using these polymers, no particular alignment was observed

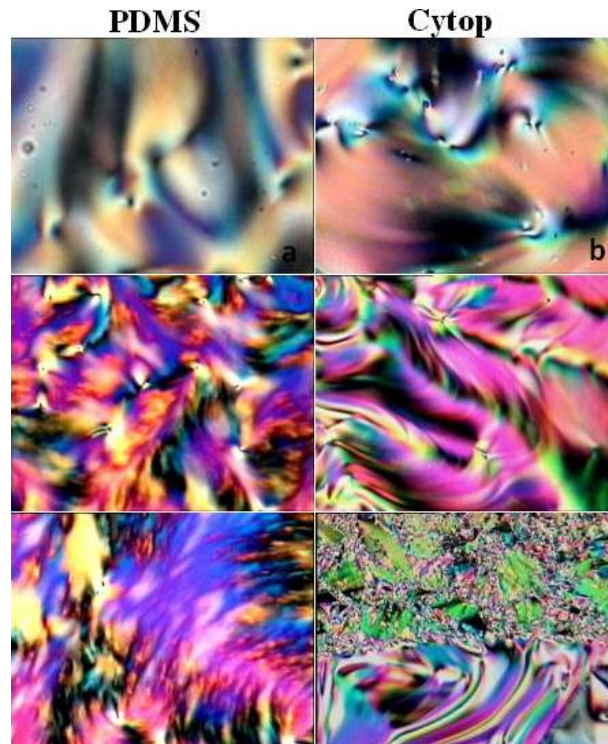


Figure 1.13: POM view of the cells filled with DSCG nematic phase using plasma treated layers of PDMS (left) and Cytop (right). Images(a,b) were acquired just after filling (magnification $20\times$). Remaining images show the texture observed after three days (magnification $5\times$).

(data not showed). The experiments reported here suggest the following conclusion on the mechanisms that induce homeotropic alignment. It is clear that the confining surfaces play a key role but the strong hydrophobicity is not the only requirement to be fulfilled. In fact, for example, homeotropic polyimides mentioned in this work are optimized in order to align thermotropic LC so over hydrophobicity, chemical affinity is important. For example alkyl side chains can help in aligning homeotropically thermotropic LC [46] but their presence is not fundamental for chromonics. In fact, we tested silane derivatives (DMOAP) and one homeotropic PI from Nissan and we were not able to obtain for DSCG an homeotropical anchoring. For this reason we used materials with low surface energy but without alkyl chains: SBS and PB. SBS surface energy is slightly higher than PB surface energy, but only PB gives a satisfactory homeotropic alignment.

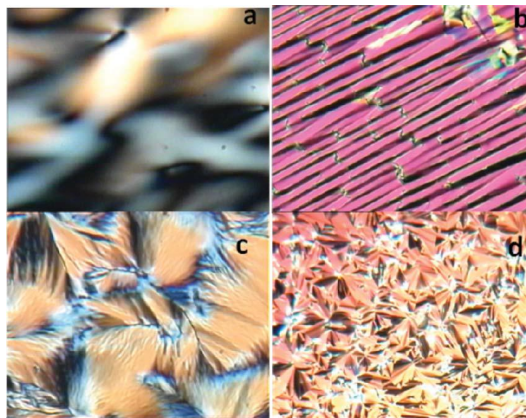


Figure 1.14: POM view of the SBS cells filled with DSCG in nematic phase (a, b) and hexagonal phase (c, d). 20 \times magnification

1.7 Conclusion

In this work we report the planar and homeotropic alignment of nematic phase of disodium cromoglycate; It is well known, for thermotropic LC, that the alignment is initially driven by the confinement surfaces. For this purpose, for planar alignment, we selected a range of films usually employed for thermotropic LC alignment like rubbed films of polyimide, films of mixed polyimides, SiO_x , rubbed films of PMMA, and polylysine covered glasses. All these materials give a good planar alignment or degenerate planar anchoring for LCLCs. In some cases the alignment is stable (SiO_x), while in others, especially if a planar degenerate anchoring is the starting texture, after few days a ribbon texture (fig. 1.9) starts to grow until there is a complete covering of the sample. Layers usually employed for homeotropic alignment, in thermotropic LC, do not work. We hence tried other hydrophobic surfaces like Cytop, PDMS and PB. Cytop cells maintain the homeotropic alignment for months. This could be due not only for the hydrophobicity but also for the chemical structure of Cytop itself. Instead for PDMS and PB, within one day, the homeotropic configuration is reached and remains stable. Unfortunately in this case ribbon textures develop. It should be noted that ribbon textures were reported in the past by Lydon [23] as a coexistence of the M phase and isotropic phase. In our samples this configuration is reached after an evolution of a nematic assembly, probably induced by water evaporation. Reorganization of molecules occurs in order to reduce the free energy. The work of Wu et al [47] supports the model of threads of molecules acting as linear polymers or worm-like structures instead of the molecular stacking model driven by $\pi - \pi$ interac-

tions of the aromatic moieties. By following the threads model we could infer that the DSCG molecules are connected through salt bridges formed by the disodium carboxylate groups on each end of the molecules. The salt bridges are stacked on top of the aromatic ring. The chromonics solution already contains a mixture of monomers, dimers, trimers, and oligomers (all noncovalent) in equilibrium since they give “isodemic” assembly (i.e. they do not show a critical aggregation concentration), but their elongation is promoted by a cooling procedure [47], thermodynamic incompatibility with non-amphiphilic small molecules and probably by slow water evaporation. The energy involved in electrostatic bonds [1] is higher than typical ones involved in liquid crystals. Consequently, the initial alignment is driven by either anchoring conditions or hydrophobicity. As soon as the anchoring symmetry is broken, for example by a gradient of concentrations, the minimum energy configuration, i.e. threads elongation, is reached ¹. It is worth noting that the energy involved in water release is of the same order of magnitude as the one involved in salt bridges bonds, suggesting that entropy plays an essential role to achieve the minimum energy configuration. This behaviour is clearly observed for samples in the nematic phase. With increasing concentration, the aggregates become longer and the viscosity increases as well, preventing the time evolution of the aggregates [48], in line with our observation. In fact, a very slow evaporation phenomenon may occur in both planar and homeotropic cells, giving rise to the formation of ribbon like textures. In the case of PMMA planar alignment, the degradation in time of the alignment layer, i.e. the surface charge decreasing in time [43], could influence as well the overall cell alignment. Regarding the homeotropic alignment, the substrate hydrophobicity strongly influences the assembly as reported in this paper, especially at lower thickness as shown in the wedge cell measurements. Other surfaces having low energy could be used obtaining similar results. In conclusion, the boundary surfaces are important in order to confine LCLCs in either a homeotropic or in planar configuration. The results are very promising for future application in biosensors and optical devices, helping to shed light on the outstanding properties of this class of molecules. The knowledge acquired for DSCG alignment has been used for the other works described in following chapter.

¹Considering that typical energies for electrostatic bonds range between 1.4 and 3 kcal/mol (5.9 to 12 kJoule/mol). From these values it is possible to estimate the energy involved in salt bridges bonds, considering assemblies of 2.6×10^{12} molecules and a uniform domain of $1500\mu m^2$ having $13\mu m$ thickness. The evaluated electrostatic energy is around 0.4nJ. If we consider in the same domain a strong anchoring condition $10^{-4} J/m^2$, the total energy in the domain due to the anchoring is 0.3pJ, that is three orders of magnitude less than the bond energy

Chapter 2

Alignment of guanosine liquid crystal solutions: an intriguing scenario

In this chapter we used the knowledge acquired from the alignment of DSCG for align DNA bases, in particular liquid crystal phases (LC) of guanosine derivatives. We report studies on the alignment of these LC solutions by varying the properties of the confining surfaces, the concentration of nucleotides in water and the effect of cations in LC solutions. We observed that if ionic and/or silver doped solution are added to the LC guanosine phases, it is possible to tune the pitch of the cholesteric phase, modifying the helix structure. Moreover, varying the nature of the confining surfaces, for pure guanosine solutions confined between hydrophobic surfaces, we observed for the first time, the formation of micrometer vesicles of guanosine. Finally, guanosine monophosphate in pre-cholesteric and cholesteric liquid crystals phases were perfectly aligned homeotropically without means of external magnetic fields.

2.1 Introduction

The knowledge that guanine-rich DNA can form unusual structures has its origin in findings that precede the double-helix structure by 50 years. However, the nature of the guanine aggregation, at the polynucleotide helix level, was only revealed in the 1960s by fibre diffraction and other biophysical studies. These studies showed that guanine polynucleotides form four-stranded helices held together by four guanines hydrogen-bonded in-plane G-quartets. Initially, this type of structure was not considered biological relevant until it was demonstrated that natural G-rich sequences in telomeric DNA at the ends of chromosomes could form such structures. The biology of quadruplexes remained a relatively unexplored area until it was demonstrated that small molecule stabilisation of the single-stranded ends of telomeric DNA into quadruplexes, is an effective way of inhibiting telomerase activity, and could therefore lead to anti-telomerase anticancer therapy. Furthermore, a growing number of quadruplex-specific proteins are being discovered. There is now the increasing realisation that non-telomeric sequences in human and other genomes can form (or perhaps can be induced to form) quadruplexes, and that these quadruplexes play a role in the regulation of gene expression. The diversity in quadruplex architecture is also of increasing interest, even though much remains to be established, and rules relating sequence to fold cannot yet be defined.

Self-association of guanosine at millimolar concentrations has been observed in solution since the 19th century as characterized by the ready formation of polycrystalline gels. In the 1960s Gellert et al. [49] determined the associated guanine bases to be in a tetrameric arrangement by crystallographic methods, described simply as a G-quartet arrangement. The four guanine bases form a square co-planar array where each base is both a hydrogen bond donor and hydrogen bond acceptor. Utilization of both the N1 and N2 of one face with the O6 and N7 of the second face on guanosine yields eight hydrogen bonds per planar G-quartet (fig. 2.1 (a-b)). With the development of chemical synthesis of extended polyguanine oligonucleotides strands additional associations were observed in the laboratory environment. CD and IR spectroscopy confirmed the same self-assembly and association of the guanines into G-quartets, while X-ray fiber diffraction studies demonstrated a four-stranded motif with stacked tetrad planes, termed quadruplexes [51, 52]. These stacked tetrads align themselves to give a similar appearance to that of duplex DNA (fig. 2.2 (a)), characterized by a regular rise and twist between the tetrad planes and generating a righthanded helical twist (fig. 2.2 (b)). In this case the phosphate backbones,

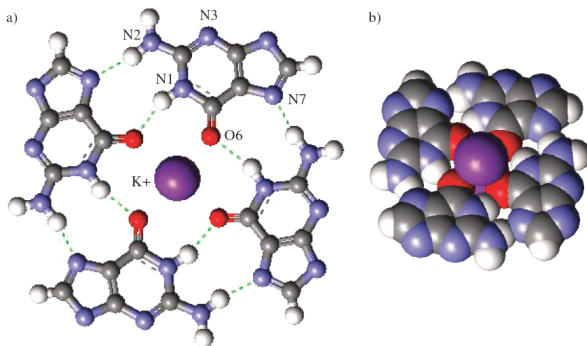


Figure 2.1: (a) A guanine quartet highlighting the hydrogen bonding network between the Hoogsteen and Watson-Crick faces of the guanine bases, including the central potassium cation, deoxyribose sugars removed for clarity; (b) space filling model of a guanine tetrad with associated K^+ metal ions located above and below plane, deoxyribose sugars removed for clarity[50]

linking the nucleosides together, generate four grooves of variable width, instead of two, giving the quadruplex DNA motif a characteristic duplex DNA feel. Interest in the structural arrangements of G-quadruplexes was ignited in the early 1990s by the identification of G-rich repetitive sequences located at the end of chromosomes and a protein, with a reverse transcriptase activity, involved in their maintenance.

2.1.1 Stabilizing factors

Base stacking

G-quadruplexes result from the hydrophobic stacking of several quartets; each quartet being a planar association of four guanines held together by eight hydrogen bonds [53]. A cation, typically Na^+ or K^+ , is located between two quartets forming cation-dipole interactions with eight guanines. In quadruplex structures, just as in duplex DNA, the stacked guanines are neither exactly symmetric or planar. This variation in geometry in the G-tetrad plane can be described in the same geometric terms as duplex DNA with rise, twist, roll tilt, and slide (fig. 2.3 (b)) for both tetrad steps and individual guanine bases. Crystal structures of quadruplexes reveal an unexpected heterogeneity in guanine stacking along the length of the quadruplex. Distortion of the planar tetrads can come from the crystal packing forces and also from linkers of reduced length that impose distance constraints on the G-tetrads. Guanines forming the top G-quartet planes as well as to those stacked below tilt and/or buckle to accommodate the induced strain. An additional

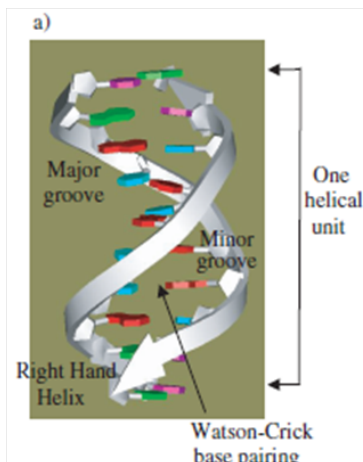


Figure 2.2: (a) A B-DNA decamer showing one full helical turn, and major and minor grooves; and (b) two stacked parallel stranded G-quadruplexes in a 5' to 5', head-to-head interaction [50]

variation in tetrad geometry, in part, comes from the stacking of guanine bases in the alternating glycosidic arrangements. This alternating pattern is found in the anti-parallel backbone arrangements where the bases need to be flipped in order to retain their Watson-Crick and Hoogsteen base pairing. In parallel stranded structures only a single stacked arrangement is observed as all the bases have anti glycosidic torsion angles (fig. 2.4 (a)). This variation in base stacking affects the arrangement of the carboxyl O6 oxygen atoms forming the cavity, located central to the quadruplex core, shown in (fig. 2.4 (a-c)), where the position of the O6 atoms are rotated relative to one another dependent upon the type of stacking. This may play a role in metal ion selectivity in the central core.

Metal ions coordination and mode of interaction

The dependence of quadruplex formation on metal ion coordination has been known since quadruplexes were first identified, while it was Arnott et al. [54] first suggested that the O6 carboxyl oxygen would coordinate cations. In fact, a range of cations both monovalent and divalent are able to stabilize quadruplex formation to varying degrees. The dependence of ions on stability can be seen from the arrangement of the carboxyl oxygen O6 atoms forming the cavity central to the stacked G-tetrad (fig. 2.4 (a-c)). Ions that coordinate effectively enhance stability. Increasing the monovalent cation concentration added little to the dissociation of the intermolecular quadruplexes but contributed significantly to their rate of refolding. The idea of the cations stabilizing one folded state over another, was first

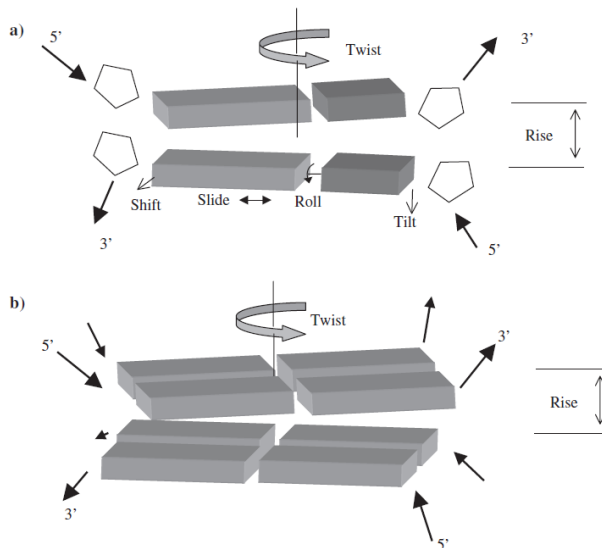


Figure 2.3: Example of base stacking between base pairs. Main geometric descriptors of twist and rise are shown in relation to helical axis and backbone strand polarity. (a) Duplex DNA and a GC base pair; (b) a stacked tetrad consisting exclusively of guanines bases [50]

described by Sen and Gilbert [55] as a Na^+ - K^+ switch. We can distinguish two different type of monocation-quadruplex interaction: the first is based on central ions which are specifically sandwiched between quartets, while the second is based on external ions which contribute to partial charge screening of the quadruplex. Xu et al. [56] demonstrated that K^+ preferentially binds to a small number of specific sites on a tetramolecular quadruplex. Quadruplex specific stabilization by cations has been evaluated for a long time. Wong and Wu have found that the cation-induced stability of a 5'-GMP structure is determined by the affinity of monovalent cations for the channel site (with the order K^+ , $\text{NH}_4^+ \gg \text{Na}^+$, $\text{Rb}^+ \gg \text{Li}^+$, $\text{Cs}^+ \text{K}^+$) [57, 58]. Cations can also disrupt quadruplexes: for example Ca_2^+ , Co_2^+ , Mn_2^+ , Zn_2^+ , Ni_2^+ , and Mg_2^+ can induce quadruplex dissociation. The two best-studied ions are Na^+ and K^+ . The preference of quadruplex central cavity for potassium over sodium ions is the result of two opposite effects: from one side the free energy of Na^+ binding to a quadruplex is more favorable than that of K^+ , but from the other side this effect is more than compensated by the much greater cost of Na^+ dehydration [59, 60]. The net result is a free energy change in favor of the potassium form. A number of guanine-rich oligonucleotides may fold into supermolecular assemblies called G-wires or frayed-wires. Formation of G-wires is dependent on the presence of Na^+ , K^+ and/or Mg_2^+ and, once formed, G-wires are resistant to denaturation. The type and concentration of the cation

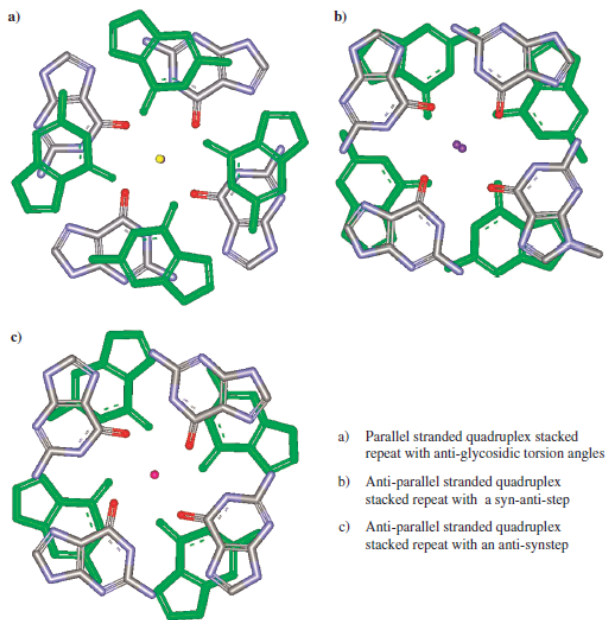


Figure 2.4: A series of stacked guanine tetrads with various strand arrangements syn and anti relationships. (a) Parallel stranded quadruplex stacked repeat where all bases have anti-glycosidic torsion angles stacked over a second tetrad containing only anti-glycosidic torsion angles. (b) First step in an anti-parallel stranded quadruplex with a syn-anti-syn-antitetrad stacked arrangement over an adjacent anti-syn-anti-syn tetrad. (c) Second step in an anti-parallel stranded quadruplex with anti-syn-anti-syn tetrad stacked over a syn-anti-syn-anti-tetrad [50]

Table 2.1: Ionic radii of quadruplex stabilizing cations

<i>Element</i>	K^+	Na^+	NH_4^+	Rb^+	Cs^+	Li^+	Ca_2^+
<i>Ionic Radii</i>	1.52	1.16(0.97)	1.43	1.66	1.81	0.9	0.99

present in solution determines which conformation the oligonucleotide will adopt. However the process of G4-wire formation in dilute aqueous solutions is quite well resolved [61, 62]. The wires assemble above a critical concentration c^* , which is in the range of 5-30%wt at room temperature and their length in solution can reach tens of nanometers depending on the selected G-derivative and on solution parameters such as concentration, temperature, pH, and ionic strength. In this chapter we will give a brief introduction to guanosine structure, aggregation and stabilizing factors. In particular, the first part is devoted to the study on the alignment of chromonic liquid crystal phases (LC) of guanosine derivatives confined between amorphous surfaces. We focused on the effect observed on LC textures when the specificity of interaction among confining surfaces and guanosine solutions is

varied, and on the the effect of cations in LC solutions, as well as their concentration in water. We studied LC phases of guanosine 5'-monophosphate ammonium salt and guanosine 5'-monophosphate free acid (i.e.guanylic acid 5'GMP) in pure water and in presence of silver sulphate. In a second part, a brief section is devoted to the interaction of guanosine LC solution with a non conventional anticancer molecules, synthesized at Chemistry Department of Univeristy of Calabria. Atomic Force Microscopy (AFM) measurements were performed on deposition of guanosine wires formed in a Langmuir trough onto mica substrates.

2.2 Alignment of Guanosine LC phases

Construction of surface architectures via controllable self-assembly processes is a challenging goal, which can lead to a broad range of applications in nanoscale molecular electronic devices and to new perspective in materials science and nanotechnology creating functional nanostructured materials. In literature the driven assembly of either thermotropic or chromonic LCs, has been achieved fabricating periodic structures with a periodicity comparable with the visible light wavelength. In particular the fabrication of periodic structures in polymeric slices represents a low cost procedure and the use of anisotropic soft biocompatible materials which combine fluidity and self assembly properties allows the optical control of the built up devices [63, 64]. Because of the difficulties encountered in aligning long chains of oligonucleotides into stable structures, we focused on the alignment of a particular nucleotide, guanosine and its derivatives, that are promising candidates for these purposes and belong to a special class of chromonic LC. Of the five nucleotides found in DNA and RNA, only guanosine shows the ability to self associate in stable structures, especially tetrameric unit. The inclination of guanosine monophosphate (GMP) or guanine-rich poly and oligonucleotides to self-assemble has been known since the pioneering work of Gelleret et al. [49]. This property is related to the presence of two hydrogen-bond donor and acceptor group quasi perpendicular one to another, which give cyclic Hoogsteen-type hydrogen bonding (fig. 2.5). Tetramers tend to self associate by stacking: ordered gels and fibers from guanosine, 5' and 3' guanosine monophosphate, polyguanosine and deoxy guanosine have been studied extensively [54],[65, p.315].

In the past, guanosine derivatives phase diagram in water, in absence and presence of monovalent or multivalent salts, has been extensively studied; Columnar polymorphism is then observed: cholesteric (pitch is of the order of tenth of microns) and hexagonal phases

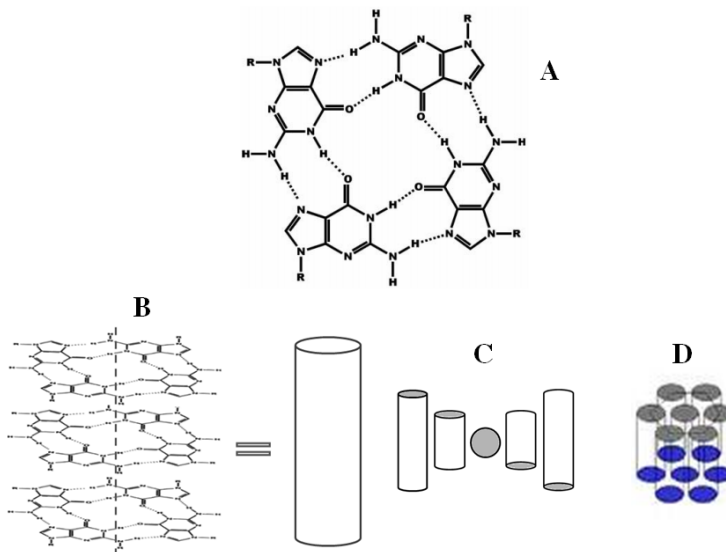


Figure 2.5: Self assembled structure of guanosine: G quartets bonded by four Hoogsteen hydrogen bond (A). The stack between tetramers could be considered as a cylinder (B) and schematic representations of cholesteric and hexagonal aggregations are given in (C) and (D) respectively.

are clearly documented by X-ray diffraction, optical microscopy and circular dichroism [66]. The interaction of guanosine and its derivatives with crystalline substrates have been investigated as well. The adsorption of DNA to mineral surfaces is of great interest because of the danger of genetically modified DNA persisting in the environment and adsorption studies of short single stranded deoxyribonucleic acid oligomers on different mineral surfaces (olivine, hematite, pyrite, calcite and rutile) have been reported [67]. Furthermore guanosine derivatives have been imaged by AFM after depositing starting from a dilute solution onto crystalline substrate like mica [68]. G quartets and DNA are commonly considered as chromonic liquid crystals, i.e., a class of plan like molecules with polyaromatic cores and peripheral groups. In 1960s highly birefringent phases were observed using an anti-inflammatory drug dissolved in water, disodium cromoglycate (5'DSCG). Differently from DSCG, the self-assembling of G derivatives was well known as was its phase diagram, even if, recently, Loo et al. [69] demonstrated the influence of Ag^+ in the assembly of guanosine monophosphate and the formation of dimers, showing an alternative arrangement of nucleobases by coordinating with electron rich functional groups. Here we present our studies on the alignment of LC phases of guanosine nucleotides by varying the surface properties of the confining surfaces, the concentration of nucleotides in water and the effect of cations in LC solutions. We studied LC phases of guanosine 5'-monophosphate

ammonium salt and guanosine 5'-monophosphate free acid (i.e. guanylic acid 5'GMP) in pure water and in the presence of silver sulphate. It is well acknowledged that 5'GMP at $\text{pH} \sim 5$ forms continuous helices with tetramers slightly tilted with respect to the helix axis. The ammonium salt, in contrast, forms planar stacked tetramers, with one rotated with respect to the other, giving rise to cylindrical helices and hence cholesteric and hexagonal mesophases [58, 70]; the addition of salts is crucial for gel formation and some cations (Na^+ , K^+ , Rb^+) has the right size either to penetrate or to position themselves slightly above and between adjacent layers, coordinating to all eight surrounding oxygen atoms. Furthermore it has been recently demonstrated that the addition of silver ions promotes hydrogels formation at higher GMP/Ag ratio due to the presence of higher dimer population [69, 71]. Here, for the first time, we succeeded in aligning cholesteric phases homeotropically without applying an external magnetic field, as done before in literature [72]. All liquid crystalline solutions were confined between polymeric and inorganic aligning layers and showed peculiar rearrangements according to the confining substrate surface energies. In addition, for pure GMP solutions confined between hydrophobic surfaces, we observed for the first time, the formation of "micrometer vesicles".

2.2.1 Materials and methods

Materials

Guanosine 5'-monophosphate free acid (98-100% purity) was purchased from MP Biomedicals, USA. Silver sulphate (2.2×10^{-4} M) was obtained from Fluka. Polymethylmethacrylate (PMMA), pure polybutadiene and SiO_x powder were purchased from Sigma Aldrich, while Cytop and polydimethylsiloxane (PDMS) were obtained respectively from Asahi Glass and Sylgard. Glass slides used for the preparation of the cell, were obtained from Pearl, China. Pure distilled water (Millipore, Millipore $18\text{M}\Omega\text{cm}$) and NH_4OH were used as solvents.

Solution preparation

Liquid crystal solutions called GMP10 and GMP20 were prepared dissolving in Millipore water, guanosine nucleotide as received from the producer, at a concentration in weight of 10% and 20% respectively. These two concentrations are respectively the pre-cholesteric and the cholesteric phase of liquid crystal guanosine solutions. GMPAg10 and GMPAg20, were made following the same procedure of the previous LC solutions but silver sulphate

Table 2.2: Surface Energy values of the alignment layers

<i>Material</i>	PMMA	SiO _x	PB	PDMS	Cytop
<i>Surface Energy (mN/m)</i>	41.1[41]	40-60[73]	33[40]	19.8[41]	19

(used as received from the company) were added to the solutions. The samples called GMPNH4 was prepared by titration of guanosine nucleotide with NH_4OH , followed by subsequent lyophilization. A solution at 20%wt (cholesteric phase) was prepared without the adding of any buffers or other ionic agents were added in order to avoid the introduction of additional assembly-promoting cations to the solution.

Methods and procedures

Glass slides were cleaned in a NaOH bath, sonicated for 15 minutes and rinsed several times with Millipore water before drying under heat flow. Hence, they were pre-treated (as explained in the following) in order to obtain planar or homeotropic alignment of the LC solutions. Standard materials and procedures extensively used for thermotropic LC alignment have been employed, such as SiO_x evaporation, rubbed PMMA layers and spin coated hydrophobic polymers, whose ability in aligning chromonics LC has been recently demonstrated [1]. The surface energy of these aligning layers are reported in table 2.2.

For the planar/oblique anchoring SiO_x evaporation and rubbed PMMA layers were used. SiO_x depositions were made under vacuum with an angle between the evaporation direction and substrate plane of 82° . PMMA films were obtained by spin coating the solution and curing them at $80^\circ C$ for 1 hour; after cooling down, PMMA films were rubbed using a custom built machine with a velvet cloth. To achieve homeotropic anchoring different materials, characterized by a very low surface energy, were used: polybutadiene (PB), a synthetic rubber, polydimethylsiloxane (PDMS), a polymeric organosilicon compound and Cytop, a transparent amorphous fluoropolymer. Preparation of PB and PDMS layers were carried out following the procedures explained in the previous chapter (Materials and methods section) while concerning Cytop deposition, the solution was used as received from the producer, and spin coated at 3000 rpm for 40 seconds and baked at $100^\circ C$ for 30min. Cells were prepared using two glasses with the same surface treatment, assembled together using two mylar strips ($12.7\mu m$) as spacers, then they were filled with the guanosine solution in isotropic phase and sealed by an epoxy glue. This procedure avoid water evaporation. After filling, each cell was slowly cooled and observed by polarized optical

microscopy (POM).

2.2.2 Results

The behavior of LC guanosine derivatives confined between amorphous substrates is quite complex hence, we group the results on the basis of the alignment layer surface energy, from the highest to the lowest. In the first part, i.e. higher surface energies, we present the results obtained using GMP solutions, then the ones obtained with GMPNH₄ and GMPAg; in the second part, i.e. lower surface energies, all solutions give similar results and are discussed all together. A brief insight is devoted to the peculiar texture observed in PDMS cells. An home - made program written in *Mathematica* has been used to highlight periodicity in the textures.

High surface energy materials

Evaporated silicon oxide is a standard material for planar alignment of thermotropic LC and it has been successfully used, as well as rubbed PMMA, in the alignment of chromonic phases of DSCG, as shown in the previous chapter. We expected that these alignment layer should be suitable also for planar alignment of guanosine LC phases.

GMP on SiO_x and PMMA

The texture observed for the cells assembled using SiO_x and PMMA treated glasses and filled with GMP10 and GMP20 are shown in fig. 2.6. As discussed in the introduction, guanosine nucleotides forms continuous helices in solution; the cholesteric phase appears starting from 20%wt, hence at 10%wt we are in a pre-cholesteric regime. The cell assembled using SiO_x as alignment layer and GMP10 solution, just after filling, presents a slightly birefringent texture with a modulation of $2 - 3\mu m$ (fig. 2.6 (a)), instead GMP20 shows temporary stable fiber-like structures with a superimposed modulation of 3 to $4\mu m$ (fig. 2.6 (b-c)). POM images of the cells assembled using PMMA as alignment layer, are shown in figure 3.9. The texture of the cell filled with GMP10 is characterized by a fiber-like “network” (fig. 3.9 (a-b)) whose inner space ranges from 10 to $14\mu m$. Cells filled with GMP20 show a texture of elongated fibers, locally aligned on a scale of about $20\mu m$ (fig. 3.9 (c)) and present the same superimposed modulation (fig. 3.9 (b)) with a pitch slightly smaller ($2 - 3\mu m$) than the one observed in the SiO_x cell (fig. 2.6 (b)) .

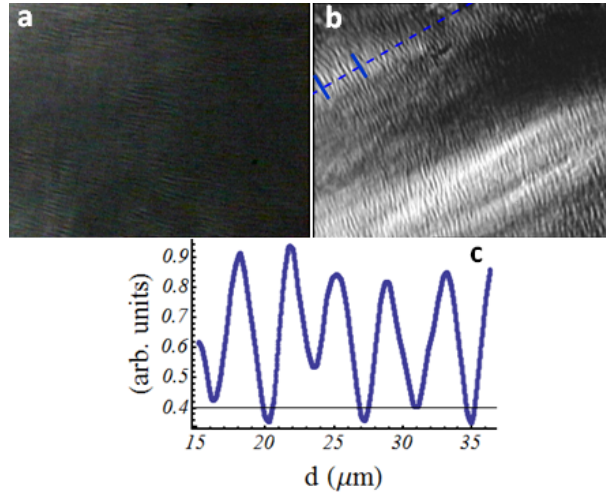


Figure 2.6: POM view of the cells filled with GMP10 (a) and GMP20 (b) on SiO_x deposited at 82°, acquired with a 20× objective. In (c) line profile of the texture in the region indicated on (b).

GMPNH₄⁺ on SiO_x and PMMA

Elongated fibers which orient following two preferred directions with respect to the evaporation axis, are observed in GMPNH₄ cells when the solution is confined between SiO_x glasses (fig. 2.8). This direction are clearly visible rotating the cell under POM. The same solution has been tested among PMMA treated glasses; in this case it is possible to observe the elongated fibers aligned homogeneously in a larger scale (fig. 2.9). Probably, the grooves created on the surfaces by rubbing help the fibers alignment while the SiO_x evaporation produces rough surface [74] promoting more alignment directions, as observed.

GMPAg on PMMA

Here we report optical observations on GMPAg, at 10%wt and 20%wt, confined between two rubbed PMMA glasses. The network observed with GMP10 (fig. 3.9 (a-b)) is broken in GMPAg10 sample; birefringent structures develop, whose dimensions range from 5μm in width (for small structures) to 13μm (for large structure)(fig. 2.10). In contrast, GMPAg20 present textures similar to GMP (figure 3.9 (c-d)) but with an increased pitch (6 – 7μm instead of 3μm) (figure 2.11). Form the results showed, we can infer that the silver sulphate, in a low molar percentage, does influence the structure, probably breaking the ribbon structures, slightly increasing the modulation along the fibers.

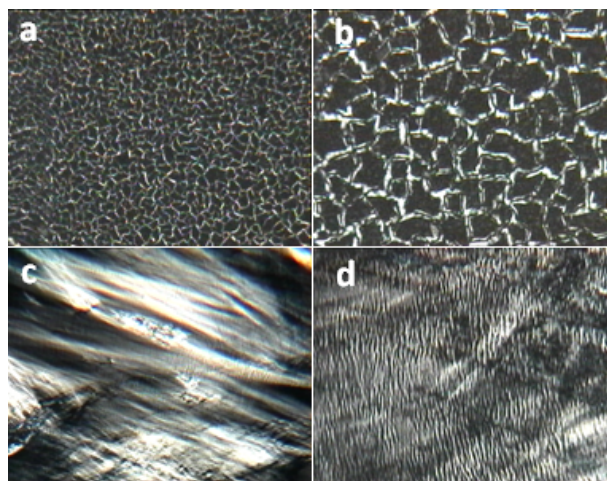


Figure 2.7: POM view of the cells filled with GMP10 (a,b) and GMP20 (c,d) on rubbed PMMA, acquired with a 5 \times objective (a,c) and a 20 \times objective(b,d).

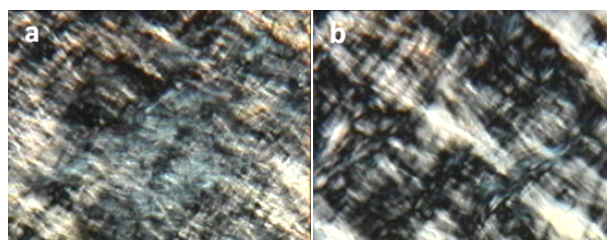


Figure 2.8: POM view of the cell filled with GMPNH4 on SiO_x deposited at 82 $^\circ$ treated glasses. Pictures are acquired using a 20 \times objective.(b) the cell is rotated of 45 degrees with respect to (a).

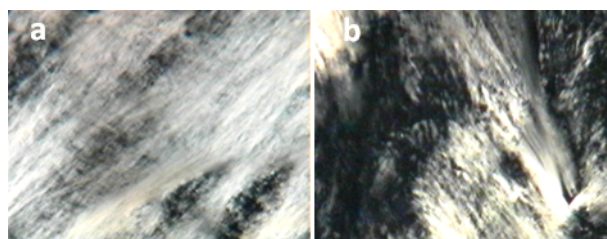


Figure 2.9: POM view of the PMMA cell filled with GMPNH4. Pictures are acquired using a 5 \times objective (a) and a 20 \times objective (b).

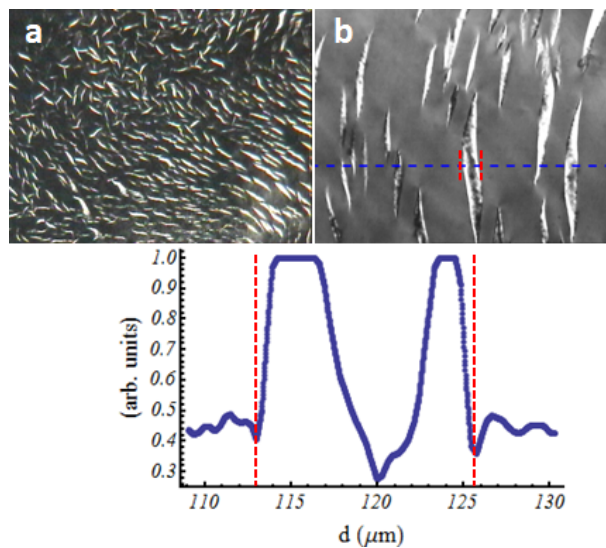


Figure 2.10: POM view of the cell filled with GMPAg10 on PMMA treated glasses. Pictures (a-b) acquired using a $5\times$ objective (a) and a $20\times$ objective (b). In (c) line profile of a “leaf-like” structure.

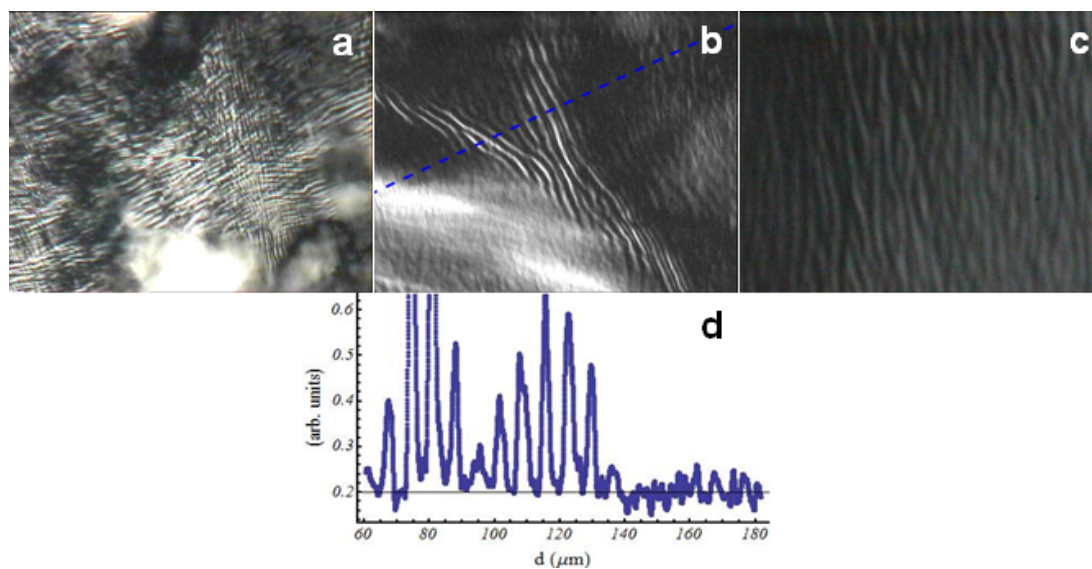


Figure 2.11: POM view of the cell filled with GMPAg20 on PMMA treated glasses. Pictures (a-b) acquired using a $20\times$ and (c) a $100\times$ objective respectively, in (d) line profile of the texture in (b).

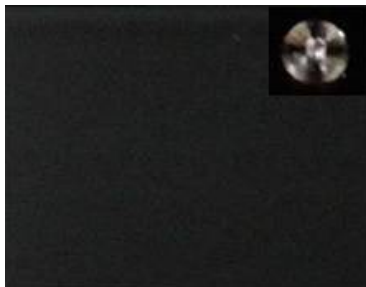


Figure 2.12: POM view of the cell filled with GMPNH4 using Cytop as alignment layer. In conoscopy a well defined Maltese cross is observed (inset)



Figure 2.13: POM view of the cell filled with GMPNH4 using PB as alignment layer. All images are acquired using a $20\times$ mag objective. (a) region with homeotropic anchoring and characteristic defects. (b-c) defect free region with a “modulation” of transmitted light intensity, indicating a tilt from normal alignment of the molecule.

Low surface energy materials

Homeotropic anchoring is achieved using alignment layers with low surface energy: Cytop, PB and PDMS. For all these alignment layers and for all guanosine solutions we were able to obtain a good homeotropic anchoring, confirmed also by Maltese cross in conoscopy (inset of figure 2.12). Due to the peculiar arrangements of guanosine LC solutions confined between PDMS substrates, we present the results starting from Cytop cells, then the ones observed with PB substrates and finally we discuss the results for PDMS cells. The homeotropic anchoring is stable in time for all the solutions tested (GMP10, GMP20, GMPNH4 and GMPAg), especially when Cytop is used as alignment layer. We report only one POM image as an example (fig. 2.12). In case of PB, the texture inside the cell exhibits black regions with and without defects. In particular, after few days, defects disappear and the cell shows a “modulation” in light intensity when it is rotated under crossed polarizers, meaning that the molecules, though aligned in the out of plane direction, are not perfectly perpendicular to the surface (fig. 2.13 (b-c)). Cells assembled with PDMS treated glasses

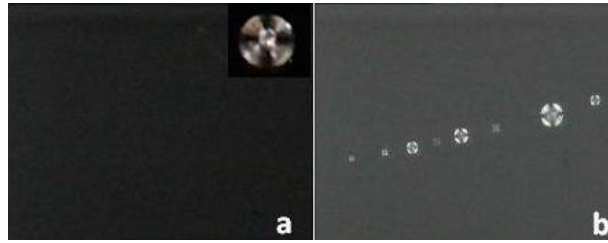


Figure 2.14: POM view of the cell filled with GMPNH4 using PDMS as alignment layer. Pictures are acquired using a $20\times$ objective. In b, guanosine vesicles are visible.

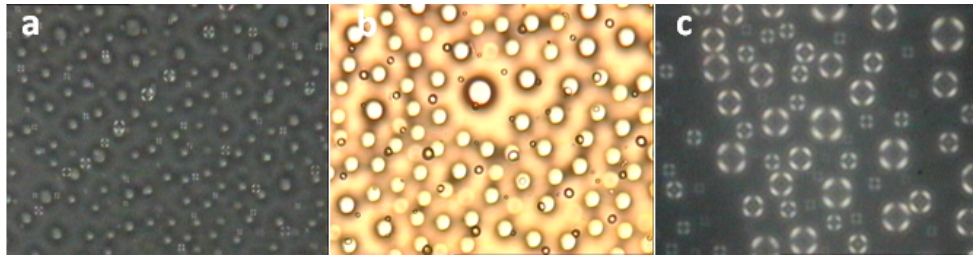


Figure 2.15: POM view (a,c) and reflection image (b) of the cell filled with GMPAg10 using PDMS as alignment layer at $20\times$ magnification. In (c) the cell is heated up to 50°C (reflection-transmission image).

exhibit a homeotropic anchoring which coexists with the presence of spherical aggregates, for all the solutions (fig. 2.14). In particular, the presence of these vesicles is enhanced for silver sulphate doped LC solutions. Moreover their stability is related to the solution used to fill PDMS cells, i.e., the defects are “metastable”. In fact after several hours (ranging from 3 to 24h) they start to shrink and finally disappear. The final texture inside the cell depends on the solution used: for GMP10 micrometric stripes start to grow, GMP10Ag cell become completely black after three days and GMP20 show a crystalline-like structure. It is interesting to note that these vesicles are visible only if guanosine mixtures are confined between PDMS treated glasses. They appear to be anchored to the surfaces and we infer that they are surface stabilized (fig. 2.15). Furthermore, we observe that, upon reducing the GMP concentration to 5% wt (in presence of silver sulphate) vesicles are still present in an isotropic medium and they are still anchored at the surfaces. An estimation of their diameter by optical microscope gives a value of tenth of micrometers. Two parameters seem to influence vesicles: the presence of Ag^+ in the solution, which seems to favor their formation, and the temperature. In fact, for all the solutions, it is possible to induce vesicles formation by heating of the cell up to 50°C .

2.2.3 Discussion and conclusions

We report on the behavior of LC phases of guanosine in water solution. From our observations we conclude that the planar alignment of liquid crystal solutions of guanosine derivatives is not straightforward, even if the alignment layers used, generally work for common thermotropic LC and chromonic mesogens. The alignment is hindered by the presence of fibers, in the case of GMPNH₄, or by the growth of a network of birefringent structures as for GMP and GMPAg. In fact, when “fiber-like” structures are present, it is quite difficult to totally align them, even if, locally (about $10\mu\text{m}$ scale), good birefringence contrast for the aligned fibers can be observed under POM. Some improvements are obtained using PMMA instead of SiO_x as confining surfaces, in fact, fibers seem to align on a larger area ($20\mu\text{m}$). This behavior could be ascribed to the different morphology of the aligning layer: a preferred aligning direction or grooves induced by rubbing procedure in one case (PMMA) and a corrugated surface in the other (SiO_x evaporation). Furthermore GMP alone presents strands, referable to the continuous helices reported in literature, which arrange in microdomains: strands are compact with a transversal periodicity of $2 - 3\mu\text{m}$ at 20%wt. GMPNH₄ presents an increased modulation of $4\mu\text{m}$ and GMPAg20 of $6 - 7\mu\text{m}$. In the pre-cholesteric region (i.e.10%wt) GMP and GMPAg behave differently since the birefringent network, present in the former, breaks down even at low Ag⁺ concentration, in favor of highly birefringent structures whose dimensions range from $5\mu\text{m}$ in width for the smaller ones, to $13\mu\text{m}$ for the bigger ones. Concerning homeotropic alignment we succeeded in obtaining a stable-in-time homeotropic anchoring for LC guanosine phases. As the surface energy decrease, the alignment improves. In particular for PB we observe a “modulation” in light intensity, meaning that the molecules, though aligned in the out of plane direction, are not perfectly perpendicular to the surface. The best homeotropic alignment for all the solutions, pure and doped, is achieved using Cytop, that has the lowest surface energy among the alignment layer tested. We infer that the interaction among tetramers and hydrophobic surfaces prevail; cylinders tend to stack perpendicularly to the surface while the phosphate groups and sugars create a “surrounding medium”. PDMS cells deserve a separate discussion since beside a good homeotropic anchoring, we observe also the growth of particular defects, i.e. what we imagine are “guanosine vesicles”. Comparing our data with literature [75, 69] we could suppose that a vesicle consists in an isotropic guanosine nucleotides core covered by ordered guanosine lamella. In fact guanosine nucleotides tend to aggregate forming tetramers, that are usually not stable. In presence of Ag⁺, the tetrameric structure could be destroyed in favor

of dimers formation [76, 69]. In particular it has been demonstrated that coordination of Ag^+ with the phosphate suggests that compensation of electrostatic repulsion could be an important factor for nucleotide assembly. In literature the production of inverse guanosine vesicles formed by symmetric dimer, in which the two guanosines are held together by two hydrogen bonds, when solved in DMSO, is reported [77]. Lamellar guanosine vesicles have been reported in literature starting from modified guanosine[4], so our guess is that the properties of the alignment layer (i.e. the presence of Si in PDMS) help vesicles formations. This idea is strengthened by the observation that vesicles are anchored to the confining surfaces and they are present only in PDMS cell and not in Cytop cells, even though both confining surfaces are highly hydrophobic. It is worth noting that in literature, the formation of unilamellar vesicles of guanosine are reported starting from a modified guanine base (alkylsilylated guanosine derivatives)[3, 4, 5]. In all of these studies the presence of Silicon (Si) is of fundamental importance for vesicles stability and formations. In our case, we obtain guanosine vesicles starting from pure GMP solutions, placing the solution between two glasses treated with a silicon based polymer (PDMS), so the properties of the alignment layer help vesicles formations. In order to better understand the mechanism of formation and the stability of the structures, we heated the cell up to 50°C , inducing the formation of isotropic bubbles, anchored at PDMS surfaces, eventually covered by guanosine lamella as visible from POM analysis. Similar isotropic guanosine derivatives cores are visible in cell confined by other hydrophobic surfaces, i.e. Cytop, but vesicles are scarcely present even under thermal treatment (no vesicles formation). Ions and heat are also important in the vesicles formation as discussed previously; Our guess is that the formation of vesicles is due to a combination of all these effects. The mechanism of aggregation is under study.

In conclusion we demonstrated the possibility to control the alignment of guanosine liquid crystal phases by using as confining surfaces substrates with different surface energy. Large area planar alignment is difficult to obtain, but relatively large ordered microdomains were observed. We showed how to control the pitch of the ordered helical structures by adding ions to guanosine nucleotides solutions. Homeotropic alignment has been obtained using different low surface energy materials. The result is particularly important for possible applications since many biosensors, based upon reorientation induced by molecular interactions in liquid crystals, are more sensitive in a homeotropic configuration than in a planar one [78]. In fact, the presence of a molecule which modifies the stacking or the interactions of chromonic assemblies, disturbs the overall alignment. For

this reason, this kind of cells can be easily used to verify the chromonic-external agent interaction. Moreover, we observed the formation of guanosine nucleotides vesicles in water and without any chemical modification. The addition of Ag^+ in LC guanosine solution favors self association of guanosine nucleotides and derivatives in dilute solutions and also promotes formation of a specific type of structures within the aggregates. This alternative base rearrangement with a relatively high concentration of Ag^+ , remaining below the critical value for which hydrogels are formed, could influence the electronic properties of this aggregated form of GMP, thereby expanding their functionality. The work reported on the alignment of a DNA bases and the ability to control the pitch of the helical structure, could represent a new route for developing low cost biosensors and biophotonic devices.

2.3 Atomic Force Microscopy studies on Langmuir-Blodgett film of guanosine derivatives

The capability of DNA to form layers and complexes with charged cationic lipid-like monolayers at the air/water interface has recently attracted much attention as it can be used for the assembly of sensitive layers for DNA chips and as it can clarify fundamental aspects of the DNA-biological membranes interactions. In this section, we will describe briefly the methods of preparations and the technique used to investigate guanosine derivatives films. A first part is devoted to describe both Langmuir - Blodgett technique and AFM operating system. Then, a brief description of the molecules used as intercalant for guanosine films are given as well as the comments on the results obtained.

2.3.1 Brief history of Langmuir-Blodgett films and applications

The formation of films at air water interface has been known for centuries. To describe the history of Langmuir and Langmuir-Blodgett films it is nice to begin with the words of Benjamin Franklin, that in 1774, at the British Royal Society, said: *“At length at Clapman where there is, on the common, a large pond, which I observed to be one day very rough with the wind, I fetched out a cruet of oil, and dropped a little of it on the water. I saw it spread itself with surprising swiftness upon the surface.. the oil, though not more than a teaspoonful, produced an instant calm over a space several yards square, which spread amazingly and extended itself gradually until it reached the leaside, making all that quarter of the pond, perhaps half an acre, as smooth as a looking glass.”* Franklin made some simple quantitative calculations according to which if a teaspoonful (2 ml) of oil is spread over an area of half an acre, the thickness of the film on the surface of water must be less than 2 nm. A number of years later, Agnes Pockel, a German woman that developed a rudimentary surface balance in her kitchen sink, reported that the movable barriers on the water surface might control the oil film (in 1891 her work was published on Nature). In the next two decades, Rayleigh, Devaux and Hordy studied various properties. Lord Rayleigh deduced that these films were of only one molecular thickness. However, Irwing Langmuir [79] was the first to carry out systematic studies, which led him to win the Nobel Prize, on monolayers floating on the water from the last years of 1910 until the end of the 20s. It was Katherine Blodgett [80], some years later, to develop the technique for transferring films on solid substrates and obtain multilayers film. These built-up monolayer

assemblies are therefore referred to as Langmuir-Blodgett (LB) films. The term “Langmuir film” (L) is normally reserved for a floating monolayer. After the pioneering work done by Langmuir and Blodgett it took almost half a century before scientists all around the world started to realize the opportunities of this unique technique. The first international conference on LB-films was held in 1979 and since then the use of this technique has been increasing widely among scientists working on various different fields of research. Today, the production of ultrathin organic films with the LB-technique has slowly started to find possible practical applications in many fields. However, even though the ideas for practical applications are growing the L and LB films are still mostly used as model systems for example for biomembrane research and multilayer coatings.

Short background and experimental methods

A boundary surface between two different phases is called an interface. Generally, the thickness of the interface is only of the order of a few molecular diameters. It is approximated truly two-dimensional. The most important feature of an interface is the sudden change in both density and composition that gives rise to an excess free energy at the interface. In most of the LB works the air/water interface are considered. The reasons for choosing water, are that it has high dielectric constant, dipole moment and has ability to form hydrogen bonds, have predominant effects on the properties of this interface. The interfacial free energy is measured by the surface tension γ , defined as

$$\gamma = \left(\frac{\partial G}{\partial S} \right)_{T,P,n} \quad (2.1)$$

where G is the Gibbs free energy of the system and S the surface area at constant temperature, T , pressure P , and composition, n . Moreover, water has a remarkably high surface tension value compared to most other liquids, 73 mN/m at 20°C, due to strong intermolecular attraction leading to pronounced ordering of the water molecules. This exceptionally high value of surface tension, compared to other liquids, makes water a very good subphase for monolayer studies, moreover, the high ordering of the water also influences the electrostatic properties of the air/water interface. When a solution of amphiphile molecules (i. e. molecules that has a hydrophobic tail part and hydrophilic head group) in a water insoluble solvent, is placed on a water surface using a microsyringe, the solution spreads rapidly to cover the available area. As the solvent evaporates, a monolayer of molecules, with the hydrophilic head in water, is formed. A classical L-B trough (see fig.2.16) has barriers that are used to compress the film.

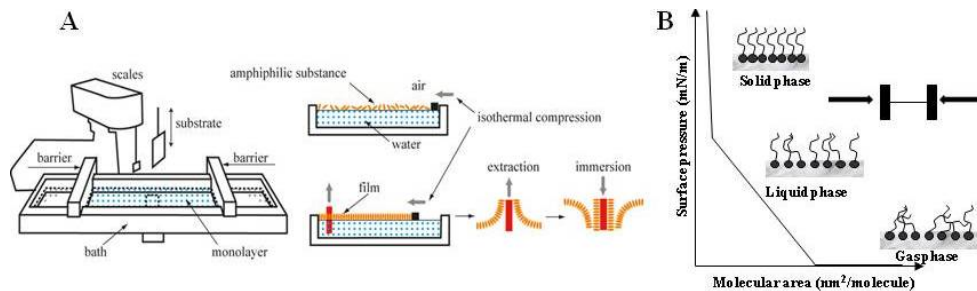


Figure 2.16: Schematic representation of a Langmuir - Blodgett trough (A) that contains the Wilhelmy plate for measuring surface pressure using an electrobalance and the dipper employed for transferring Langmuir - Blodgett onto a solid substrate. Typical Pressure - Area isotherm (B) with a schematic molecular arrangements shown for the gaseous phase, liquid-condensed phase and solid-condensed phase.

Since the molecules of the spread monolayer are confined to the air/water interface, this system is most suitable for studies of two dimensional association processes. The surface tension, γ is a measure of the free energy at the surface and the presence of other substances at the interface will normally lead to a lowering of γ . Therefore, the surface pressure, Π can be defined as the difference between the surface tension γ_0 of the “clean” surface and the surface tension γ in the presence of lipid molecule. Therefore, $\Pi = \gamma_0 - \gamma$. Using a Wilhelmy plate arrangement, Π can be measured as a function of monolayer area that in turn easily may be converted to the mean area available for a single lipid molecule (area/molecule) of the monolayer.

2.4 Brief introduction to “Atomic Force Microscopy”

The atomic force microscope (AFM) is a very high-resolution type of scanning probe microscope, with resolution of fractions of a nanometer. The AFM is one of the foremost tools for imaging, measuring, and manipulating matter at the nanoscale. The information is gathered by sensing the surface with a mechanical probe. Piezoelectric elements that facilitate tiny but accurate and precise movements on (electronic) command enable the very precise scanning. The AFM consists of a cantilever with a sharp tip (probe) at its end that is used to scan the specimen surface. The cantilever is typically made of silicon or silicon nitride with a tip radius of curvature on the order of nanometers (around $100 - 200\mu\text{m}$ long and $10 - 20\text{nm}$ radius of curvature). When the tip is brought into proximity of a sample surface, forces between the tip and the sample lead to a deflection of the cantilever according to Hooke’s law. Depending on the situation, forces that are

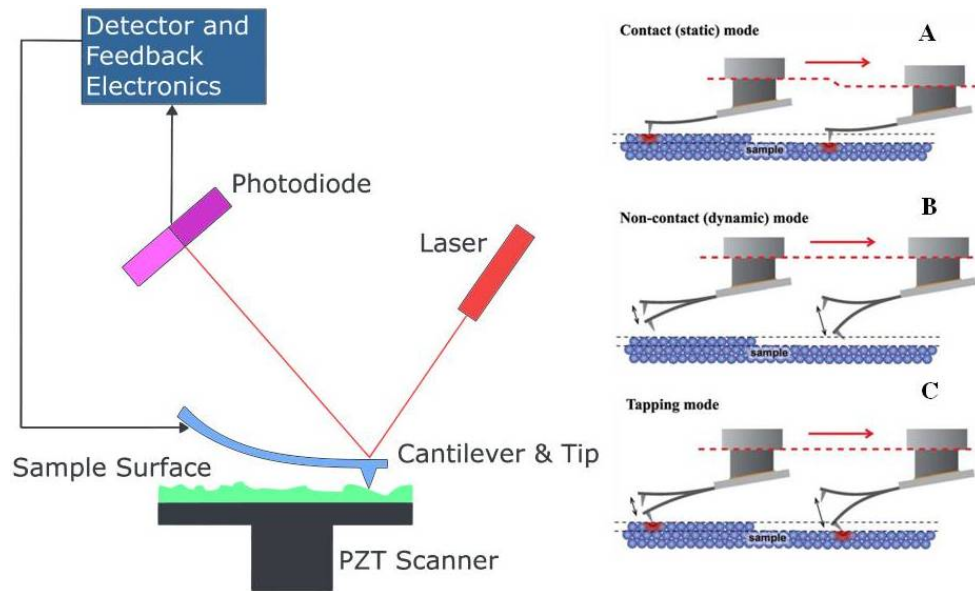


Figure 2.17: Schematic representation of an Atomic Force Microscope (AFM) (on the left) and operating mode (on the right). (A) contact (static) operation mode, (B) non-contact (dynamic) operation mode, (C) tapping mode.

measured in AFM include mechanical contact force, van der Waals forces, capillary forces, chemical bonding, electrostatic forces, magnetic forces etc. However, additional quantities may simultaneously be measured through the use of specialized types of probes, along with force. Typically, the deflection is measured using a laser spot reflected from the top surface of the cantilever into an array of photodiodes. The cantilever scans above the surface of the sample by progressively moving backward and forward across the surface. If the tip was scanned at a constant height, a risk would exist that the tip collides with the surface, causing damage. Hence, in most cases a feedback mechanism is employed to adjust the tip-to-sample distance to maintain a constant force between the tip and the sample. Traditionally the tip or sample are mounted on a ‘tripod’ of three piezo crystals, with each responsible for scanning in the x,y and z directions.

Three main operation mode have been established: contact mode, non-contact mode and/or “tapping mode”.

Contact mode: the cantilever is in full contact with the surface and the static tip deflection is used as a feedback signal. Because the measurement of a static signal is prone to noise and drift, low stiffness cantilevers are generally used to boost the deflection signal. However, close to the surface of the sample, attractive forces can

be quite strong, causing the tip to “snap-in” to the surface. This technique is capable of detecting the topography of atomic scale resolution but could destroy the sample.

Non-contact mode/tapping mode: the tip mounted on the cantilever does not contact the sample surface. The cantilever is instead oscillated at either its resonant frequency (frequency modulation) or just above (amplitude modulation) where the amplitude of oscillation is typically a few nanometers (<10 nm) down to a few picometers. The van der Waals forces, which are strongest from 1 nm to 10 nm above the surface, or any other long range force which extends above the surface acts to decrease the resonance frequency of the cantilever. This decrease in resonant frequency combined with the feedback loop system maintains a constant oscillation amplitude or frequency by adjusting the average tip-to-sample distance. Measuring the tip-to-sample distance at each (x,y) data point allows the scanning software to construct a topographic image of the sample surface.

Schemes for dynamic mode operation include frequency modulation and the more common amplitude modulation. In frequency modulation, changes in the oscillation frequency provide information about tip-sample interactions. Frequency can be measured with very high sensitivity and thus the frequency modulation mode allows the use of very stiff cantilevers. Stiff cantilevers provide stability very close to the surface and, as a result, this technique was the first AFM technique to provide true atomic resolution in ultra-high vacuum conditions. In amplitude modulation, changes in the oscillation amplitude or phase provide the feedback signal for imaging. In amplitude modulation, changes in the phase of oscillation can be used to discriminate between different types of materials on the surface. Amplitude modulation can be operated either in the non-contact or in the intermittent contact regime. In dynamic contact mode, the cantilever is oscillated such that the separation distance between the cantilever tip and the sample surface is modulated. For our experiments, we used the so called “tapping mode” in which the tip is in intermittent contact with the sample. This operating mode is the most preferred for high-resolution topographic imaging of subcellular structures, and soft and delicate biological samples.

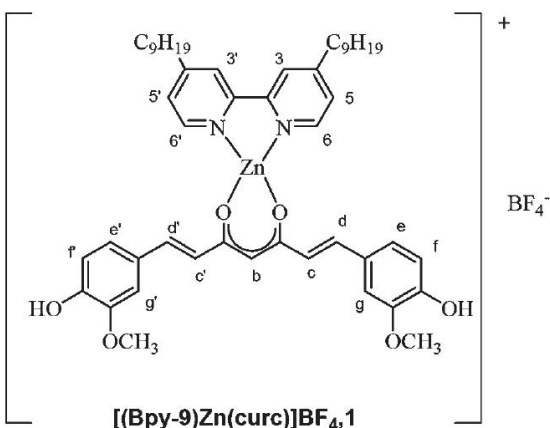


Figure 2.18: Molecular formula of D2.

2.5 Experiment

2.5.1 Intercalating materials

Over the last decade medicinal chemistry has been the scene of a massive investigation into cytotoxicity and genotoxicity of new metal-based antitumor complexes able to overcome cisplatin resistance and toxicity. A rational drug design has focused on a number of transition metal complexes other than platinum which could offer unique properties such as variable redox states, photophysical properties, the possibility of tailoring substrate specificity and ability of targeting DNA through non covalent modes of action [81, 82]. In this context, due to the physiological roles of Zinc in cells and organs, a large interest is growing in the use of Zn(II) coordination complexes with low toxicity and low side effects in medicinal therapeutic applications [83], for treating diabetes mellitus or cancer [84, 85]. The complex studied in this work, synthesized at Chemistry department of Univeristy of Calabria, [(bpy-9)Zn(curc)](BF₄), here in after called D2 for simplicity, has been selected among the new inorganic complexes recently proposed, as effective alternatives to platinum based antitumor agents currently used in chemotherapy, in order to overcome toxicity and drug-resistance phenomena and to improve activity and selectivity [86]. Indeed, [(bpy-9)Zn(curc)](BF₄) shows interesting anti-tumor properties in vitro on several human tumor cell lines, with value of IC₅₀ of micromolar order [86] and high stability in solution, factors that allow it to overcome the curcumin disadvantage of being relatively poor bioavailable and photodegradable. In particular [(bpy-9)Zn(curc)](BF₄), is an heteroleptic Zinc(II)

complex containing in the same time an N,N chelating ligand (the 2,2'-bipyridine), a diketonate O,O chelating ligand (the curcumin) and a monodentate ligand (chloride), whose overall molecular structure suggests that it may act as metallo-intercalating agent. For all this reason, we choose this compound as candidate for studying the interactions that occur between metalloincalator compounds and DNA bases (guanosine derivatives in our case).

2.5.2 Materials and methods

Films were prepared on Milli Q purified water ($18.2M\Omega cm$), used as subphase, in a NIMA 622/D1/D2 film balance with coupled barriers and transferred via the Langmuir-Blodgett (LB) technique onto hydrophilic mica (dipping speed 5 or 10 mm/min). Water surface was characterized prior to film dispersion to ensure purity, by a complete compression cycle while measuring the surface pressure, to detect the presence of any contaminant. The subphase is a $24\mu mol$ solution of GMPNH₄ (the same used for previous experiment) in water. Guanosine were allowed to stand into the subphase for 12hours, then a micro liter syringe was used to deposit, drop by drop, a solution of D2 solved in chloroform at concentration of $1.4mg/ml$ onto the bath, and after several minutes, needed for allow the complete evaporation of the solvent, compression of the monolayer was performed at a speed of 70 mm/min.

2.5.3 Results

$\Pi - A$ isotherms of D2 on guanosine subphase are shown in figure 2.19. The compression of the film were started after 20 minutes, in order to allow the evaporation of the solvent used for D2, and the repeated after 45 minutes. The area per molecule, in time, increases from 104 to 115 \AA^2 indicating the possible formation of aggregates onto the water surface. Probably these aggregates are due to the interaction of D2 with the guanosine in water subphase, that can lead to G-wire formations, as then confirmed by AFM studies done on dried LB films. A second step in the self-organization of guanosine molecules, is the stacking of G-quartets into long 1D assemblies, called G4-wires.

The self-assembly process depends on several external factors, such as concentration of the solution, temperature etc. In figure 2.20 and 2.21 are reported the topography of the sample acquired with AFM in Tapping Mode and a line profile of the wire. As visible in figure 2.20, G-4 wire structures are formed. The height of the wires is about 1 nm. This

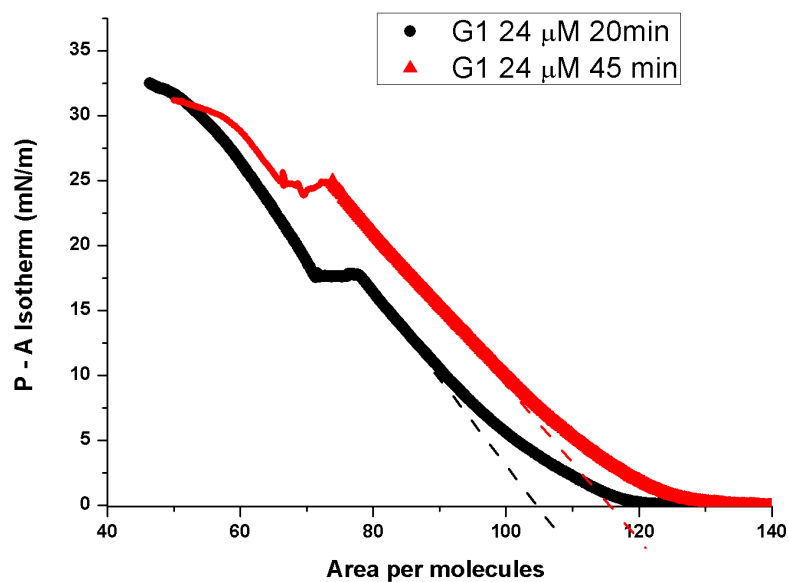


Figure 2.19: Pressure-Area isotherms of D2 on guanosine subphase after 20min (black curve) and 45min (red curve).

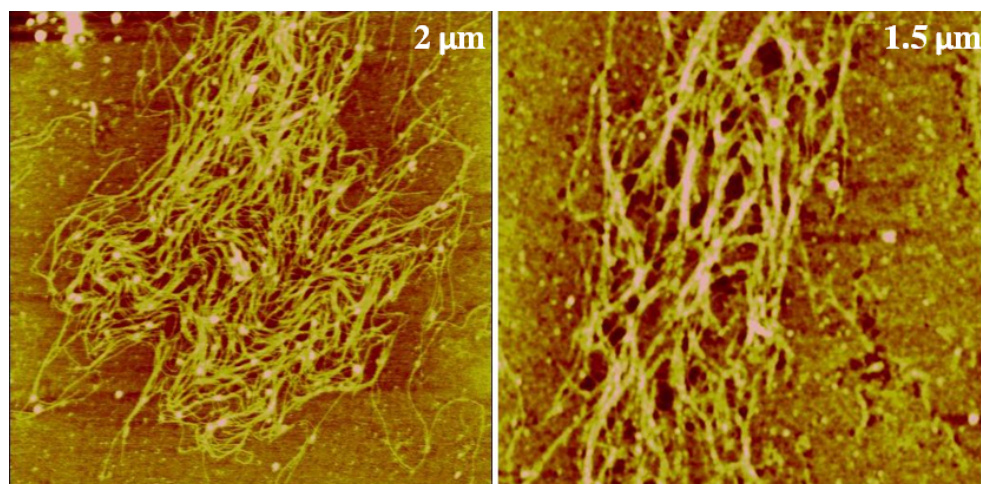


Figure 2.20: AFM topography images of two different places of LB deposition on mica substrates. On the left the dimension of the scan is of $2\mu\text{m}$, while on the right $1.5\mu\text{m}$.

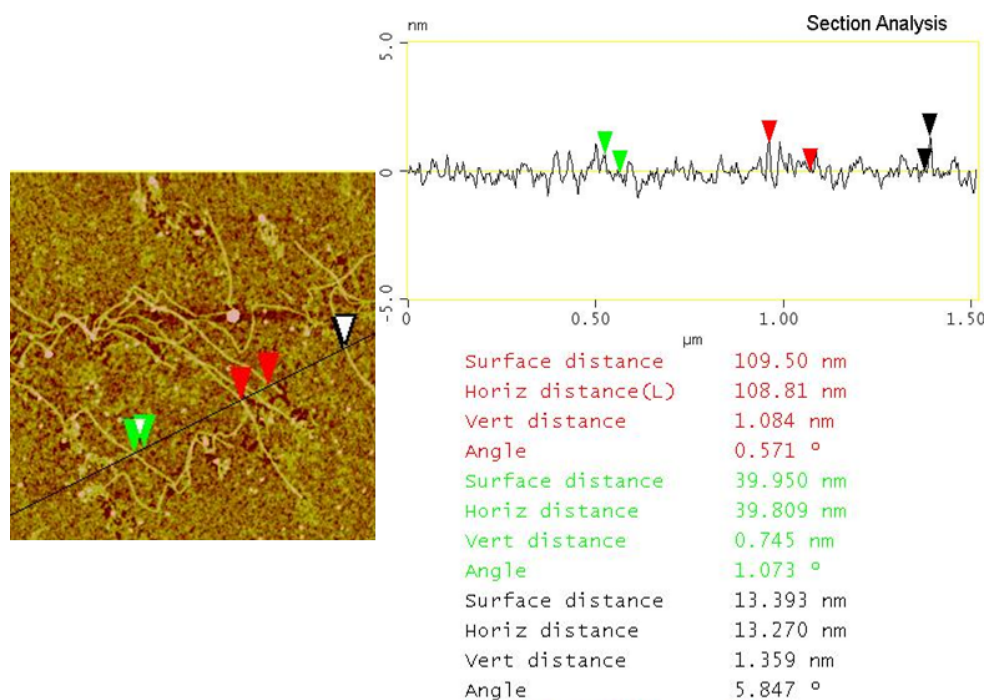


Figure 2.21: Line profile of AFM topography of the LB deposition of G1-D2 on mica. The “height” of the wire are about 1 nm.

value is different from the one reported in literature for G-wire investigated with AFM, mainly for two reasons: first, usually the G-wire are formed adding salts into guanosine solution [87, 88], and as explained in the introduction, the dimensions of the cations between the tetramers influence the structure; second, the data reported in literature are collect carrying out the measurements in a buffer environment, while we are investigating dried films.

However the work is in progress and further investigation are required in order to understand if the D2 is intercalated into the wires or if it only favors their formation.

Chapter 3

New synthesized chromonic molecules: non classical anticancer agents

This chapter is devoted to the study and characterization of new chromonic complexes, synthesized at Chemistry Department of UNICAL, with possible application as anticancer drugs. A complete characterization of liquid crystal phases of these compounds were done (X-Ray Diffraction measurements, phase diagrams with optical microscope pictures, etc), and also for their LC phases, we developed a “route” to drive the alignment, particularly important for future application in biophotonic devices. We used one of these complexes as intercalator of a well known chromonic system, for miscibility studies, important in biomedical field.

3.1 Introduction

Under the name of “Chromonics materials” are collected a large class of molecules and materials, ranging from various drugs (anti-asthmatic and anti-allergic), dyes and nucleic acids. In particular, nucleic acids may adopt different structures according to the hydrogen bonds that can be formed between nucleotides. Guanine-rich (G-rich) nucleic acid sequences have a high propensity to self-associate into planar guanine quartets (G-quartets or tetrads) stabilized by a central, coordinating cation (usually K^+ or Na^+), to give unusual structures called G-quadruplexes, first reported by Davies and co-workers in 1962 [89]. Since guanine-rich sequences are present in important regions of the eukaryotic genome, such as telomeres and regulatory regions of many genes, such structures may play important roles in the regulation of biological events. A telomere is a region of repetitive nucleotide sequences at each end of chromatid, i.e. one copy of a duplicated chromosome, which is responsible of the duplication of the cell. Telomerase is the most important enzyme involved in the maintenance of telomeres length, it prevents their shortening, and it is also an important selective target, since it is expressed in about 85% of tumor cells compared to normal somatic cells. The inhibition of this enzyme is capable of inducing the death of cancer cells, but more important, does not produce toxic effects on healthy cells. This happens because the chromosome ends of cancer cells are morphologically different from those of the normal somatic cells. In normal cells, during replication, telomeres are subjected to a progressive shortening which lead to arrest of cell proliferation. This usual behaviour is not maintained in cancer cells, where telomeres are shorter than those of healthy cells with a constant length, that avoid the normal death of the cell. Telomeric DNA inhibits telomerase activity, organizing in G-quadruplex structures and stabilizing them. For all these reasons, in the past two decades, G-quadruplexes have been considered as valid targets for new anticancer drugs [90, 91]. In the last years, several studies have shown that G-quadruplexes ligands are able to selectively inhibit the growth of cancer cells, thereby opening interesting perspectives for the development of new drugs. Many studies have been performed in order to better understand the factors governing the stability and order of these self-organizing systems, but their structure-property relationships are still not clearly understood. A deeper understanding of the parameters and of the structure-properties relationships that guides the organization of single stranded DNA, can be obtained through miscibility studies that, for chromonic systems, consist in the intercalation of guest molecules into the columns formed by the chromonic mesophases. The

so called *intercalation*, should light the structure-properties rules of this kind of lyotropic mesogens. A recent development concerns the use of mixtures of chromonics and non mesogenic or thermotropic discotic species, whose association produces alternating stacks by “complementary polytopic interactions” (CPI). In this context, the research on new biomaterials, compatible with G-quadruplexes ligands, especially in the field of oncology, have attracted the interest of researchers. Over the last decade medicinal chemistry has been the scene of a massive investigation on cytotoxicity and genotoxicity of new metal-based antitumor complexes able to overcome cisplatin resistance and toxicity. A rational drug design has focused on a number of transition metal complexes other than platinum which could offer unique properties such as variable redox states, photophysical properties, the possibility of tailoring substrate specificity and ability of targeting DNA through non covalent modes of action [92, 93]. New metal-based therapeutics are continuously proposed as effective alternatives to antitumor agents currently used in chemotherapy, with the intention to overcome toxicity and drug-resistance phenomena typical of platinum-based anticancer drugs. In the field of non-classical anticancer agents, Zn(II) derivatives have proved to be potential anticancer agents with low in vivo toxicity and perhaps new modes of action and cellular targets with respect to the classical metallodrugs. However, the limited solubility of neutral metal-based drugs, which often imply low bioavailability, together with toxic side effects and resistance, represent major limitations on their effective use [94]. A pharmacological approach extremely promising is based, therefore, on the possibility of inhibiting telomerase activity in tumor cells and promote, consequently, apoptosis by the administration of substances capable of inducing and / or stabilize quadruplex structures in telomeres [95]. One of the ultimate goals of our current research is the study of parameters that guide and influence the self-assembly of tetrameric aggregates of DNA and of the forces that stabilize them, through studies of miscibility and intercalation. The G-quadruplex stabilization occurs through $\pi - \pi$ interactions and electrostatic interactions existing between the aromatic part of the molecule with the planar structure identified by the guanosine tetrads. Because the tetrads possess a large area, an efficient G-quadruplex binder must present a large aromatic surface, larger than those of a duplex binder, in order to increase the aromatic-aromatic overlap and the selectivity. Electrostatic interaction with the positive charge of the binder contributes too to the stabilization. This means, that a compound should possess both hydrophilic and hydrophobic nature in order to be suitable to interact with the G-quadruplex structure of DNA. Generally, the practice followed to obtain this properties is to add amminic group to the molecule. In this way, the

molecule is both charged and water soluble. Metal-organic compounds are very attractive due to their versatility of synthesis and promising properties of binding to G-quadruplex, thus stabilizing structures:

- The metal occupy the center of the tetrads, electrically stabilizing the structure, replacing the K^+ or Na^+ that normally occupy this site.
- The binder, with a large aromatic surface, favors the aromatic-aromatic overlap with the wide area of tetrads.

Only few examples of metal complexes capable of stabilizing telomeric quadruplex structures are reported nowadays, but thanks to the versatility of the coordination chemistry of transition metals, the complexes of transition metals are configured as excellent potential G-quadruplex ligands. In this context we aim to investigate the coordinative ability of these functionalized ligands towards other metals with respect to the conventional Pd(I) or Pt(II) ones, such as Ag(I) and Zn(II), to obtain non conventional geometries, (from the tetrahedral to octahedral), novel topologies, further and interesting supramolecular interactions (argentophilic) between molecular entities and consequently new phases and properties in the resulting mixtures. Starting from these premises, in this work, a series of ionic silver(I) complexes in which has been changed the nature of the counterion, has been synthesized starting from nitrogen ligands with an extended aromatic portion, able to favor intercalation in DNA, in particular 2,2'-bipyridines functionalized in position 4,4' with hydrophilic groups. These compounds are ideal candidates to achieve CPI mixtures and to investigate their influences on the G-quadruplex structures. They will be used as intercalating additives in well known chromonic systems, used as a model, to study their interference with G-quadruplexes. In particular, a first step was to obtain a complete characterization of these compounds, (liquid crystal phases, optical properties) and then to use them as active intercalating agents in well known chromonic system (disodium chromoglycate in nematic phase).

3.2 Structure of complex I, II and III

Three new metal-containing chromonic complexes (I, II III) have been synthesized and characterized. The proposed structure of the complexes is a ionic molecule or a ionic polymer with a silver/bipyridine 1:2 molecular ratio. They are Ag(I) bipyridine-based

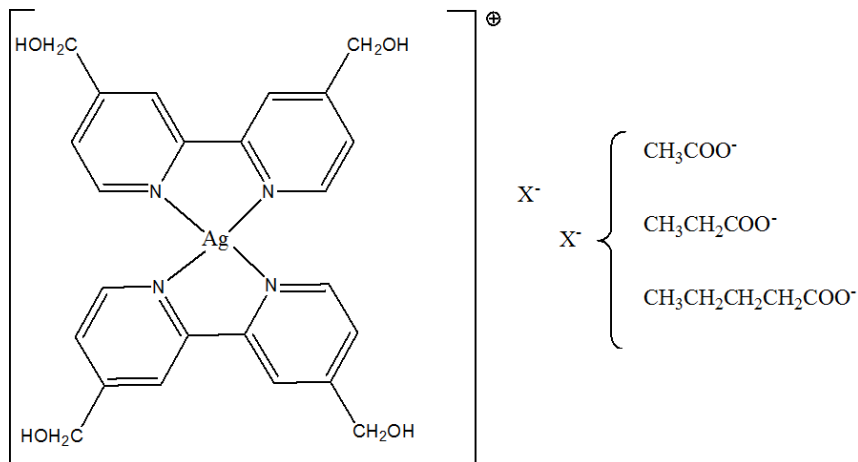


Figure 3.1: Proposed structures for Complex I, II and III, where X represent the counterion that changes for them. From TGA measurement we know that there is a molecule of water, not reported in the picture, because of the lack of information on the real structure.

complexes which differ between them for the length of the alkyl chain on the acetate silver salt used (simple, ethyl or penthyl acetate). Before starting the experiment, the presence of LC phases was tested by mixing a small amount of powder and water and observing a drop of this solution between two glasses. We focused our attention on complex I and II, because complex III presents nematic phase only at very high concentration (50%wt). In addition to phase diagrams, X-Ray Diffraction measurements were done on both complexes powder and their LC phases. X-ray diffraction was carried out, at room temperature (25°C), with a D8 discover Bruker-AXS with a Cu anode, operating with a wavelength of 1.5418Å. The LC solution was hosted in a glass capillary (Mark tubes, Hilgenberg, 80 mm length, outside diameter 0.8 mm or 1 mm and wall thickness 0.1 mm) placed in a home-made sample holder.

3.2.1 Materials and methods

Liquid crystal solutions were prepared by dissolving complex I and II in pure distilled water (Millipore, 18MΩcm) in a range of concentrations between 15%wt and 60%wt. For the phase diagram studies, cells were assembled using two glasses cleaned in a NaOH bath, without any other treatment, filled with the LC solutions in isotropic phase, and sealed using epoxy glue. This procedure avoid water evaporation. After filling, each cell was slowly cooled down and observed by polarized optical microscopy (POM).

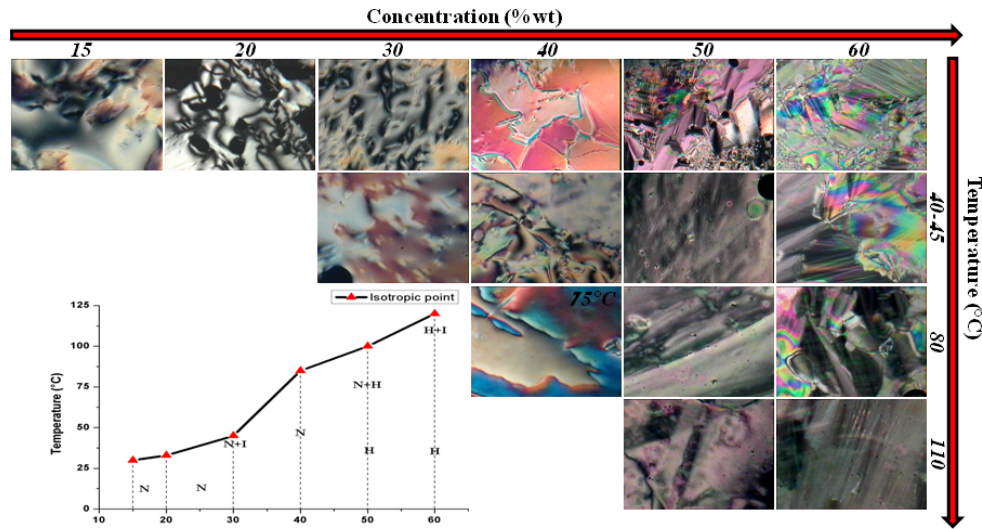


Figure 3.2: (a) Phase diagram of complex I. *N* indicates the nematic phase, *H* the hexagonal phase and *I* the isotropic phase. On *x* axes is reported the concentration of complex I in water, while on *y* the temperature *T* ($^{\circ}\text{C}$)

3.2.2 Complex I: Phase diagram

A phase diagram is a common way to represent the various phases of a substance and the conditions under which each phase exists. Water solutions of complex I exhibit liquid crystal phases from 15%wt to 60%wt. At room temperature, aggregation begins when complex I concentration reaches approximately 10%wt. In figure 3.2 is reported the phase diagram of complex I with some pictures of the textures observed inside the cell, until it reaches the isotropic temperature. Before doing the experiment, we tested the goodness of the “microscope-oven” used to make the phase diagrams, by heating a cell filled with E7, a well known liquid crystal and checking its isotropic temperature transition. We observe the presence of extensive two phase-regions, that is a common features for chromonic mesogens and dyes diagram’s mesophase. From 15%wt to 40%wt complex I is in the nematic (*N*) region, while at 50%wt we observe a coexistence of both nematic and hexagonal phases and 60%wt in the hexagonal one.

At concentration of 50%wt we observe a coexistence of hexagonal and nematic phase between $(65 - 90)^{\circ}\text{C}$. Nematic region goes from 100 to 110°C until the complete transition to isotropic state (*I*). This coexistence is lost when the concentration is increased up to 60%wt. In this case we observe only hexagonal phase until 115°C , where transition starts with coexistence of both *H* and *I* phase. In addition to phase diagrams, X-Ray Diffraction

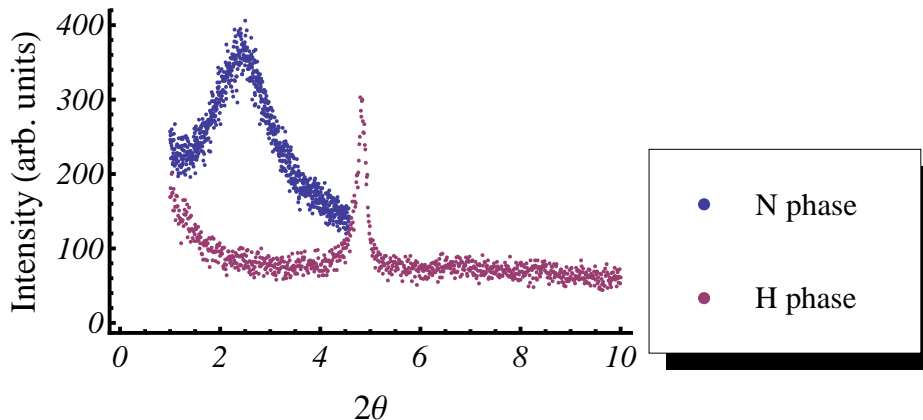


Figure 3.3: X-Ray diffraction pattern obtained at room temperature (25°C) from nematic phase (blue line) 20%wt, and hexagonal phase (magenta line) 60%wt of complex I. (Thanks to Dr. F. Ciuchi for the measurements)

measurements (XRD) were done, at room temperature, on powder and both 20%wt and 60%wt LC phases of complex I.

The structure of the liquid crystalline phases can be derived from the analysis of the corresponding X-ray diffraction profiles. Typical X-ray diffraction patterns for the two mesophases observed in the present system are reported in figure fig. 3.3. The peak is centered at $2\theta = (2.5 \pm 0.4)$ for nematic phase, that correspond to $d = (35, 3 \pm 0.2)\text{\AA}$ and $2\theta = (4.8 \pm 0.2)$ for hexagonal phase, corresponding to $d = (18, 41 \pm 0.2)\text{\AA}$. These values are comparable with the ones usually observed for nematic and hexagonal phases of common liquid crystals.

3.2.3 Complex II: Phase diagram

Complex II differs from the former for the counterion. The phase diagram, reported in fig. 3.5, presents lower isotropic temperature and show the presence of the only nematic phase, even at high concentration. For this complex the concentrations ranges from 20%wt up to

Table 3.1: Phase diagram of complex I

<i>Concentration (%wt)</i>	15	20	30	40	50	60
<i>Phase</i>	N	N	N	N	H	H
<i>Isotropic temperature (T°C)</i>	30	32	47	87	110	120

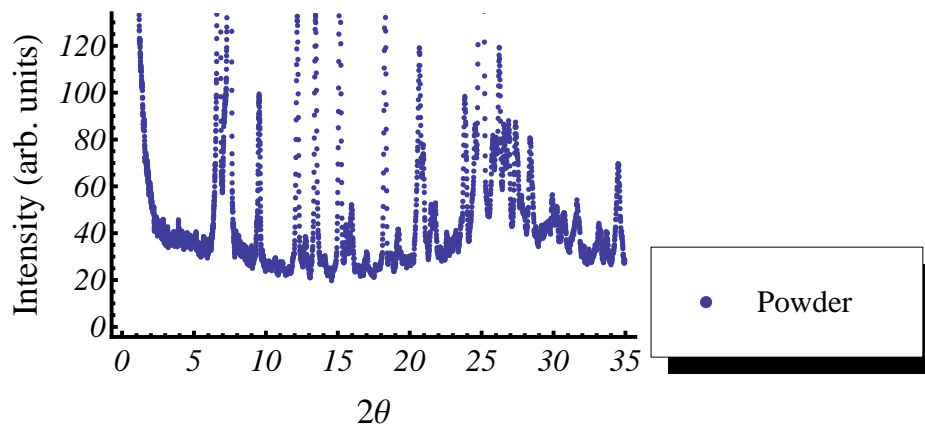


Figure 3.4: X-Ray diffraction pattern obtained at room temperature (25°C) from the powder. (Thanks to Dr. F. Ciuchi for the measurements)

Table 3.2: Phase diagram of complex II

<i>Concentration (%wt)</i>	20	30	40	50
<i>Phase</i>	N	N	N	N
<i>Isotropic temperature (T°C)</i>	34	48	73	90

50%wt. It was not possible to obtain 60%wt, because at this concentration the complex did not completely dissolve in solution.

Also for complex II we performed XRD measurements on both powder and nematic phase.

Typical X-ray diffraction pattern for the mesophase observed in the present system is reported in figure 3.7. The peak is centered at $2\theta = (2.5 \pm 0.4)$, that correspond to $d = 42.1 \pm 0.2$ Å. Powder diffraction spectra is reported in fig. 3.6. Analysis of the powder diffraction spectra, as for the case of complex I, is already under study. It is worth noting that the value of d obtained for both nematic phase of complex I and II is slightly increased for the latter. This could be ascribed to the presence of both nematic and hexagonal phases for complex I. Concerning the XRD spectra of the “hexagonal phase” of complex I, we should notice that it was not possible to observe the characteristic peak at high value of 2θ angle (which give information about the stacking of the molecules) because of the sensitivity of the detector. For this reason, and also for the lack of information on the single molecule structure, we should not say without any doubt that it is an hexagonal phase, but it is correct to say that we are in presence of a 2D packing. However, preliminary

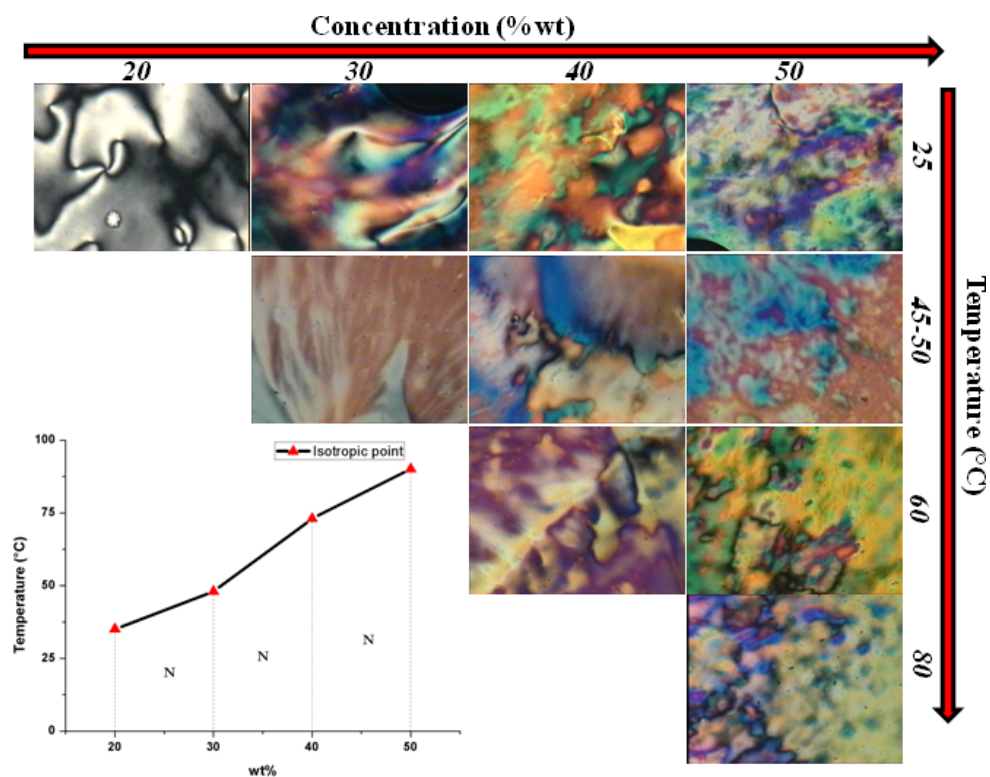


Figure 3.5: Phase diagram of complex II. *N* indicates the nematic phase, *H* the hexagonal phase and *I* the isotropic phase. On *x* axes is reported the concentration of complex I in water while on *y* the temperature ($^{\circ}\text{C}$)

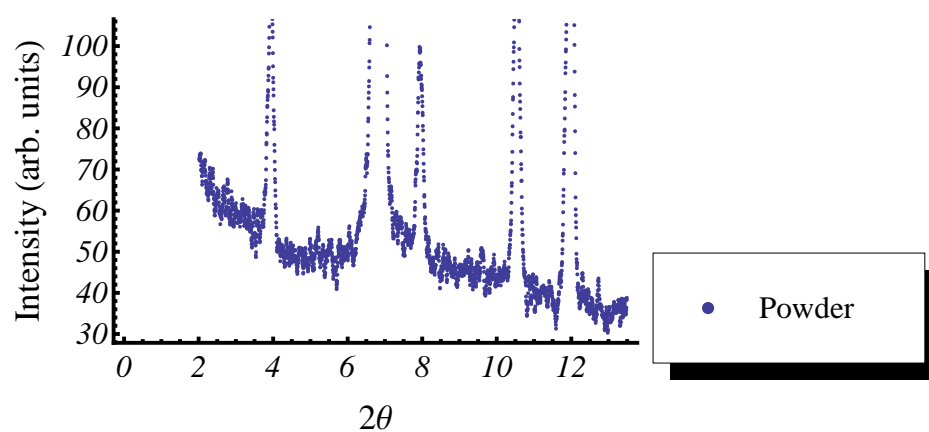


Figure 3.6: X-Ray diffraction pattern obtained at room temperature (25°C) from the powder of complex II. (Thanks to Dr. F. Ciuchi for the measurements)

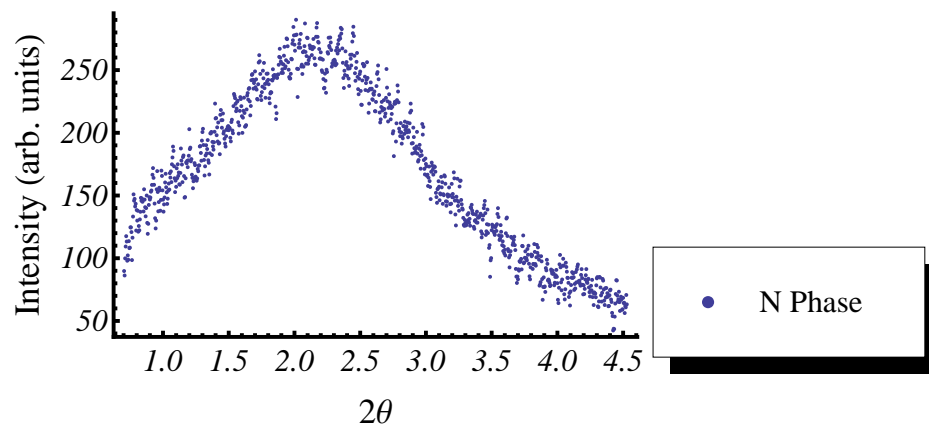


Figure 3.7: X-Ray diffraction pattern obtained at room temperature (25°C) from the nematic phase of complex II. (Thanks to Dr. F. Ciuchi for the measurements)

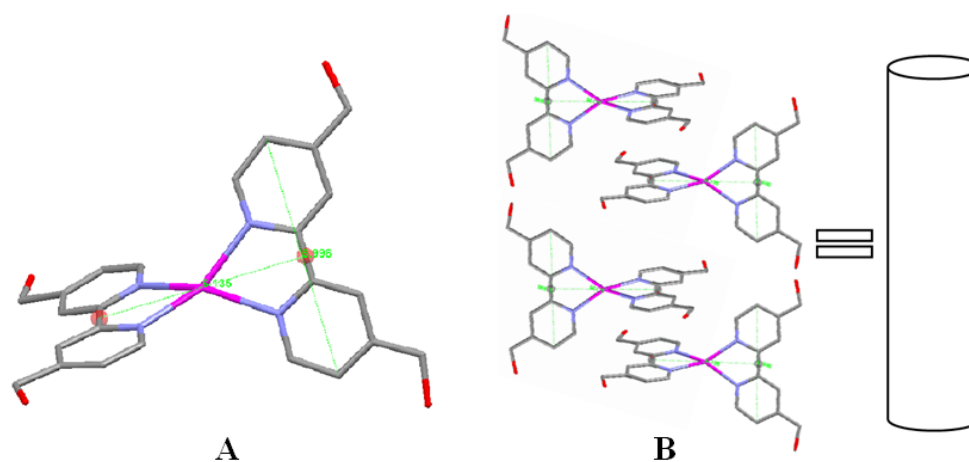


Figure 3.8: Scheme of the hypothesized structure of complex I (A) and its possible packing in (B).

studies hypothesize a model structure (reported in fig. 3.8 (A)) with a possible packing of the molecules as reported in fig. 3.8.

3.3 Alignment

In order to be suitable for optical or devices applications, the liquid crystal solutions of the pre - mentioned complexes, should be well aligned between two surfaces. In this section we will focus on the alignment of LC solutions of these new chromonic complexes, confined between two glasses, properly treated in order to obtain both planar and homeotropic

anchoring. As done before for the other chromonic mesogens, we prepared PMMA rubbed glasses, polyimides and Cytop depositions following the procedure described in the previous chapter. Generally, rubbed PMMA aligns in a planar configuration common thermotropic liquid crystal and chromonic mesogens as well [1], while Cytop depositions, highly hydrophobic, were used for the homeotropic anchoring. As reported in previous chapter, we infer that the surface energy is the driving force in the alignment of chromonic mesogens. Following this idea, we group the results starting from alignment layers with high surface energy (PMMA and PI) to low surface energy (Cytop).

3.3.1 Materials and methods

Polymeric thin films were prepared by spin coating technique, at 3000rpm, using a spin coater from Calctec (Italy) and an appropriate thermal treatment. After cooling, glasses with PMMA film were rubbed using a rotating velvet cylinder. Polyimide depositions (PI LQ1800), 2%wt in Polyvinylpyrrolidone, were prepared using a spin coater at 3000rpm. After deposition, glasses were allowed to rest on a hot plate at 90°C followed by backing in oven at 180°C for 1 hour. When cooled, they were rubbed with a custom built machine with a velvet cloth. Cells were assembled using two glasses with the same surface treatment and 12μm mylar stripes as spacers, filled with the solution in isotropic phase and sealed by an epoxy glue. After cooling down, the cells were observed under polarized optical microscope (POM). We tested LC solutions of both Complex I and II at concentration of 20%wt and 50%wt.

3.3.2 High surface energy material: PMMA and PI

The results obtained in PMMA cells for LC solutions at 20%wt and 50%wt are shown in figure 3.9. Just after filling, the texture observed for complex I in nematic phase is characterized by a coexistence of degenerate planar alignment and homeotropic anchoring. With time, the degenerate planar anchoring evolves in an ordered structure characterized by cylinder (Fig. 3.9 (a) and magnification (c)), and finally, after about 60-70 minutes, a reorientation of the molecules occurs and stable homeotropic anchoring is reached (Fig. 3.9 (b)), confirmed also from maltese cross in conoscopy. For the LC solution in hexagonal phase, just after filling, the homeotropic anchoring is reached. Nevertheless, the texture presents a “modulation” of transmitted light intensity, indicating a tilt from normal alignment of the molecule, that is completely lost after 1 hour. Similar behaviour is observed

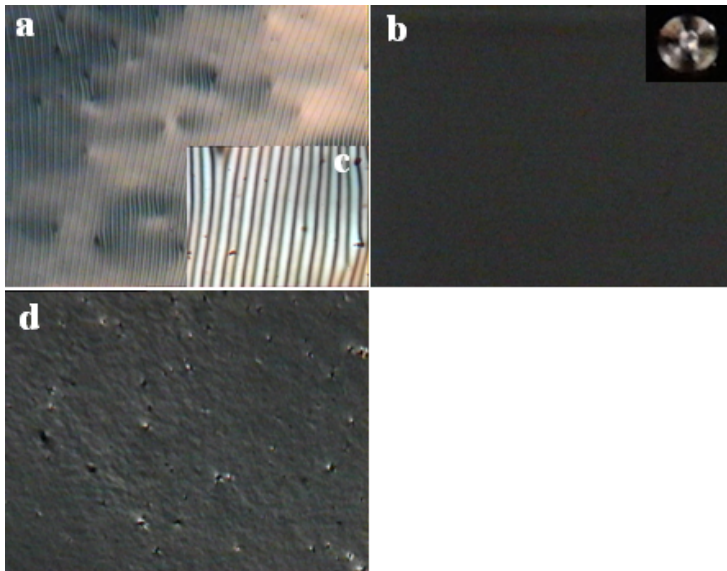


Figure 3.9: POM view of PMMA cells filled with LC solutions of complex I at 20%wt (a,b,c) and 50%wt (d). Picture were acquired using a $5\times$ objective (a) and a $20\times$ objective (b,c,d).

when LC solution in hexagonal phase of complex I are confined between PI treated glass (data not shown). The homeotropic alignment reached using PI treated surfaces is stable and does not change even under heating and successive cooling down process (i.e. the reorientation of the molecules and the rising of cylinders are not observed in PI cells). As previously mentioned, particularly interesting is the behaviour of nematic phase of complex I confined between PMMA treated glasses. In order to verify whether the rising of cylinder is a peculiar reorganization of the molecules or simply a transition that took place in an uncontrolled way, we performed a series of heating-cooling down cycles on the cell. By heating up to 60°C the cell and then slowly cooling down, we observed the same peculiar cylinder structure that “cover” the sample until the reaching of an homeotropic alignment as shown in fig. 3.10. This cylinder structure is metastable and disappear as soon as a “critical temperature” is reached (i.e. the cell reaches the room temperature). Using an home-made program written in *Mathematica*, we were able to make a line profile and measure the “pitch” of these ordered structures. The measured periodicity is $25\mu\text{m}$, with a modulation in the middle at about $12 - 13\mu\text{m}$. The same experiments were done using LC solutions at 20 and 50%wt of complex II.

When confined between PMMA treated glasses, the LC solution at 20%wt reaches a homeotropic free of defect configuration just after filling, instead at higher concentration

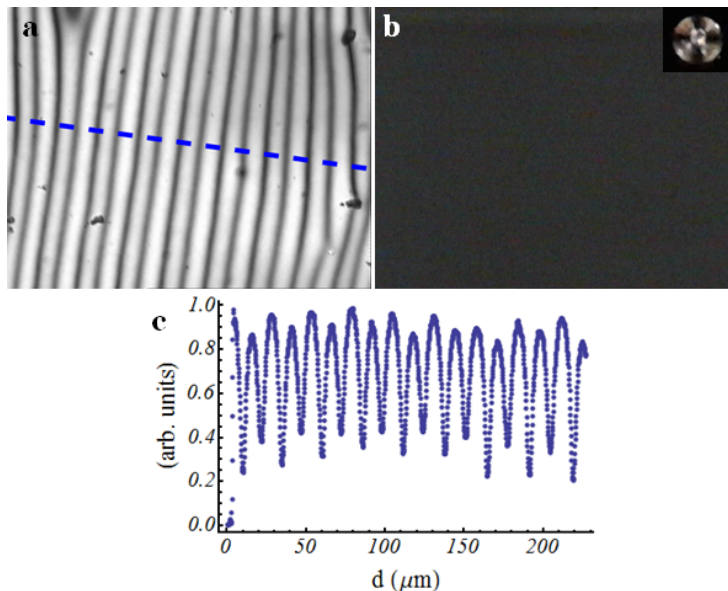


Figure 3.10: POM view at $20\times$ magnification (a,b) and line profile (c) of the cylinders inside PMMA cell during the cooling down process. (b) classical texture of the homeotropic alignment and well defined maltese cross, reached after 2hours. As visible from the line profile, the pitch of the cylinders are $25\mu\text{m}$ with a modulation in the middle (at about $13\mu\text{m}$)

($50\%wt$), it behaves similarly to complex I, i.e. in POM, the cell presents a “modulation” of transmitted light intensity that is completely lost after 1 hour. Because the difference between the two complexes is the counterion, we suppose that complex II should present the same molecules’ reorganization observed for complex I. For this reason, we performed a series of heating-cooling down cycle on the cells filled with LC phases of complex II.

Differently from complex I, the peculiar cylinders appear when the cell was cooled down from 72°C to room temperature, but are visible only in the range temperature $68 - 69^{\circ}\text{C}$. In this case, the pitch measured for the cylinders are about $10\mu\text{m}$ but, differently from complex I, they disappear as soon as the temperature goes down from 68°C . In order to re-induce their formation or to extend the life-time of cylinders, is necessary to heat again the cell and maintain the temperature between $68 - 69^{\circ}\text{C}$. When the cell is completely cooled, the molecules tend to orient in an homeotropic configuration.

3.3.3 Low surface energy material: Cytop

The results obtained for the cells assembled with Cytop treated glasses are showed in following figures. Here we report the texture observed for both nematic phase of complex

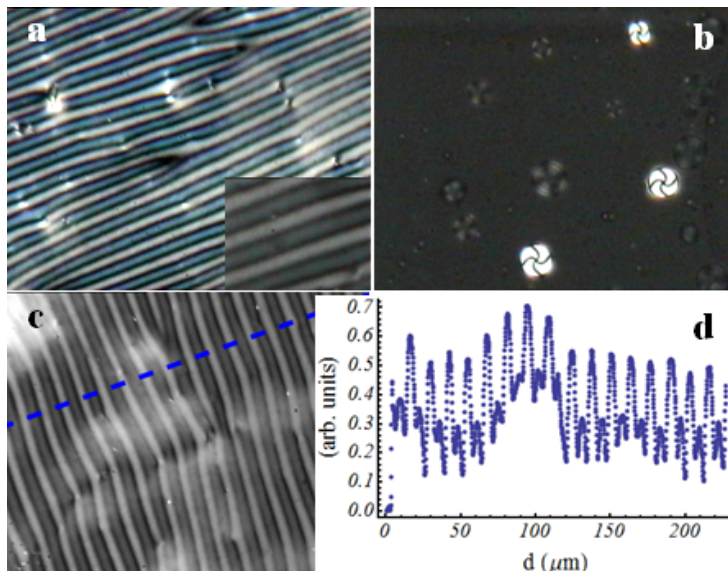


Figure 3.11: POM view of Cytop cell filled with LC solution of complex I at 20%wt. Pictures (a,b,c) were acquired using a 20 \times objective. Inset of (a) is acquired using a 100 \times objective. (d) is the line profile of figure (c) and a “double modulation” is visible. The mean pitch of the cylinders is 14 μm

I and complex II (i.e. 20%wt). Complex I present an initial quasi-perfect planar alignment with some characteristic defects (Schlieren texture), that rapidly disappear in favor of well ordered cylinders, that cover the whole cell. With time, some molecules constituting the cylinders re-organize themselves, maintaining the global external structure but not the internal ones. This reorganization is reflected in the change of cylinder’s color, as observed under POM (fig. 3.11 (a)). After 3 hours, the molecules reorient in the whole cell, reaching an homeotropic alignment. The texture observed is the classical black (maltese cross is clearly visible in conoscopy) with few defects characteristic of this alignment (fig. 3.11 (a) and inset, (b)).

Concerning the temperature cycles (heating up of the cell to 75 $^{\circ}\text{C}$ and consequently cooling down), as observed for the other cells, during the cooling down process, the cylinders appear and cover the whole cell. With time they start to slowly disappear, until the complete reaching of homeotropic configuration in 3 hours. Our explanation is that the organization of the molecules constituting the LC phase during the cooling down process, is responsible of the cylinders optically observed.

Some studies have been carried out in the past on the organization of chromonic mesogens, but the aggregations phenomena were still not well understood [24]. In order to destroy the molecules organization between glasses, we pressed the cell by applying a uni-

form stress. This process cause an immediate change in the texture. In fact, a well ordered planar orientation of the LC solution is observed under POM, but it rapidly changes in favor of cylinders formation. Note that there are no variation in the pitch of the cylinders. After 3 hours, the texture observed is the classic black of the homeotropic anchoring that remains stable in time. On the contrary, complex II, when confined between Cytop treated glasses, present a degenerate planar alignment during the I-N transition (fig.3.12 (a)), but as soon as the LC solution cools down, cylinders similar to the one observed inside PMMA cells, rise. Under POM, seems that the cylinders have two focus, meaning that probably they extend throughout the volume and are anchored to the confining surfaces (fig.3.12 (d)). The presence of cylinders, whose mean pitch in this case is of $25\mu m$ (fig.3.13), co-exists with region characterized by homeotropic orientation of the molecules. With time, the cylinders completely disappear and homeotropic anchoring is reached in the whole cell (3 hours).

3.4 Discussion and Conclusion

A detailed characterization of Ag(I)-bipyridine based complexes has been carried out. We studied the liquid crystals phases of these complexes determining their phase diagrams, performing X-Ray diffraction measurements on their LC phases and finally we tried to align them in both planar and homeotropic configuration for future application in devices. Unfortunately, because the studies on XRD powder spectra are still in progress, we are not able to give the real structure of these compounds, nevertheless some hypothesis are discussed in the following. Concerning the alignment, from our results, we can state that the planar alignment is not straightforward as usually it is, suggesting a discotic-like behaviour for the compounds. Nevertheless the planar alignment of a molecule on a surface represents, normally, the minimum energy configuration, it seems that for these complexes, the $\pi - \pi$ staking between the disks is the driving forces in the alignment process, even in nematic phase. It is worth noting, in fact, that we assembled also cells using different spacers in order to verify if the thickness could influence the alignment. Indeed, the thickness is important since if the value is close to 0, for all phases of both complexes, we observe a degenerate planar alignment, while when the spacers used to assemble the cells are of about 12 microns, the texture observed are the one reported in the experimental section (mostly homeotropic). From the experimental observation seems that when the thickness is comparable to the anchoring length, it is possible to obtain a planar

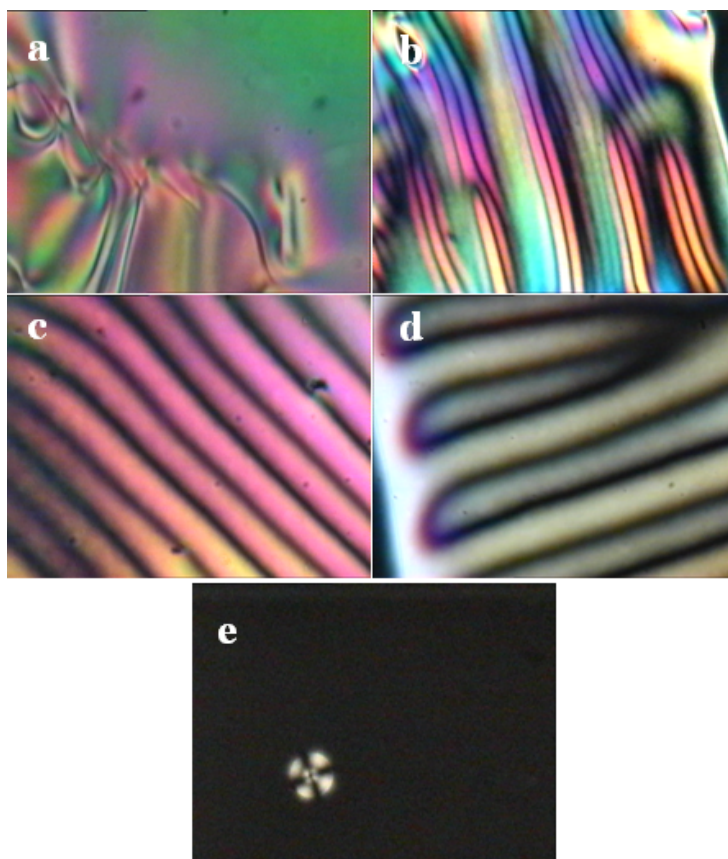


Figure 3.12: POM view of Cytop cell filled with LC solution of complex II at 20%wt. Pictures were acquired using a 5 \times (a,b), 20 \times (c,e) and 100 \times (d) objective. In (a) the initial degenerate planar alignment is visible. After about 20 minutes, a reorientation of the molecules occurs and cylinders start to rise (b) until covering the whole cell. In 3 hours the homeotropic alignment is reached and remains stable for months (e).

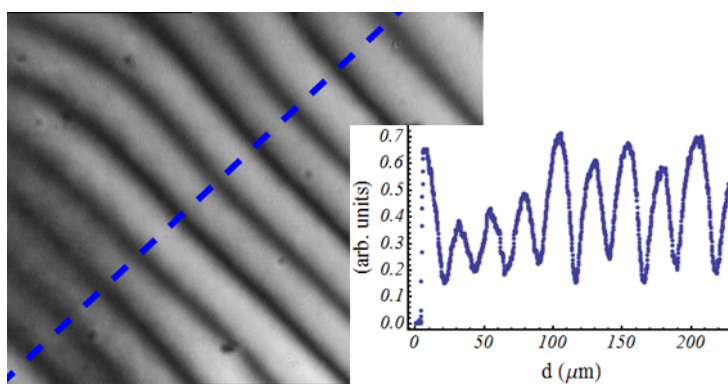


Figure 3.13: Line profile of cylinders in Cytop cell filled with LC solution of complex II at 20%wt. The POM view is a 20 \times magnification and the pitch measured is 25 μm .

configuration of the LC solutions, due to the influence of confining surfaces that restrain the stacking between molecules. As expected, this staking is stronger in hexagonal phase, in fact, even when the LC solution is confined between PMMA treated glasses, that usually promote a planar orientation, the hexagonal phase of complex I immediately organizes in a homeotropic configuration, that remains stable even under thermal treatment. Both nematic phases at 20%wt, when confined between PMMA treated glasses, show, during the cooling down process, the presence of cylinders that cover the cell. These cylinders are well ordered and the pitch of these structures ranges from 14 microns to 25, according to the LC phase used to fill the cell. However, for all cells, the homeotropic anchoring is reached after at least 3 hours. It is worth noting that complex II at 50%wt is in nematic phase, and in the cooling down process, only in a specific range of temperature, presents the characteristic cylinders that appear in the metastable re-orientation of the molecules before reaching the homeotropic alignment. Even for complex II at 20%wt, this reorganization of the molecules occur (data not shown). Concerning low surface energy material, i.e. Cytop treated glasses, we tested the nematic phase of both complexes observing peculiar textures. When nematic phase of complex I is used, the cell, after filling, present a good planar alignment in the whole cell, but after less than a minute, cylinders, with two different colors under POM, rise and cover the surface. The pitch of these cylinders is $14\mu m$. Also for Cytop cells, the final alignment of the LC phase, is the homeotropic one. Differently from complex I, where the starting point is a good planar alignment followed by the rising of cylinders that cover almost all the cell surface, until the reaching of the homeotropic anchoring, for complex II, the cylinders appear after an initial degenerate planar alignment in the I-N coexistence region, that persist for about 20 minutes, before reaching at the end the homeotropic configuration (after 3 hours). In this case, the pitch of the cylinders (about $25\mu m$) is larger than the one observed in the other cells (both Cytop and PMMA), and under POM, seems that they have two focus, meaning that probably they are “anchored” to the surfaces and extend throughout the volume. Another difference is that, differently from the one observed for complex I, these are double in dimensions and present no internal “modulation”, leaving the cell in an homeotropic configuration after three hours, with less defects compared to the texture of complex I. From the observations reported until now, we could infer that for these metal based complexes, the “surface energy rule” works in the opposite way. In fact, unlike the case of DSCG, using high surface energy materials, we were able to obtain only the homeotropic anchoring for the molecules, while with highly hydrophobic surfaces, we were able to disrupt the $\pi - \pi$

stacking between the molecules and to obtain the planar alignment, even if for a very short time. It is really interesting the fact that only inside Cytop cells we observe a good planar alignment, even for a short time, that could be re-induced by applying an external stress onto the cell. Moreover, in Cytop cells, the cylinders have a mean “life-time” longer respect the one in PMMA cells. Probably the antagonistic influence of the alignment dictated by the confining surfaces and the tendency of the molecules to reorganize affect the life time of the cylinders.

Another general observation is the following: we subjected the cell to several temperature cycles (especially to study the rise of cylinders in the cooling down processes) and it was observed that there were no evaporation effects, so the sealing procedure is effective. Moreover we confirmed that the rising of the cylinders is reproducible and there are not memory effects which come into play. This result is very important for us since it means that we found a protocol to follow in order to avoid evaporation effects that drastically cause changes in LC phases and consequently in their alignment, ensuring stability for the devices. However further investigation will be done in order to shed light on the aggregation mechanisms as well as the reorientational ones.

3.5 Use of complex I as intercalating agent in nematic phase of DSCG

As said in the introduction, miscibility studies are fundamental for understanding the structure-properties relationship that guides the organization of biological self-organizing systems. Thus, we decided to study the effect of intercalation of complex I in a well ordered chromonic system, such as DSCG aligned in planar configuration. As shown in chapter one, nematic phase of DSCG is easily aligned in planar configuration using rubbed PMMA treated glass as confining surfaces. Hence, we prepared PMMA cells filling them with the three different mixtures of DSCG and complex I and observed under POM the textures obtained. We prepared three mixtures of Complex I and DSCG as described in the following:

mixture I powder of complex I at a concentration of 8%wt was added into a nematic solution of DSCG.

mixture II two drops ($5\mu\text{l}$ per each) of both nematic phases of complex I and DSCG were deposited directly on rubbed PMMA glass.

mixture III nematic phase of both complex I and DSCG in a percentage of (50:50) were mixed into a vials and allowed to rest for some hours before the use.

The cells, after filling with the solution in isotropic phase, were allowed to rest until complete cooling down at room temperature. During the cooling down process, the texture of the LC solution inside the cell is constantly checked by means of polarized optical microscopy (POM).

3.5.1 Results

The texture observed for the three cells are shown in figure 3.14. For mixture I, as the temperature goes down (I \rightarrow N region), we observe the rising of tactoids, both symmetric and asymmetric (fig. 3.14 (a)), well documented for DSCG nematic phase by other researchers [96]. After 6 hours, the texture inside the cell changes and present a coexistence of classical nematic phase with Schlieren texture and tactoids, where some of them start to be covered by filaments (fig. 3.14 (c)). After 22 hours, the tactoids seen previously, are completely covered by filaments (fig. 3.14 (d)) and the nematic array with Schlieren defects is disappeared.

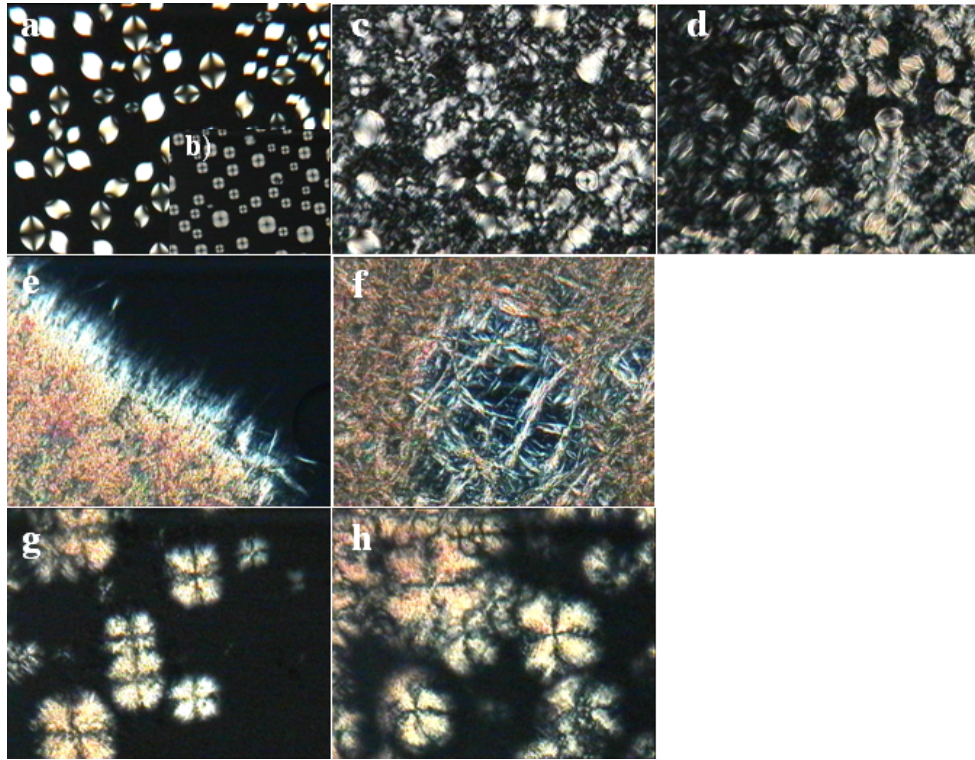


Figure 3.14: POM view of PMMA cell filled with mixture I (a,b,c,d), with mixture II (e,f) and with mixture III (g,h). All images are acquired using a $20\times$ objective. (c) is acquired after 6hours while (d) after 22hours; (f) and (h) are acquired after 2 hours.

Regarding mixture II, i.e. the direct mixing of two drops of both nematic phases, the behaviour observed is quite peculiar. In fact, starting from the point in which the two drops are mixed, a crystallization occur until complete covering of the cell, that is reached in about two hours (fig. 3.14 (e-f)). This behaviour is quite strange, and lead us to verify what happen if the amount of solutions, allowed to stay together, is larger. The last PMMA cell was filled using mixture III. The texture observed consists in an homeotropic alignment, stable in time, of the molecules with some characteristic defects that seems crystallized (fig. 3.14 (g-h)).

3.5.2 Discussion and conclusion

We performed a first step for miscibility studies using a well known chromonic mesogen and our sample as intercalator. From the optical observation we can say that the presents of complex I into nematic phase of DSCG definitively affect the orientation of DSCG

molecules causing the rise of peculiar texture inside the cell. Particularly interesting is the presence of tactoids, well documented in literature, that usually rise during the transition from $I \rightarrow N$ state of DSCG. Indeed we observed both symmetric and asymmetric tactoids in the nematic region that with time, are covered by filaments, probably due to complex I. A common observation is that when complex II is added to nematic solution of DSCG, the final alignment for the mixtures is the homeotropic one instead of the planar configuration, normally obtained for nematic phase of DSCG confined between PMMA treated glasses. This means that, in some way, complex I forces DSCG molecules to align perpendicularly to the confining surfaces. This behaviour is always observed, in fact, for mixture I, after 6 hours we observe a coexistence of tactoids and Schlieren textures, characteristic of nematic phase, but after 22 hrs we observe the rise of filaments that cover tactoids immersed in an homeotropic medium (fig. 3.14 (d)). For mixture III this behaviour is more evident, in fact from the beginning, homeotropic texture with characteristic defects appear in the cell (fig. 3.14 (g)), while for mixture II, before the complete crystallization, there are the presence of both homeotropic medium and crystallized fibers (fig. 3.14 (e)). The rising of filaments should be ascribed to chiral structure. In literature are reported an example of chiral chromonic molecules that present filaments referable to classical cholesteric textures [97]. However, we can conclude that the presence of complex I affect the orientation of DSCG nematic phase modifying its structure. Moreover it forces the molecules to orient perpendicular to the confining surfaces. Probably the interactions between the molecules constituting complex I are stronger than the ones between DSCG molecules, that, as reported in chapter one, are of the order of kcal/mol. Hence, differently from what happened for nematic phase of DSCG confined between PMMA glasses, where the total energy due to the anchoring was three order of magnitude less than that of the salt bridges, the presence of complex I, add to the system enough energy to destroy the planar configuration in favor of the homeotropic one.

3.6 Atomic Force Microscopy investigation on dried LC film

Further investigations are needed in order to obtain deeper understandings of the mechanisms involved in the aggregation of these new complexes and to extrapolate information on their structure. From the alignment studies, it seems that it is easier to achieve an homeotropic anchoring of the molecules instead of the planar one. We assume that the molecules, that probably have a discotic shape, organize in columns thanks also to the $\pi - \pi$ stacking favored by the aromatic cores. Probably the molecules start to aggregate and self-organize in solution. In order to better understand if the organization in columns is due to the interaction with the confining surfaces, or the columns are already formed in solution, we decided to put a drop of LC solution in nematic phase onto a substrate and to observe how the solution organize at the substrate/air interface. The morphology of the “film” produced has been investigated by Atomic Force Microscopy.

3.6.1 Experimental section

As substrate we choose freshly cleaved muscovite mica, because it is an atomically flat substrate and it has a negatively “charged” surface with an hydrophilic character. Complex I present an external counterion positively charged, and exhibits LC phases when dissolved in water, hence the hydrophilic character of the substrate should favor the spreading of LC drop. We prepared two samples: the first, depositing a drop of nematic phase of complex I onto mica, allow it to spread on the surface, wait for one minute in order to favor the attachment of the material on the substrate and rinsed several time with water to wash away the excess of material; the second, leaving a drop of LC solution onto mica and wait until complete drying. Measurements were performed in “Tapping Mode” (see chapter 2 for an explanation of this operating mode) acquiring simultaneously the morphology and the “error signal”.

3.6.2 Results

Form the images acquired for the first sample, we observe that even if the sample was rinsed several times with water, there exist an excess of materials attached on the surface and terrace-like aggregations are also visible. We made a line profile in order to obtain information on the height of these terraces and we interpret the data acquired as “single”

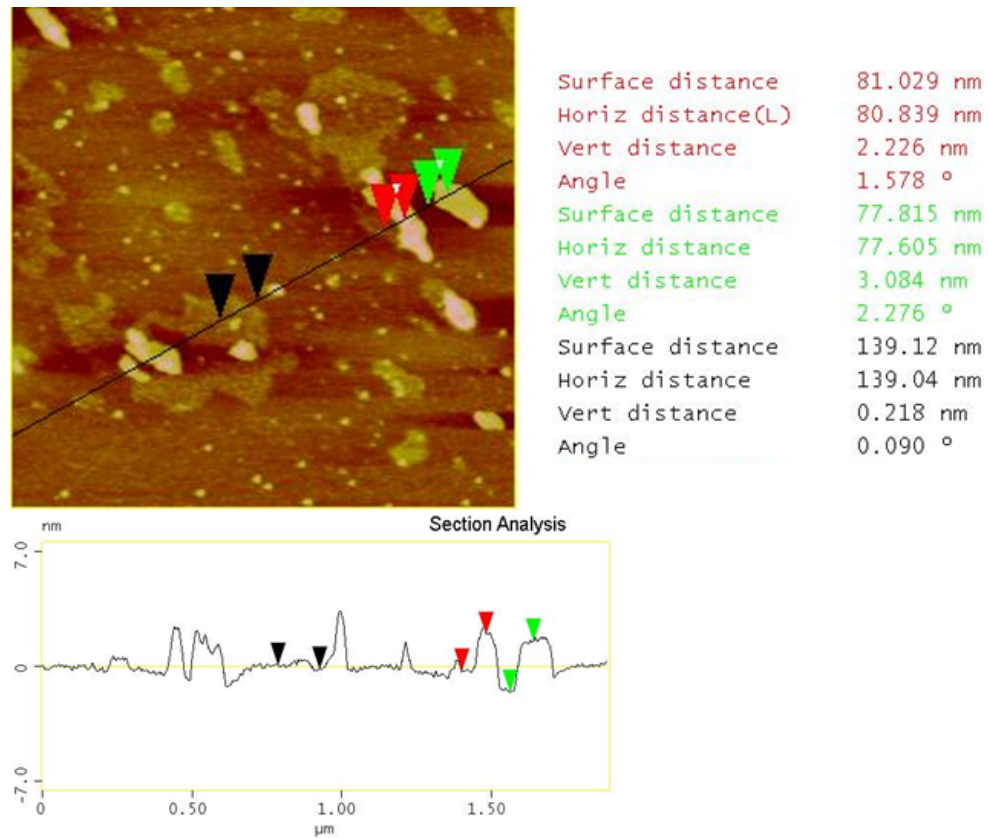


Figure 3.15: AFM topographic image and line profile of the first sample prepared depositing a drop of complex I nematic phase onto a mica substrate, followed by several rinsing with Millipore water.

and multi layers of molecule. In fact, the height of these aggregates ranges from 0.20nm , that we suppose to be only one molecule layer, to 3nm (fig. 3.15).

In figure 3.16 is shown the topography of the second sample, prepared leaving the drop of nematic phase of complex I at the air interface. As visible in the images larger and well defined terraces are formed (fig. 3.16 (A)) compared to the previous ones. Moreover, the vertical spacing of the terraces ranges from 1.4nm to 1.7nm (fig. 3.16 (B)), smaller than that of the aggregate with an height of 3nm . In figure 3.17 is reported the “signal error image”, i.e. the representation of the variation in amplitude oscillation of the cantilever from the pre-set value, obtained when the feedback circuit is operative. In other words, is an image that sometimes emphasize the presence of particular structures on sample’s surface, not completely clear in the topographic image, because of several effects. In our case, these images give us the possibility to observe that the terraces are more or less equally spaced in vertical direction and well ordered.

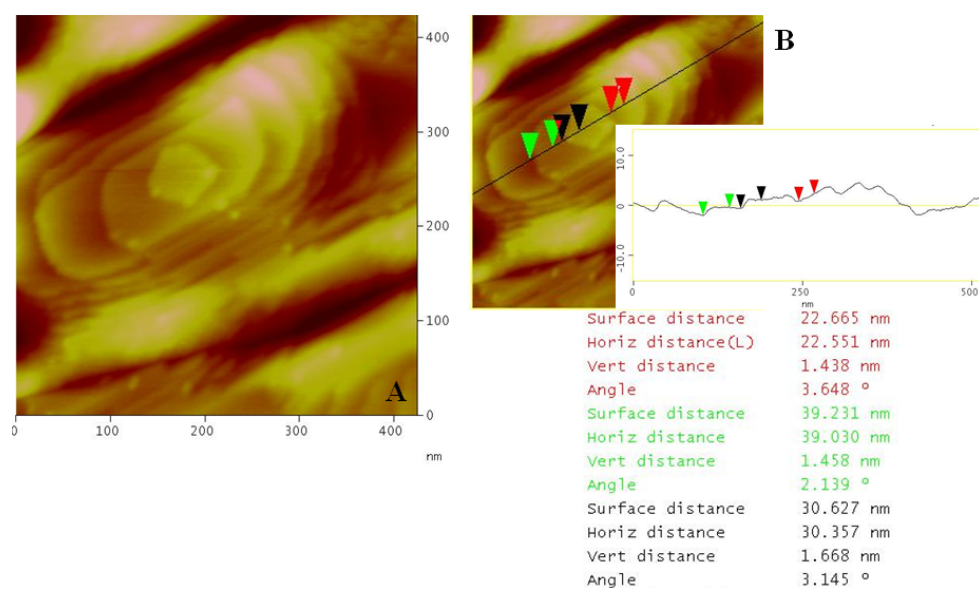


Figure 3.16: AFM topographic image (on the left) and line profile (on the right) of the second sample prepared depositing a drop of complex I nematic phase onto mica and waiting until complete drying.

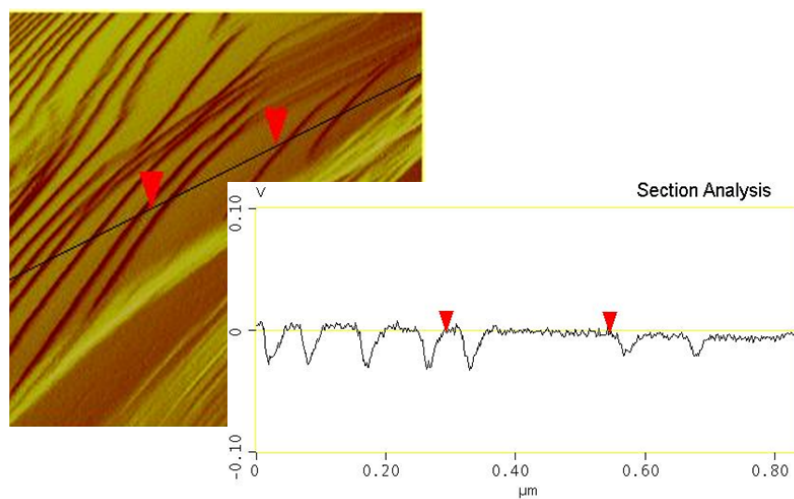


Figure 3.17: “Signal Error” image of a different place of the sample reported in 3.16. The terraces here are more or less equally spaced as visible from the line profile of the image.

3.6.3 Conclusion

In conclusion, we report on several experiments carried out in order to verify the hypothesized structure for Complex I and II. A common feature is the formation of terraces, that indicates a tendency of the molecules to stack into columns. Even if it is not possible to compare the values obtained from AFM analysis with crystallographic data, we can say that the aggregation of this molecules, for sure, starts in solution and create ordered structures. This tendency of the molecules to stack one on another is strong, and cause a reorientation also of the other molecules mixed in solution with this complexes (DSCG). More studies will be done in order to better understand the mechanisms of aggregation and to solve the real structure of these compounds. The biological activity of complex I on G-quadruplex is currently under investigation but the first results are promising.

Chapter 4

Liquid Crystal Based Biosensors: Study of the interactions between protein decorated LC interfaces and phospholipids

Studies on interactions of proteins with lipids are the area of fundamental interest due to enormous biological importance. The interest in biosensor devices is tremendously increased in recent years and the research is always focused in finding low cost raw materials with high efficiency: liquid crystals, thanks to their high sensitivity to the external conditions, represent the best candidate. In this chapter, starting from the results found in literature, we report our studies on the effect of phospholipids on protein decorated liquid crystal interfaces by means of optical microscopy and FT-IR measurements. The first technique allow us to observe the response of decorated LC film when exposed to phospholipids vesicles, while the second, give us insight on conformational changes involved in secondary structure of the protein in function of the time of interaction between protein and LC, and the pH of the surrounding environment. The results obtained show a new methods to report specific binding of vesicles on protein decorated interfaces.

4.1 Introduction

In the past two decades, the biological and medical fields have seen great advances in the development of biosensors and biochips capable of characterizing and quantifying biomolecules. From the biotechnological and biomedical applications point of view, studies on lipids and proteins have been playing a significant role in developing protocols for drug delivery and immunosensing system, various biomolecular devices etc. Recent studies demonstrated that it is possible to report biomolecular interactions at phospholipid laden interfaces between thermotropic LCs and aqueous phases and to trigger ordering transitions in thermotropic liquid crystals by absorbing amphiphiles and polymers at the interface between nematic LC and immiscible aqueous phase. The approach revolves around the assembly of phospholipids at interfaces between aqueous phases and micrometer thick films of thermotropic liquid crystals [98]. Brake et al. demonstrate that the presence of phospholipids at the interface of the liquid crystals (LC) led to well defined orientations of the LC and that specific binding and enzymatic activity of proteins at these lipid-laden interfaces triggered orientational transitions in the LC. Past studies reported the transfer of phospholipids from aqueous dispersion of vesicles to interfaces to be a complex process that depends on a number of parameters, including the type of interface [99], vesicles size and concentration [100], phase state of the lipid [101], and solution conditions such as pH and ionic strength [102]. In recent years, the assembly of synthetic surfactants and biological lipids at aqueous-LC interfaces attracted the interest of many researchers for the possible application as biosensor. The ordering of LCs at these aqueous interfaces is fundamentally different from the ordering at solid interfaces, because the mobility of molecules is high at the aqueous interface and the interface is deformable. Because one side of the interface is an aqueous phase, the LC-aqueous interface enables investigations of the influence of biomolecular interactions on the ordering of LCs. A variety of approaches have been used to create LC-aqueous interfaces for investigations of interfacial phenomena, including planar interfaces created by stabilizing films of LCs in microfabricated structures (such as TEM grids, microwells, and micropillar systems). In addition, recent studies have shown that LC-aqueous interfaces formed by the emulsification of LCs within an aqueous phase are also promising for fundamental studies of the influence of confinement on the ordering of LCs. An example of the system used to prepare stable LC-aqueous interfaces is shown in fig. 4.1. The approach uses a metallic grid (TEM grid) supported on a chemically functionalized solid surface to form a stable LC film with a thickness that

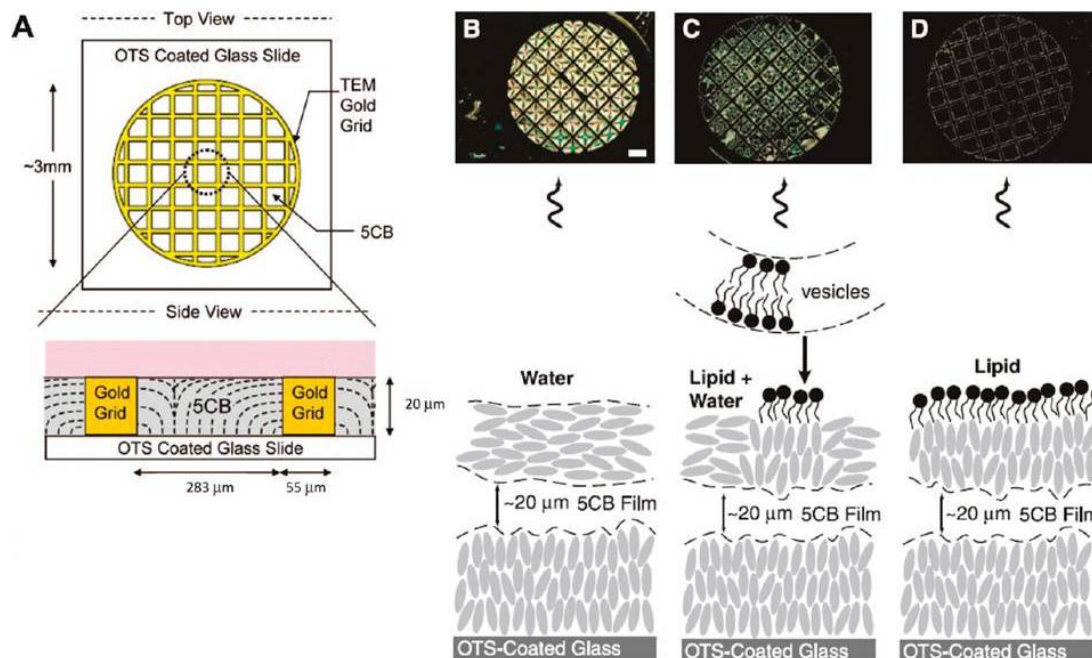


Figure 4.1: (A) Schematic illustration of an experimental system that can be used to create stable LC-aqueous interfaces. (B) Optical image and cartoon representation of the anchoring of 5CB and the state of the aqueous-5CB interface immediately after the injection of a dispersion of vesicles formed from 0.1 mM L-DLPC in tris-buffered saline (TBS) (aqueous 10 mM Tris, 100 mM NaCl, pH 8.9). The optical image above the cartoon shows the transmission of polarized light (cross polars) through 5CB. The scale bar is $200\mu\text{m}$. (C) Optical image and cartoon representation of the anchoring of 5CB after 10 to 20 min of contact with the dispersion of L-DLPC vesicles. (D) Optical image and cartoon representation of the anchoring of 5CB after 2 h of contact with the dispersion of L-DLPC vesicles.

[103]

is controlled by the metallic grid. The underlying solid surface is treated to define the orientation of the LC on the bottom surface [104]. For example, surfaces treated with octadecyltrichlorosilane (OTS) or dimethyloctadecyl - [3-(trimethoxysilyl)propyl] ammonium chloride (DMOAP) will give rise to homeotropic anchoring [105], whereas SAMs formed from hexadecanethiol (C_{16}) and many other alkanethiols on gold films will give rise to a planar orientation of the easy axis of the LC. The pores of the grid provide a mechanically stable support for the LC and prevent dewetting phenomena. The pores are filled with LC thanks to capillary forces, then the supported LC film is immersed in an aqueous solution to create an approximately flat LC-aqueous interface. In the illustration shown in Figure 4.1, the director of the LC is shown. At the bottom of the LC film, inside one square of the grid, the director of the LC is perpendicular to the surface

(homeotropic alignment on OTS), and on the top surface, the LC shows an orientation parallel to the interface. Here we note that common LCs such as 5CB and E7 exhibit an easy axis that is parallel to the aqueous-LC interface (where E7 is a nematic LC consisting of a mixture of four alkylcyanobiphenyls with different aliphatic chain lengths). Figure 4.1 (B-D) shows optical micrographs (cross polars) of ordering transitions induced in films of nematic 5CB by the adsorption of lipid L-R-dilauroyl phosphatidylcholine (L-DLPC) at the LC-aqueous interface [104]. In the absence of adsorbed lipids, the LC exhibits a bright optical appearance, consistent with degenerate planar anchoring of the LC at the aqueous interface (see discussion above). The first indication of the influence of adsorbed lipid on the ordering of the LC is the appearance of dark domains in the LC. These dark regions correspond to areas of the LC-aqueous interface at which the LC has adopted a perpendicular orientation [104]. A number of observations (including observations based on the use of fluorescence microscopy to image DLPC doped with fluorescently labeled lipid Texas red dihexadecanoyl phosphatidylethanolamine (TRDHPE)) indicates that the domains of homeotropically anchored LC correspond to lipid-rich areas (i.e., lipid domains) at the interface [106].

In this work we concentrate on the interactions of phospholipids with protein-decorated interfaces of LC. In past studies, specific binding of phospholipid vesicles to protein attached at the surfaces of solids [107, 108] has been investigated, but in this work, the LC interface on which the protein are adsorbed, is deformable and mobile [109, 110]. We investigate how the competitive interactions of protein and phospholipids at LC interfaces influence the ordering of LCs. Differently from previous published work, where the ordering transition of LC were studied using fresh and aged protein as decorative elements for LC interfaces, we adopt another approach, leaving the fresh protein on LC surface for long incubation time (6, 24, and 48hrs) and observing the optical response. In order to better understand the phenomena involved in the interaction at protein-liquid crystal interface, we performed also FT-IR measurement on LC droplet-protein emulsion. FT-IR is a technique widely used to investigate an infrared spectrum of absorption, emission, photoconductivity or Raman scattering of a solid, liquid or gas. In particular we used FT-IR to study changes in protein conformation. The information gained from FT-IR has been used to strengthen the optical observations. Moreover, it is worth noting that the choice of β -lactoglobulin (BLG) as protein to decorate the LC interface is not trivial. Amyloid aggregation, the self-assembly of proteins in nano-fibrils stabilized by cross-b interactions, has long been associated with neurodegenerative disorders such as Alzheimer's,

Parkinson's, Huntington's and Creutzfeldt–Jakob diseases [111]. The discovery of (non-pathological) functional roles of amyloid fibrils in biological processes [112, 113] has also opened a new perspective in materials science and nanotechnology: creating functional nanostructured materials from the amyloid linear self-assembly of 'design' proteins and polypeptide units [114]. BLG has been extensively studied owing to its abundance in cow milk whey, ease of purification, making it an ideal 'building block' for studying the general molecular mechanisms underlying amyloid aggregation. BLG consists of 162 amino acid residues, with a molecular weight of about 18 kDa and a globular shape with a radius of about 1.5 nm [115].

4.2 Experimental Section

4.2.1 Materials

1,2-Dilauroyl-sn-glycero-3-phosphocholine (DLPC) was purchased from Avant Polar Lipids, Inc. (Alabaster, AL). 2-Propanol and Fisher's Finest Premium grade glass slides were purchased from Fisher Scientific (Pittsburgh, PA). Beta lactoglobuline (BLG), octyl-trichlorosilane (OTS), deuterium chloride, mono and dibasic sodium phosphate were obtained from Sigma Aldrich (St Louis, MO). Gold specimen grids ($20\mu m$ thickness, $283\mu m$ grid spacing, and $50\mu m$ bar width) were obtained from Electron Microscopy Sciences (Fort Washington, PA). The nematic LC 4'-pentyl-4-cyanobiphenyl (5CB) was obtained from EMD Chemicals (Spring Valley, NY). Deionization of a distilled water source was performed with a Milli-Q system (Millipore, Bedford, MA) to give water with a resistivity of $18.2M\Omega cm$.

4.2.2 Methods

Preparation of Protein-5CB droplet emulsion for FTIR

BLG were dissolved at 1%wt/v in DCl phosphate buffer at two different pH (5 and 7). Protein solutions were allowed to stand for 5 minutes in order to guarantee a complete solvation in the buffer. After this time, 5CB, in a concentration of 40%wt/v, was added to protein solution. Five cycles, each comprising 30 seconds of vortex mixing (at 3000 rpm), yielded milky white emulsions.

Preparation of Protein-Decorated Interfaces of Nematic 5CB

A detailed description of the method used to prepare micrometer-thick films of LC hosted within gold specimen grids can be found in previous work from Abbot's group [110]. Briefly, glass microscope slides were cleaned according to published procedures and coated with OTS. Gold specimen grids were placed onto the surface of the OTS-treated glass slides. The grids were filled with 5CB using a blunt-tipped glass syringe and the excess LC was removed such that the grid was uniformly filled with LC. The quality of the OTS layer was assessed by checking the alignment of a film of 5CB confined between OTS-treated glass and air. The LC-impregnated grid supported on an OTS-treated glass slide was immersed in a dish of deionized water. Formation of an adsorbed layer of protein on the interface of the LC was accomplished by introducing a solution of BLG (1%wt in DCl-sodium phosphate buffer, at pH 5 and 7) into the deionized water in contact with the interface of 5CB. The interface of the LC was incubated against the protein solution for three different incubation time, 6hrs, 24hrs and 48hrs for both pH solutions, 5 and 7. At the end of the equilibration period, free BLG in the bulk aqueous solution was removed by sequential exchange or dilution of the aqueous phase with deionized water.

Preparation of Phospholipid Vesicles

Dispersions of vesicles of phospholipid were prepared using methods previously published [116]. Briefly, DLPC (dissolved in chloroform) was dispensed into glass vials. The solution was dried under a stream of nitrogen to remove the chloroform and the vial containing the phospholipids was placed under vacuum for at least 1 h. The dried lipid was resuspended in an aqueous solution of sodium phosphate buffer and then extruded several times through a polycarbonate membrane filter (pore size of 100 nm) (Millipore, Bedford, MA). The above described procedure yielded unilamellar vesicles with an average diameter of 120 nm, as determined using dynamic light scattering (DLS) [107]. All phospholipid dispersions were used within 24 hours of their preparation.

Interactions of Phospholipid Vesicles with Protein-Decorated Interfaces of 5CB

After formation of protein-decorated aqueous LC interfaces (as described above), an aliquot of a dispersion of phospholipid was added to the aqueous phase. The LC-filled grids were incubated against the dispersion of vesicles and the orientation of the nematic film of 5CB was then optically characterized according to the methods described in the

dedicated section.

Optical Characterization of LC Ordering

The orientation of 5CB was examined by using plane-polarized light in transmission mode on an Olympus BX60 microscope with crossed polarizers. The gold grid hosting the film of 5CB was placed on a rotating stage located between polarizers. In-plane birefringence was determined by rotating the stage by 45° and observing modulation in the intensity of transmitted light. Homeotropic alignments were determined by first observing no transmission of light over a 360° rotation of the stage. Insertion of a condenser below the stage and a Bertrand lens above the stage allowed conoscopic examination of the cell. An interference pattern consisting of two crossed isogyres indicated homeotropic alignment. The camera was set to a f-stop of 2.8 and a shutter speed of 1/60 s.

Determination of the Tilt of 5CB at the Aqueous-LC Interface

The color of the LC under white-light illumination was matched against a Michel-Levy chart to determine the effective birefringence Δn_{eff} of the $20\mu m$ thick film of 5CB. For each value of Δn_{eff} , the tilt angle of 5CB at the aqueous-LC interface (measured relative to the surface normal), θ , was determined solving of the equation

$$\Delta n_{eff} \approx \left(\frac{1}{d}\right) \int_0^d \left(\frac{n_{\parallel} n_{\perp}}{\sqrt{n_{\perp}^2 \sin^2 \left(\frac{z}{d}\right) \theta + n_{\parallel}^2 \cos^2 \left(\frac{z}{d}\right) \theta}} - n_{\parallel} \right) dz. \quad (4.1)$$

where n_{\parallel} and n_{\perp} are the refraction indices parallel and perpendicular to the optical axis of 5 CB, respectively (at $\lambda = 632nm$ at $25^\circ C$ ($n_o = 1.711$ and $n_e = 1.5296$)[117]), and d is the thickness of the LC film. The tilt angles reported in this work are an average of nine different random locations for each of the two independent grids.

FT-IR measurements and analysis

To investigate the conformational changes in the secondary structure of the protein after its adsorption at LC-aqueous interface, we recorded FT-IR spectra of protein solutions in pure buffer and of the emulsions with liquid crystal droplets. FT-IR provides some insight into the conformation of BLG and the spectra acquired with this technique allow semi-qualitative analysis. This technique gives valuable information at the molecular level by

analyzing the so-called amide I region of the infrared spectra, whose vibrations originate from the amide vibrations of the peptide bonds (mainly the C=O stretching vibration). The segments of protein adopt secondary structures which differ in the geometry and hydrogen bond strength. Consequently the secondary structures of a protein give rise to vibrations located at specific wavenumbers [118]. However, since they are very close to each other, they have to be separated by mathematical treatments such as a second derivative or a Fourier self deconvolution. The study reported here concentrate on the second derivative spectra of FT-IR absorption in the amide I region. We prepare a series of samples at different pH (5 and 7) and with different incubation time for protein at the LC droplet interface (6, 24 and 48 hours). Each emulsion was centrifuged (at 12000rpm for 45 min) before the FT-IR measurement in order to investigate both the LC-protein rich phase (or cream phase) and the bulk. The FT-IR spectra of cream phase and bulk were compared with the FT-IR spectra of the protein in the pure buffer in order to verify the presence of some differences in protein structure due to the interaction with the LC. To avoid the problem of absorption bands arising from H_2O in the FT-IR spectra, which would obscure the amide I bands of the protein, we adopted the general practice of dissolving freeze-dried protein in 20mM phosphate buffer, prepared using Na_2HPO_4 , D_2O and DCl, at both pH 5 and 7. Infrared spectra at $2cm^{-1}$ resolution were recorded with a Magna 560 Nicolet spectrometer (Madison,WI) equipped with a nitrogen cooled mercury-cadmium-telluride (MCT) detector. The spectrometer was continuously purged under a N_2 continuous flux. Samples were placed between two CaF_2 windows separated by $12\mu m$ teflon spacers. Each spectrum is the result of an average of 128 scan. The study of the amide I region of the protein (the so-called amide I in D_2O), were performed with the software Omnic, given by the producer of the instrument. Before all experiment, we collected the spectra of the empty cell, in order to subtract its contribution during final data analysis. Second derivative spectra were calculated using an home made program in *Mathematica*.

4.3 Results

4.3.1 Orientational transitions in 5CB protein decorated interfaces

Preliminary studies on incubation of the LC interface against a dispersion of vesicles of DLPC showed, in absence of proteins bound at the LC interface, the nucleation and growth

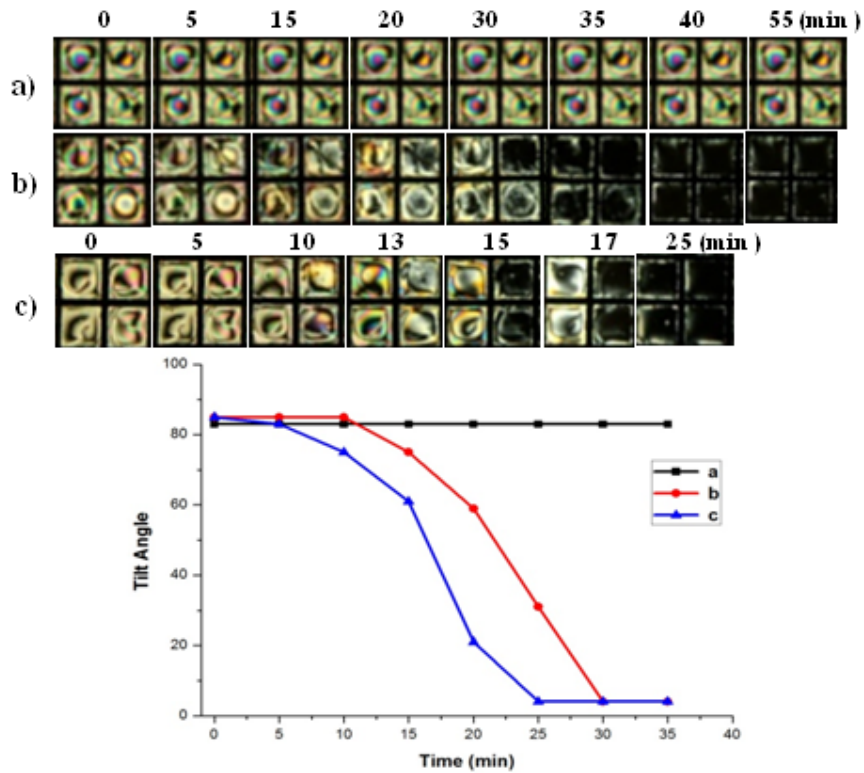


Figure 4.2: Optical images (crossed polarizers) of the ordering transition induced in films of nematic 5CB protein-decorated aqueous interfaces against incubation of DLPC vesicles (0.1mM (a), 0.2mM (b) and 0.3mM (c)). Protein incubation time of 6hrs at $pH \sim 5$. (d) Tilt angle of 5CB at the aqueous-LC interface, plotted as a function of time following incubation against dispersion on vesicles.

of dark domains. These domains correspond to regions with homeotropic anchoring of the LC, a result of fusion of vesicles with the interface of the LC and transfer of phospholipid onto the LC interface [104]. In our experiment, according to the concentration of DLPC vesicles solutions tested (i.e. 0.1mM, 0.2mM and 0.3mM) a uniform dark appearance of the LC interface against the dispersion of DLPC was achieved after 20 minutes, for the lower DLPC vesicles concentration, up to 10 minutes for the highest (data not shown). Moreover, each dark square in the grid is framed by a bright edge (as we will report in the following images). The bright edge is the result of perpendicular anchoring of the LC on the vertical walls of the grid. We present the results according to the protein incubation time at the liquid crystal-water interfaces, for the two pH values. Incubation of β -lactoglobulin decorated interfaces against a dispersion of DLPC vesicles (6 hours incubation time) resulted in a slow but continuous progression of interference colors (fig.

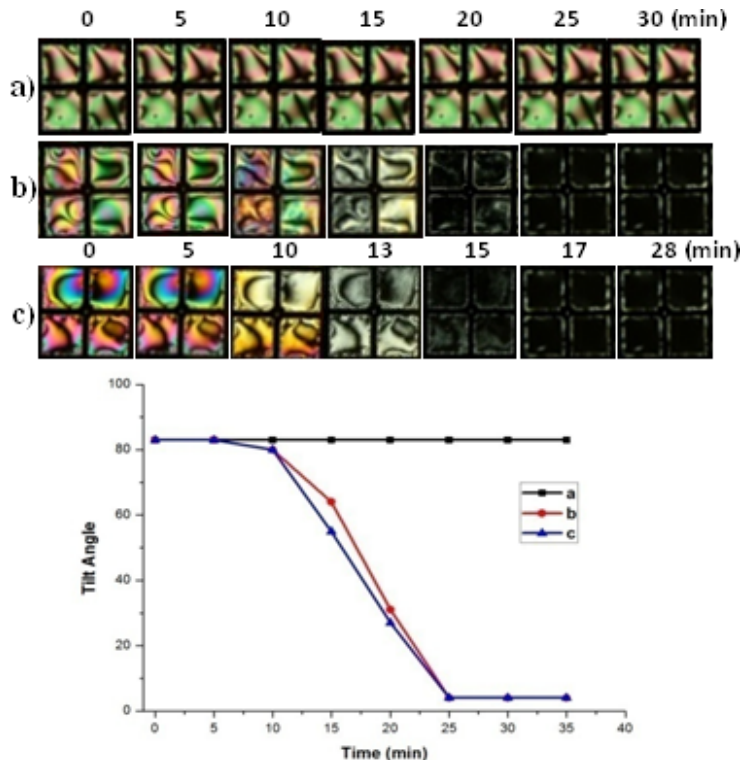


Figure 4.3: Optical images (crossed polarizers) of the ordering transition induced in films of nematic 5CB protein-decorated aqueous interfaces against incubation of DLPC vesicles (0.1mM (a), 0.2mM (b) and 0.3mM (c)). Protein incubation time of 6hrs at $pH \sim 7$. (d) Tilt angle of 5CB at the aqueous-LC interface, plotted as a function of time following incubation against dispersion on vesicles.

4.2), a consequence of a continuous change in the tilt of the LC at the aqueous-5CB interfaces over >20 minutes (fig. 4.2 (b,c)).

At $pH \sim 7$, instead, the transition starts about 15 min after exposure against vesicles dispersion (fig. 4.3 (b)). This change in the tilt angle is not observed when the decorated LC interfaces is exposed to 0.1mM concentrations of DLPC vesicles for both pH.

Since the LC assumes a planar orientation at a protein decorated interface (fig. 4.2 first images of a,b,c) whereas phospholipids at the interface induces a homeotropic orientation (fig. 4.2 black squares), we interpret the tilting of LC as the competitive influence of proteins and phospholipids at the interface on the LC [107]. As reported in recent work from Abbott's group, it is possible to observe that the dynamics of the continuous transition in the orientations of LC are accelerated in presence of modified vesicles with specific binding enzymes [116]. To quantify the difference in the orientations of the LC induced by the interactions of the vesicles, the interference colors generated by the LC

under white light illumination, were used to determine the tilt of the LC at the aqueous interface as a function of time. It is visible that change in the tilt of LC is slightly faster for $pH \sim 7$. From the observation it is possible to infer two important conclusion: first, the presence of β -lactoglobulin adsorbed at the LC interface does not prevent but retards phospholipids adsorption relative to the protein-free interface of the LC (from < 10 min to > 30 min); second, in contrast to the protein-free interface of LC, for which the LC ordering transition was discontinuous with the appearance of micrometer-sized domains of patterned LC, the LC ordering transition induced by phospholipids in the presence of interfacial protein was continuous. This continuous tilting of the LC orientations hints that the presence of the protein on the LC interface limits the size of the phospholipids domains to suboptical sizes.

4.3.2 Effect of aged protein adsorbed at the LC interface

Past studies have demonstrated that the interfacial shear viscosity of a protein film increases with age due to conformational changes and physical cross-linking of protein on the interface [119]. In additions, it is well documented in literature that adsorbed layer of aged proteins, produce interfacial elastic films that are displaced only by application of large external surface pressure. Our hypothesis, is that aging of the beta-lactoglobulin would produce a state of adsorbed protein that would be less readily displaced by phospholipids, resulting in a slower/retarded ordering transition of the LC. To test this hypothesis, we incubated the aqueous-5CB interface against a 1%wt solution of β -lactoglobulin at $pH \sim 5$ and 7 for 24 and 48 hours. After this time, the samples was rinsed at the interface, in order to wash away the protein not bounded to LC surface and then exposed to a dispersion of vesicles as in the previous experiment. The optical observations are reported in Figures 4.4 and 4.5.

After 24 hours of protein incubation at LC interface we observe the reordering of LC molecules also when the film is exposed to the lower concentration of DLPC vesicles (0.1 mM). The transition time from planar to homeotropic anchoring is comparable and in some case equal to the one observed after 6 hours of incubation. Nevertheless it is worth noting that at $pH7$ the transition to homeotropic configuration is slightly accelerated and in the optical images, bright objects start to rise.

The appearance of “objects” becomes more important when the protein incubation time at LC interface is increased up to 48 hours. In fact, in this case, we observe “filaments”

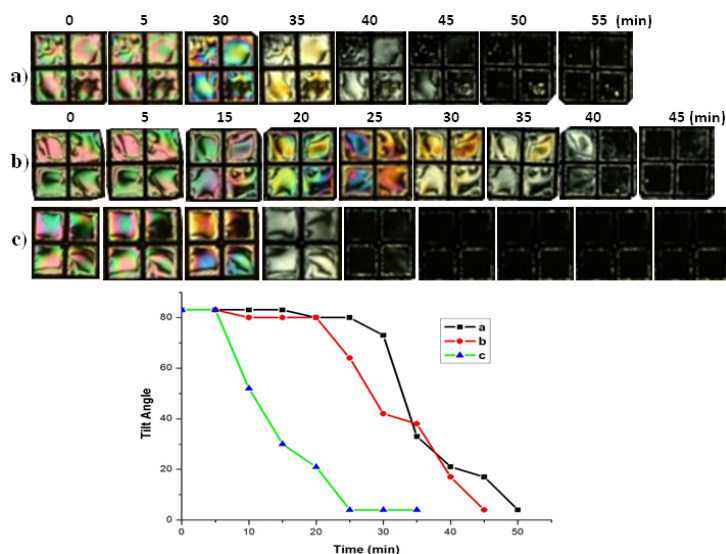


Figure 4.4: Optical images (crossed polarizers) of the ordering transition induced in films of nematic 5CB protein-decorated aqueous interfaces against incubation of DLPC vesicles (0.1mM (a), 0.2mM (b) and 0.3mM (c)). Protein incubation time of 24hrs at $pH \sim 5$. (d) Tilt angle of 5CB at the aqueous-LC interface, plotted as a function of time following incubation against dispersion on vesicles.

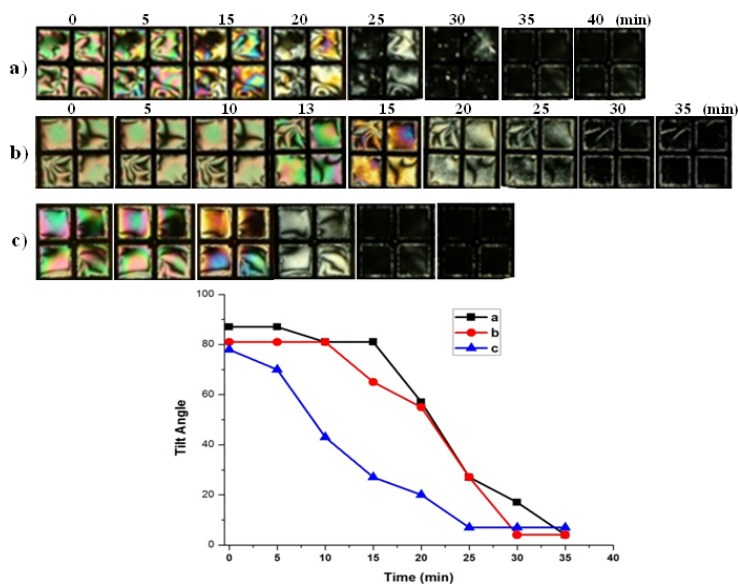


Figure 4.5: Optical images (crossed polarizers) of the ordering transition induced in films of nematic 5CB protein-decorated aqueous interfaces against incubation of DLPC vesicles (0.1mM (a), 0.2mM (b) and 0.3mM (c)). Protein incubation time of 24hrs at $pH \sim 7$. (d) Tilt angle of 5CB at the aqueous-LC interface, plotted as a function of time following incubation against dispersion on vesicles.

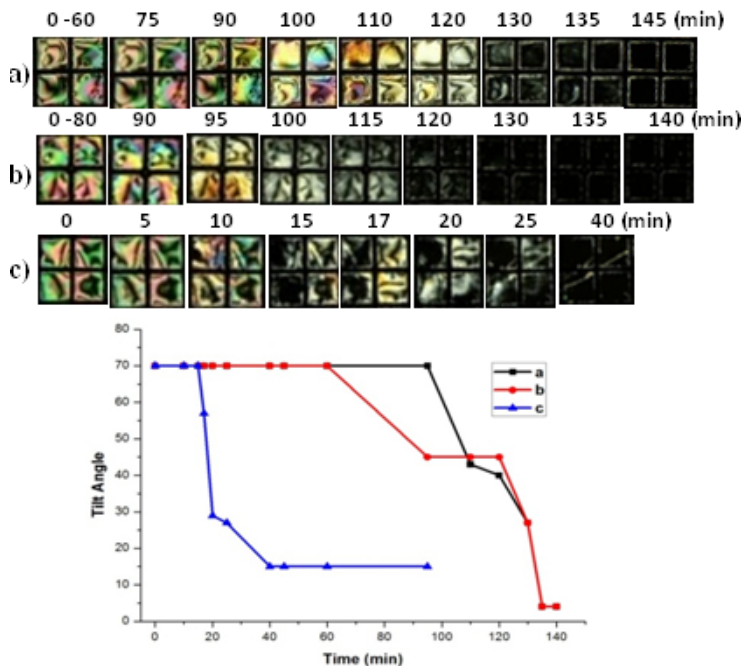


Figure 4.6: Optical images (crossed polarizers) of the ordering transition induced in films of nematic 5CB protein-decorated aqueous interfaces against incubation of DLPC vesicles (0.1mM (a), 0.2mM (b) and 0.3mM (c)). Protein incubation time of 48hrs at $pH \sim 5$. (d) Tilt angle of 5CB at the aqueous-LC interface, plotted as a function of time following incubation against dispersion on vesicles.

(especially at pH7) that we hypothesize to be fibrils of β -lactoglobulin, indicating a strong denaturation of the protein and consequently aggregation, probably due to hydrophobic interaction between protein and LC and protein-protein itself fig. 4.7.

In some case (fig. 4.6) the LC ordering transition induced by the presence of vesicles at the interface was accelerated increasing β -lactoglobulin interfacial density. This result is, at first sight, seemingly contradictory of the above-described hypothesis. As mentioned above, unfolding of proteins permits intermolecular interactions between neighboring proteins, as well as stronger adsorption of proteins to the interface [120]. Thus, we interpret the results described above, to suggest that the ordering transition of 5CB induced by binding of vesicles to the LC interface is accelerated at high interfacial densities of β -lactoglobulin due to either weaker inter-protein associations and/or weaker adsorption of the proteins onto the LC interface, both of which permit facile displacement of proteins from the interface by phospholipids. This interpretation is consistent also with the above-noted effects of aging of the proteins on the LC interface. However, if the presence of protein aggregation is important, we observe two different behaviour related to the pH of

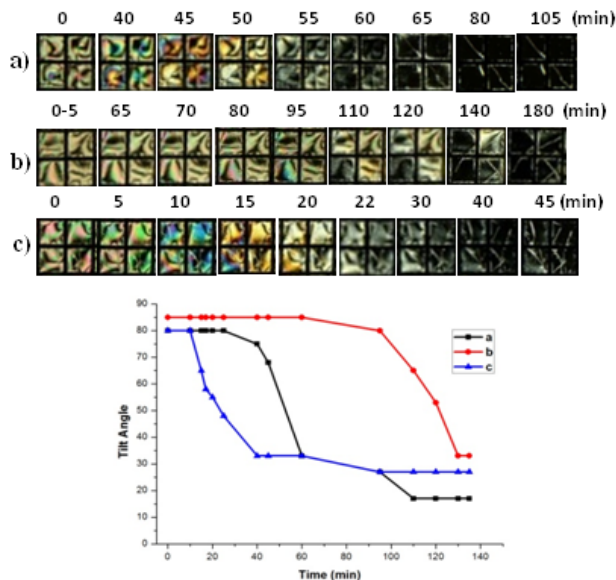


Figure 4.7: Optical images (crossed polarizers) of the ordering transition induced in films of nematic 5CB protein-decorated aqueous interfaces against incubation of DLPC vesicles (0.1mM (a), 0.2mM (b) and 0.3mM (c)). Protein incubation time of 48hrs at $pH \sim 7$. (d) Tilt angle of 5CB at the aqueous-LC interface, plotted as a function of time following incubation against dispersion on vesicles.

the aqueous interface. After 48 hours of protein incubation at the LC interface, the time needed to the LC molecules to reorient when exposed to phospholipid vesicles is tremendously increased at pH5, even if there are no protein aggregation at the interface (fig. 4.6 (a-b)) while in presence of protein aggregation, the characteristic reorientation time is comparable to the previous (about 40 minutes to reach the homeotropic alignment). At pH7, instead, the presence of protein aggregations is important and cover almost all the grid (fig. 4.7 and fig. 4.13). In this case, the characteristic transition time ranges from 10 to 45 minutes (i.e. the begin of reorientation of LC molecules at the interface), from the higher vesicles concentration to the lower. However it should be noticed that the time needed to completely reorient the LC molecules, in some case, increase up to 3 hours for both pH values.

4.3.3 FT-IR measurements

As noticed in the previous section, the aim of this work was to better understand the interaction between protein and liquid crystals and to figure out which kind of conformational changes could be induced in the protein due to the long time contact with LC and

Table 4.1: Band assignments in the FT-IR Spectra of β -lactoglobulin

<i>Wavelength (cm^{-1})</i>	<i>Assignment</i>
1622	<i>β-Sheet (exposed or intermolecular)</i>
1632	<i>β-Sheet (antiparallel)</i>
1637	<i>Intramolecular β-Sheet</i>
1645	<i>Unordered</i>
1649	<i>α-Helix</i>
1678	<i>β-Sheet</i>
1682	<i>Intermolecular β turns, bends</i>
1694	<i>β-Structures</i>

how these modifications could influence the reorientation of LC molecules when exposed to phospholipids. A powerful instrument that allows us to investigate the conformational changes in protein secondary structure is an FT-IR spectrometer. As described in the methods section, we investigate different 5CB droplet emulsion and compare the spectra focusing on the modification in second derivative of the Amide I region. In the following, are reported the second derivative spectra of both cream phase (LC-protein rich phase) and bulk. This spectra is compared with the spectra of amide I region of β -lactoglobulin recorded in the pure buffer.

Secondary structure of β -lactoglobulin adsorbed at LC-water interface at pH7

The spectrum of native BLG in the buffer at pH7 consists of two major bands at 1632 and 1622 cm^{-1} , which are thought to arise from β -sheet structures [121]. The band at 1678 cm^{-1} together with the band at 1632 cm^{-1} demonstrates the presence of antiparallel β -sheet, while the band at 1649 cm^{-1} has been assigned to the α -helix [121]. The band at 1645 cm^{-1} , usually assigned to unordered structure is small in this spectrum (fig. 4.8, fig. 4.10). The spectrum of "freshly" adsorbed protein at the LC interface, i.e. 6 hours of incubation time with 5CB droplets, is different from that of the native protein with a noticeable decrease in the band 1622 cm^{-1} , an increase in the overlap of the bands at 1632 and 1622 cm^{-1} , and an increase in the band appearing at 1682 cm^{-1} , possibly from increased intermolecular β -structures [122] or from an increased contribution from turns and bends [123]. It is worth noting that, two important bands rise at 1603 and 1610 cm^{-1} , assigned to residue side chain vibrations, not present in the spectra of native protein, for

both pH. Despite these changes, the structure of the protein remain well defined, i.e.the secondary structure is not totally lost(fig. 4.8). The spectrum after 24 and 48 hours have noticeable different characteristics. There is a large increase of the band at 1645cm^{-1} from unordered structure, and the two bands at 1622 and 1632cm^{-1} shift to 1624 and 1634cm^{-1} become much less separated from one another. The band of the α helix was affected by the adsorption of the protein. This surface denaturation is similar to the initial stage of heat denaturation characterized by an increase in the unordered structure and an increasing in the overlap of the β -sheet absorption bands at 1622cm^{-1} and 1632cm^{-1} [121]. These two bands altered in relative intensity, both with adsorption and with the age of the emulsions. Since these bands are associated with β -structures, this suggest that the structure of the β -barrel of the protein is progressively altered as the emulsion ages. It is noticeable also an increasing in the size of the band at 1682cm^{-1} meaning an increase in intermolecular β structures or from the contributions of bends. After 48 hours the spectra dramatically change: the band at 1635cm^{-1} decreases, but remains visible, while the band related to α helix, strongly decreases in the intensity. Other peaks related to segments connecting alpha helices rise, meaning that a modification in the structure occurred [121]. Moreover, an important band at 1694cm^{-1} that is assigned to β type structures, probably related to the fibrillation of the protein, as observed by optical microscope [124], appears. The slow alteration of the conformation of β -lactoglobulin on the LC-water interface correlates well with the optical observation reported above. The FT-IR results showed that the protein unfolds after being adsorbed to the interface, but there was still residual β -sheet structure present. The α helix after 48 hours is still present but the signal dramatically decreased in intensity meaning that the adsorption at the interface may did not require the completely unfold of the α -helix but certainly drastically modified it. However, simulation studies on the conformational changes involved in β -lactoglobulin secondary structure in presence of 5CB, show that the protein, tends to open and expose the α helix. ¹

Secondary structure of β -lactoglobulin adsorbed at LC-water interface at pH5

The structure of pure β -lactoglobulin at pH5 is very similar to that at pH7 except for some bands attributed to *beta*-sheet structures that are shifted to higher value, from 1632

¹The tendency of the protein to open its structure at high pH is a well known phenomena called Tanford transition. In simulation, this behaviour is visible at pH7, when the protein, whose structure could be imaged as a chalice, tends to open exposing the α helix that becomes more flexible (private communication regarding an ongoing work).

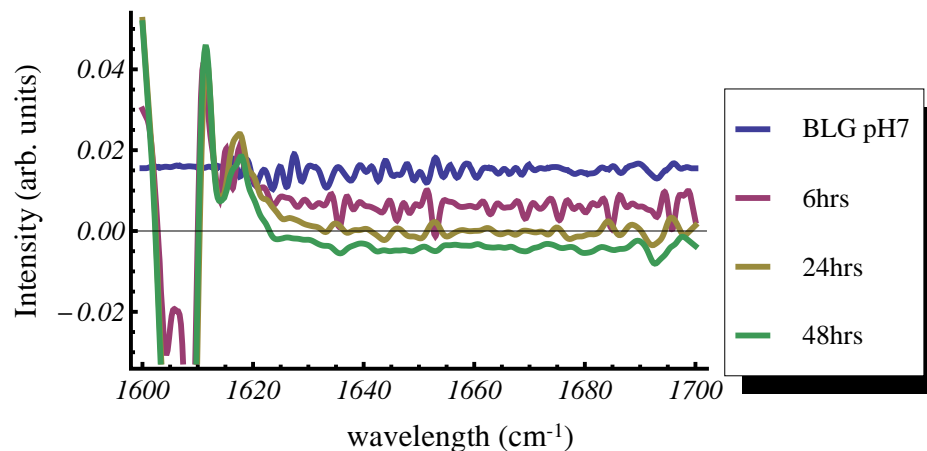


Figure 4.8: Second derivative FT-IR spectra of 5CB- β -lactoglobulin emulsion in the region of Amide I ($1600-1700\text{ cm}^{-1}$). Spectra of BLG in pure buffer at pH7 is reported in the blue line. The spectra of the cream phase after 6, 24 and 48 hours are respectively represented with the magenta, olive and green lines.

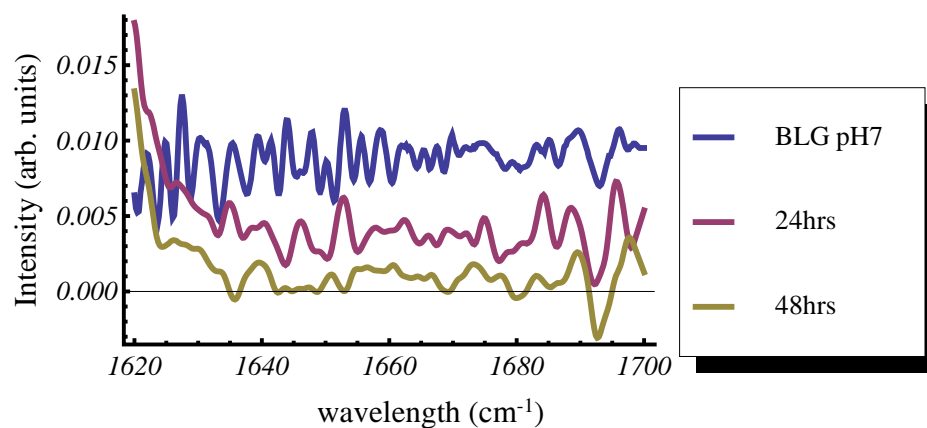


Figure 4.9: Particular of second derivative FT-IR spectra of 5CB- β -lactoglobulin emulsion in the region ($1620-1700\text{ cm}^{-1}$). Blue, magenta and olive lines are respectively the spectra of β -lactoglobulin in pure buffer at pH7 and the cream phase after 24 and 48 hours).

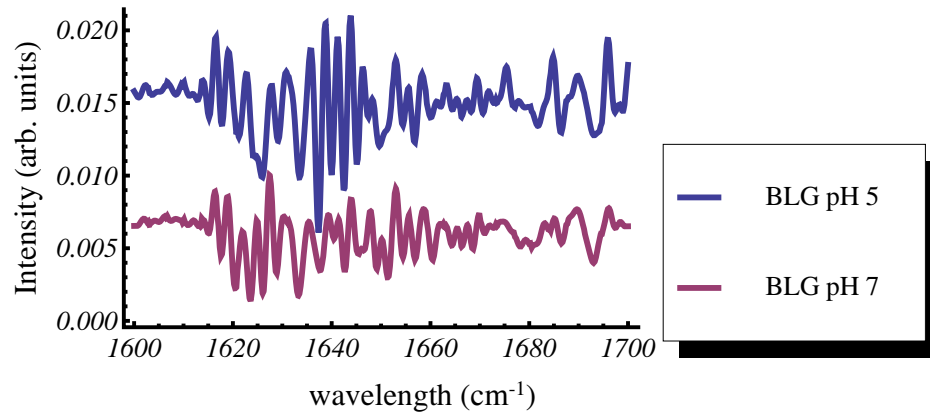


Figure 4.10: Second derivative spectra FT-IR of β -lactoglobulin in pure buffer at pH5 and 7 in the region of Amide I ($1600\text{-}1700\text{ cm}^{-1}$).

and 1622cm^{-1} at pH7 to 1634 and 1624cm^{-1} and there is an overlap at 1624cm^{-1} and at 1678cm^{-1} for the β sheet. The band assigned to the α helix is more defined at pH5 and a contribution from intermolecular β -sheet and bends appear at 1684cm^{-1} . Thus, the un-adsorbed protein appear to possess similar but not identical structures at pH5 and 7, but, when adsorbed at LC-water interface, the protein structures at the two pH values are different. The denaturation of β lactoglobulin at pH7 occurred faster and resulted in a larger proportion of unordered structures. It seems that at pH5 it is necessary to wait 48hours before seeing differences in the spectra. After 24 hours in fact, we observe only an overlap in β structures 1658cm^{-1} and the rise of bands related to antiparallel β -sheet (1688 cm^{-1}). Even at pH5, after 48 hours, there is the rise in the spectra of the band related to β type structures, but, differently from pH7, it is not important as in the previous spectra. The difference in the structures of adsorbed β lactoglobulin lies in the extent of denaturation and in the much larger amount of unordered structure and possibly intermolecular β -sheet structure found in β lactoglobulin adsorbed at pH7 and 5. It is possible that different parts of the molecule are active in the adsorption on the interface according to the pH of the aqueous environment. In fact, considering the optical observation, even after 48 hours of incubation time of protein at LC-aqueous interface, at pH5 the presence of fibrils is not so important as in the case of pH7, where, the huge covering of fibrils at LC interface, in some case, restrain the transition of LC molecules when exposed to phospholipid vesicles.

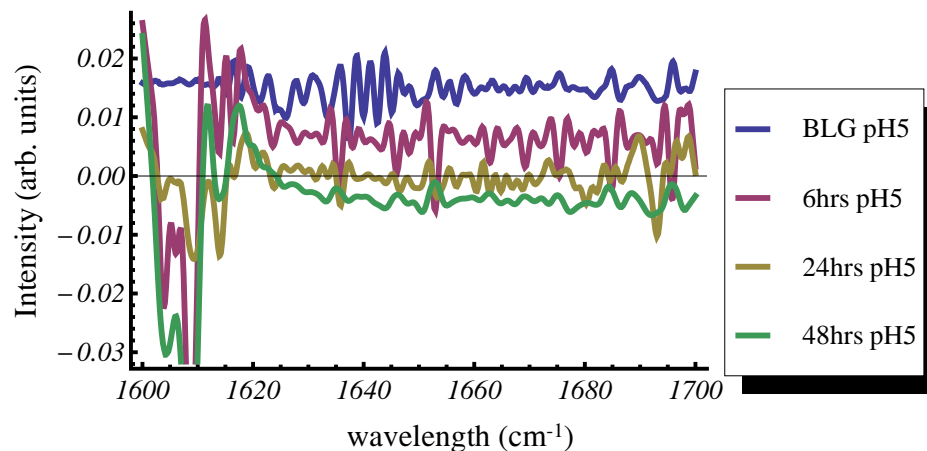


Figure 4.11: Second derivative FT-IR spectra of 5CB- β -lactoglobulin emulsion in the region of Amide I (1600-1700 cm^{-1}). Spectra of BLG in pure buffer at pH5 is reported in the blue line. The spectra of the cream phase after 6, 24 and 48 hours are respectively represented with the magenta, olive and green lines.

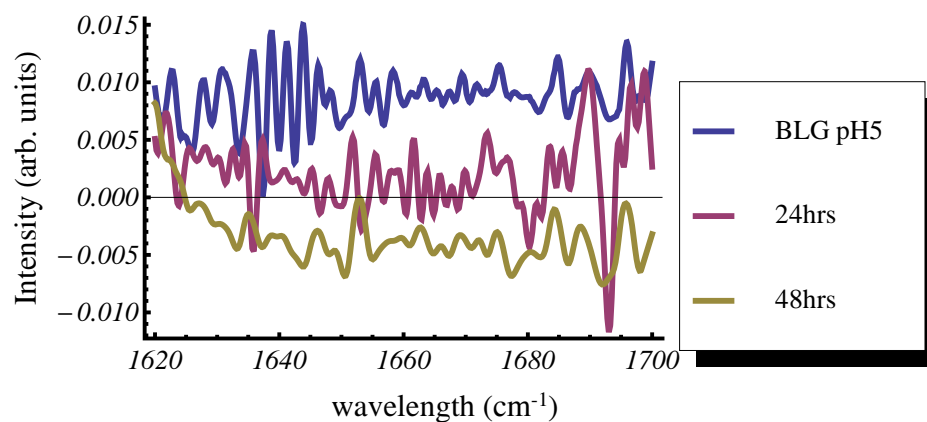


Figure 4.12: Particular of second derivative FT-IR spectra of 5CB- β -lactoglobulin emulsion in the region (1620-1700 cm^{-1}). Blue, magenta and olive lines are respectively the spectra of β -lactoglobulin in pure buffer at pH5 and the cream phase after 24 and 48 hours).

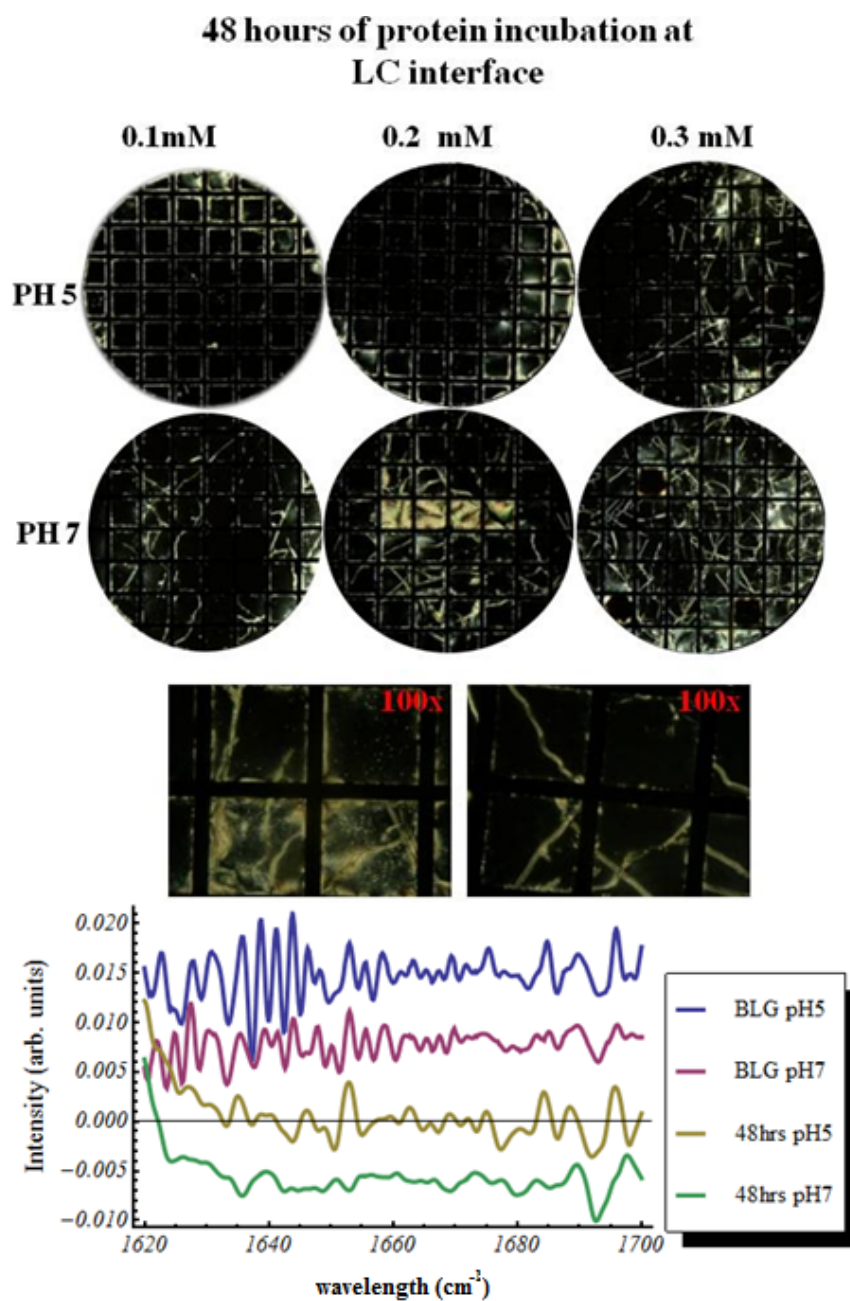


Figure 4.13: POM images (20 \times magnification) of TEM grid with the LC-protein decorated films at aqueous interface of both pH5 and 7 after 48 hours of incubation time. Magnification at 100 \times of the fibrils present at LC-aqueous interface at pH5 (right) and pH7 (left). Graphic of the second derivative FT-IR spectra at pH5 and pH7 in pure buffer compared to the spectra of cream phase after 48 hours incubation of the protein-LC emulsion.

4.3.4 Discussion and conclusion

For simplicity we will divide the discussion into two parts: the first part focuses on the discussion on the optical observation and the second focuses on FT-IR measurements. One key finding from the optical observation is that the antagonistic influence of adsorbed proteins and phospholipids on the orientational ordering of LCs gives rise to continuous ordering transitions in LCs. These findings are significant in the light of the previous studies. Specifically, Brake and co-workers showed that when a monolayer of phospholipid (containing 2 mol% biotinylated lipid) was formed at an aqueous-LC interface by fusion of vesicles and subsequently exposed to a solution of neutravidin, micrometer-scale domains comprised of segregated proteins and lipids were observed at the LC interface [104]. This segregation of species led to patterned orientations of the LC. Furthermore, de Tercero et al. demonstrated that nonspecific interactions of proteins with interfaces of 5CB decorated with partial monolayer of DLPC also led to formation of micrometer-sized, patterned domains of LC, consistent with penetration of the protein into the lipid-laden interface (and segregation of the species at the interface) [125]. In contrast to these past studies, the interaction of vesicles with protein-decorated LC interfaces, does not lead to micrometer-scale, lateral segregation of phospholipids and proteins leading to domains of either planar or homeotropic ordering of LCs. Instead, the continuous tilting of the LC observed in these experiments suggests a physical picture where phospholipids and proteins form sub-optical domains. The above-described interpretation of the continuous ordering transition is inspired by previous studies in which are reported that heterogeneous interfaces comprised of nanoscopic patches, that cause homeotropic or planar anchoring of LCs, can give rise to micrometer-scale tilting of the molecules. The pattern of local surface-imposed orientations of the LC becomes homogeneous in the bulk of the LC in order to minimize the elastic energy of the LC (by relaxing the discontinuity in the director field near the alignment layer). In contrast, a mixture of two species, one of which causes homeotropic alignment and the other causes planar alignment, if mixed homogeneously at the molecular level, will not give rise to tilted states of the LC. That is, for a molecularly mixed alignment layer, the change from planar to homeotropic alignment (or vice versa) occurs in a discontinuous manner [126, 127]. For example, Bos and co-workers demonstrated that a homeotropic alignment layer, when deposited as a continuous film over a first layer that causes planar anchoring of a LC, leads to a discontinuous transition of the orientation of the LC from planar to homeotropic as the thickness of the top layer is increased [128]. In contrast, when the overlayer causing homeotropic alignment of the LC formed

a discontinuous film, a continuous transition in orientation of the LC was observed with increasing coverage of the surface by the top layer [128]. The observation of a continuous change in the tilt of the LC is, therefore, consistent with an inhomogeneous LC interface comprised of nanodomains of proteins and phospholipids. Many studies have reported that proteins undergo conformational changes upon adsorption to interfaces [129]. For example, at hydrophobic interfaces, proteins expose their hydrophobic (interior) amino acid residues to maximize interactions of these residues with the hydrophobic interfaces. This restructuring (denaturation) of the protein can promote cross-linking of proteins on the interface and the formation of a cohesive gel-network [130]. Of particular relevance to our studies, Mackie and co-workers have shown that surfactant-driven displacement of a protein film becomes increasingly difficult with increasing age of the protein film [131]. The extent of conformational change of the proteins is also affected by the degree of crowding of proteins at interfaces: The lower the interfacial density of proteins, the more space proteins have to spread and unfold to maximize their interactions with the interface [132]. For example, Norde and coworkers have demonstrated that the α -helix content of serum albumin decreases along with the surface coverage [133]. Our observation that LC ordering transitions induced by specific capture of vesicles is influenced by both aging and crowding of proteins at the interface, suggests that the conformational state of the proteins at the LC interface is a central factor underlying these LC ordering transitions. We interpret our results to suggest that the LC ordering transitions involve at least two key processes. The first process involves the accumulation of phospholipid near the interfacial region of the LC via specific binding of the vesicles to the protein decorated interface. The second process is the phospholipid driven displacement of the proteins from the LC interface. Protein films that are difficult to displace impede incorporation of lipids into the interface of the LC [131]. At this point, the FT-IR measurements help us to give more insight in the nature of the interaction that involves at the LC interface. There is a strong correlation between FT-IR measurements and optical observation. The phenomena optically observed are confirmed by the FT-IR spectra: with time, the protein at the LC interface unfold, but the differences in secondary structure are different for the two pH buffer solution. At pH7, the transition to a more unfolded state of the protein is much faster than at pH5, and the protein almost completely unfold, giving rise to structure, called β -type structure, probably due to the fibrillation of the protein (also observed in the POM images). The presence of these structures is confirmed in FT-IR spectra, where a large band at 1694cm^{-1} , (more important in the spectra acquired at pH7), rises, probably because of the increasing in

the hydrophobic interactions. Instead, for the emulsion at pH5, important changes in the spectra start to be visible after 24 and in particular 48 hours. Also this behaviour is in agreement with optical observations. The fibrillation of the protein occur also at pH5, but it is not so important as for pH7. In conclusion, the study of the interfaces between LCs and aqueous solutions, when decorated with proteins, permit to observe in an amplified way, specific binding events involving vesicles into orientational transitions in the LC. The ordering transition reflects the competitive interactions of the interfacial proteins and phospholipids with the LCs. Our results reveal that the LC ordering transition is influenced by aging and crowding of interfacial proteins. Both effects are consistent with the proposition that the state of the protein adsorbed onto the LC interface influences the ease of displacement of the proteins from the interface by phospholipids, a process that seems necessary for the LC ordering transition to be observed. Finally, the increase in hydrophobic interaction between the unfolded protein and the LC molecules, in particular condition (the change of pH), leads to the formation of protein fibrils, that are clearly visible under optical microscope and whose presence, cause a restrain the LC molecules' orientation. Overall, the results showed offers the basis of a novel tool for fundamental studies of proteins and amphiphiles at interfaces and, specifically, they offer new methods to report specific binding of vesicles on protein decorated interfaces.

Chapter 5

Conclusion and Perspectives

In this work we have analyzed some properties related to the phenomena involved at the interfaces between liquid crystals and biomolecules, which offer a wide range of potential technological applications and represent an important field for fundamental research. The work reported in this thesis is just a small contribution to the fascinating world of Science. The first part of the thesis was concerned with the study of the effect of different confining surfaces on the alignment of a special class of lyotropic liquid crystals, called “chromonics”, which, in addition to their LC properties, are bio-compatible. Our main goal was to achieve, without the help of external field, a stable in time alignment of LC phases of DSCG, that should be obtained using the properties of the alignments layer and avoiding the water evaporation, that causes drastic change in LC phase. In the first chapter we demonstrated the role of confining surfaces’ surface energy in the alignment of a particular chromonic liquid crystal, disodium chromoglycate (DSCG), showing how it is possible to control both planar and homeotropic anchoring of its LC nematic phase in confined geometry, exploiting alignment layers with high surface energy (for the planar alignment) or low surface energy (for the homeotropic one). Hence, we give a general rule to follow for other chromonic mesogens alignment. For the first time in the literature, we reported a stable-in-time homeotropic alignment [1], achieved using highly hydrophobic surfaces and tested also the use of plasma treatment on these hydrophobic surfaces in order to observe the effects. In particular this point is interesting because it should be useful to create confining surfaces with both hydrophilic and hydrophobic pattern that give the possibility to obtain, in the same device, pattern of planar and homeotropic region of LC phases for application in photonics. With the knowledge acquired in the alignment of DSCG, we focused our attention on the alignment of DNA and its bases for applica-

tion in biophotonic devices. It is well known that in the last years the interest in DNA based devices experienced huge growth. The main problem, however, is to obtain large domain of well ordered periodic structure, comparable with the visible light wavelength. The fabrication of periodic structures in polymeric slices represents a low cost procedure and the use of anisotropic soft biocompatible materials, which combine fluidity and self assembly properties, allows the optical control of the built up devices [64, 63]. Because of the difficulties encountered in aligning long chains of oligonucleotides into stable structures without means of prefabricated structure, we focused our interest on the alignment of a particular nucleotide, guanosine and its derivatives, as a preliminary case of study. The second chapter of this thesis reports our efforts on the studies of the alignment of guanosine LC solutions, achieved using the properties of the confining surfaces, varying the concentration of nucleotides in water and the effect of cations in LC solutions. We observed that if ionic and/or silver doped solution are added to the LC guanosine phases, it is possible to control the pitch of the cholesteric phase, modifying the helix structure. Moreover, we observed the formation of micrometer guanosine vesicles when the LC phase was confined between two hydrophobic surfaces. Differently from what reported in literature [3, 4, 5], we observed the formation of guanosine vesicles, starting from pure solution of guanosine monophosphate instead of alkylsilylated guanosine derivatives. Our interpretation for the rise of these vesicles is that, the silicon present in the alignment layer (PDMS), helps in the formation a well ordered guanosine lamella, that cover the isotropic guanosine bubbles. The presence of these vesicles are enhanced when the LC solution used to fill the cell, is silver doped. From the studies reported in literature, the presence of silver ions favor the formation of dimers instead of tetramers in guanosine solutions. This, combined with the properties of the alignment layer, should drive the formation of ordered lamella that cover guanosine bubbles. Finally, we demonstrated that guanosine monophosphate in pre-cholesteric and cholesteric liquid crystals phases were perfectly aligned homeotropically, without means of external magnetic fields, as reported in the past [72]. Concerning the planar alignment, that as previously said is the “hot topic”, we showed that long “fiber-like” structures could be aligned on a micrometer scale (20 microns). This represent an important result, however further investigation are necessary in order to deeply understand the alignment mechanism. Indeed, our efforts are directed at improving and/or finding new materials in order to increase the scale of the alignment. A short paragraph is devoted to an initial work focused on the formation of G-wires in a Langmuir trough and their interaction with potential anticancer drugs synthesized at Chemistry Department

of University of Calabria. Then, remaining within the framework of lyotropic chromonic liquid crystals, we characterized newly synthesized metal based chromonic compounds, with promising application as anticancer drugs. We performed X-Ray Diffraction measurements (XRD) on both powder and LC phases, phase diagrams of their LC phases and, for possible future application in devices, we studied also their alignment, finding that the “general rule” that worked for DSCG and DNA is not valid. The reason could be ascribed to the “structure” of these compounds. In fact, the $\pi - \pi$ interaction between the aromatic cores of the molecules, lead them to stack into columns and this stacking seems to be more effective than the alignment imposed by the confining surfaces. Indeed, we were able to align LC phases of these compounds perfectly in homeotropic configuration. However, from the experimental observation we can infer that when the thickness is comparable to the anchoring length, it is possible to obtain a planar configuration of the molecules, due to the influence of confining surfaces that restrains the stacking between molecules. In order to verify the goodness of the alignment, we subjected all the cells to several temperature cycles and the behaviour of the LC phases, when they are cooled down from isotropic state to room temperature is quite interesting. Whatever polymer is used as alignment layer, we observed the rising of well ordered cylinders, anchored to both surfaces, meaning that these cylinders extend through the volume. Moreover we observed that the nature of the confining surfaces affect the cylinders “life-time”. Even though we do not know the real structure of the compound (analysis on XRD spectra is currently going on), from the experimental observations, we hypothesize a possible structure and a schematic view of how the molecules organize in order to stack into columns. In order to overcome the lack of information and to strengthen the idea of the stacking, we performed AFM analysis on LC films deposited on mica. Even from this experiment, we observe the tendency of the LC phase to create terraces more or less equally spaced. However more investigation should be done in order to better understand the aggregation mechanisms, that could also explain the presence of cylinders, now interpreted as the results of molecules’ reorientation. Moreover, the anticancer properties of these compounds are still under investigation and the preliminary results are promising, giving good hopes for their use as intercalating agents in G-quadruplex. Following the field of application of liquid crystals to bio-inspired devices, we focused our attention on LC based biosensors, that use thermotropic LC as a probe. From the biotechnological and biomedical applications point of view, studies on interactions of proteins with lipids are the area of fundamental interest due to enormous biological importance. The interest in biosensor devices is tremendously

increased in recent years and the research is always focused in finding low cost raw materials with high efficiency: liquid crystals, thanks to their high sensitivity to the external conditions, represent the best candidate. It has been demonstrated that aqueous interface of LC has an instantaneous response when exposed to phospholipids [98]. This is a good base to study the interaction between biomolecules using LC as probe. Starting from the results found in literature, we studied the effect of phospholipids on protein decorated liquid crystal interfaces by means of optical microscopy and FT-IR measurements. The first technique allow us to observe the response of decorated LC film when exposed to phospholipids vesicles, while the second, give us insight on conformational changes involved in secondary structure of the protein in function of the time of interaction between protein and LC, and the pH of the surrounding environment. The study of the interfaces between LCs and aqueous solutions, when decorated with proteins, allows to observe in an amplified way, specific binding events involving vesicles into orientational transitions in the LC. The ordering transition reflects the competitive interactions of the interfacial proteins and phospholipids with the LCs. Our results reveal that the LC ordering transition is influenced by aging and crowding of interfacial proteins. Both effects are consistent with the proposition that the state of the protein adsorbed onto the LC interface influences the ease of displacement of the proteins from the interface by phospholipids, a process that seems necessary for the LC ordering transition to be observed. Finally, the increase in hydrophobic interaction between the unfolded protein and the LC molecules, in particular condition (the change of pH), leads to the formation of protein fibrils, that are clearly visible under optical microscope and whose presence, cause a restrain the LC molecules' orientation. The results obtained show a new methods to report specific binding of vesicles on protein decorated interfaces. In conclusion, we succeeded in aligning chromonic phases of different mesogens and materials by using confining surfaces with specific properties. The evaporation phenomena were eliminated, ensuring stability in the alignment of liquid crystalline phase and resistance to the devices. Moreover, a general rule to follow for the alignment of chromonic mesogens has been given as well as an explanation of mesogens behaviour inside the cell. Regarding the findings on LC based biosensor, we can state that the study of protein decorated liquid crystal - water interfaces, allows to observe in an amplified way, specific binding events involving vesicles into orientational transitions in the LC, offering the basis of a novel tool for fundamental studies of proteins and amphiphiles at interfaces and, specifically, they offer new methods to report specific binding of vesicles on protein decorated interfaces.

Bibliography

- [1] C. M. Tone, M. P. De Santo, M. G. Buonomenna, G. Golemme and F. Ciuchi, *Soft Matter* **8**, 8478 (2012).
- [2] C. M. Tone, M. P. De Santo and F. Ciuchi, *Molecular Crystals and Liquid Crystals* **576**, 2 (2013).
- [3] I. Yoshikawa, J. Sawayama and K. Araki, *Angew.Chem.* **120**, 1054 (2008).
- [4] H. Sakaino, J. Sawayama, S. Kabashima, I. Yoshikawa and K. Araki, *J.Am.Chem.Soc.* **134**, 15684 (2012).
- [5] J. Sawayama, H. Sakaino, S. Kabashima, I. Yoshikawa and K. Araki, *Langmuir* **27**, 8653 (2011).
- [6] P. Collings and M. Hird, *Introduction to Liquid Crystals* (Taylor & Francis, London, 1997).
- [7] P. Collings, *Liquid Crystals: Nature's Delicate State of Matter* (Princeton University Press, Princeton, 1990).
- [8] F. Reinitzer, *Monatshefte fur Chemie* **3**, 752 (1883).
- [9] P. De Gennes and J. Prost., *The Physics of Liquid Crystals* (Oxford University Press, Oxford, 1993).
- [10] A. Jakli and A. Saupe, *One and Two-Dimensional Fluids: Properties of Smectic, Lamellar, and Columnar Liquid Crystals* (Taylor and Francis, Boca Raton, FL, 2006).
- [11] T. Attwood, J. Lydon and F. Jones, *Liq. Cryst.* **1**, 499 (1986).

-
- [12] T. Attwood, J. Lydon, C. Hall and G. Tiddy, *Liq. Cryst.* **7**, 657 (1990).
- [13] J. Lydon, *Curr. Opin. Colloid Interface Sci.* **3**, 458 (1998).
- [14] N. Hartshorne and G. Woodard, *Mol. Cryst. Liq. Cryst.* **23**, 343 (1973).
- [15] V. Horowitz, L. Janowitz, A. Modic, P. A. Heiney and P. J. Collings, *Phys. Rev. E* **72**, 897 (2005).
- [16] G. Tiddy, D. Mateer, A. Ormerod, W. Harrison and D. J. Edwards, *Langmuir* **11**, 390 (1995).
- [17] P. Mariani, F. Spinozzi, F. Federiconi, H. Amenitsch, L. Spindler and I. Drevensek-Olenik, *J. Phys. Chem. B* **113**, 7934 (2009).
- [18] L. Spindler, I. Drevensek-Olenik, M. Copic, R. Romih, J. Cerar, J. Skerjanc and P. Mariani, *Eur. Phys. J. E* **7**, 95 (2002).
- [19] C. Woolverton, E. Gustely, L. Li and O. Lavrentovich, *Liq. Cryst.* **32**, 417 (2005).
- [20] Y. Luk, C. Jang, L. Cheng, B. Israel and N. Abbott, *Chem. Mater.* **17**, 4774 (2005).
- [21] P. Gaubert, *Seances Acad. Sci.* **163**, 392 (1916).
- [22] P. Gaubert, *Seances Acad. Sci.* **197**, 1436 (1933).
- [23] J. Lydon, *J. Mater. Chem* **20**, 10071 (2010).
- [24] A. S. Vasilevskaya, E. V. Generalova and A. S. Sonin, *Russian Chemical Reviews* **58**, 904 (1989).
- [25] S. Tam-Chang and L. Huan, *Chem. Commun.* **30**, 1957 (2008).
- [26] M. Nakata, G. Zanchetta, B. Chapman, C. Jones, J. Cross, R. Pindak, T. Bellini and N. Clark, *Science* **318**, 1276 (2007).
- [27] S. Shiyonovskii, T. Schneider, I. Smalyukh, T. Ishikawa, G. Niehaus, K. Doane and O. Woolverton, C.J. and Lavrentovich, *Phys. Rev. E* **71**, 020702(R) (2005).
- [28] B. Clare and N. Abbott, *Langmuir* **21**, 6451 (2005).
- [29] J. Cox, G. Woodard and W. McCrone, *J. Pharm. Sci.* **60**, 1458 (1971).
-

-
- [30] Y. Nastishin, H. Liu, T. Schneider, V. Nazarenko, R. Vasyuta, S. Shiyanovskii and O. Lavrentovich, Phys. Rev. E **72**, 041711 (2005).
- [31] T. Fujiwara and K. Ichimura, J. Mater. Chem. **12**, 3387 (2002).
- [32] K. Simon, E. Burton, F. Cheng, N. Varghese, E. Falcone, L. Wu and Y. Luk, Chem. Mat. **22**, 2434 (2010).
- [33] V. Nazarenko, O. Boiko, H. Park, O. Brodyn, M. Omelchenko, L. Tortora, Y. Nastishin and O. Lavrentovich, Phys.Rev.Lett **105**, 017801 (2010).
- [34] I. Iverson and S. Tam-Chang, J. Am. Chem. Soc. **121**, 5801 (1999).
- [35] I. Iverson, S. Casey, W. Seo and S. Tam-Chang, Langmuir **18**, 3510 (2002).
- [36] O. Lavrentovich, T. Schneider, A. Golovin and J. Lee, Aligned lyotropic chromonic liquid crystal films, patent us 7294370.
- [37] D. Matsunaga, T. Tamaki, H. Akiyama and K. Ichimura, Adv. Mat. **14**, 1477 (202).
- [38] X. Wang, P. Zhang, Y. Chen, L. Luo, Y. Pang and X. Liu, Macromolecules **44**, 9731 (2011).
- [39] S. Tam-Chang, J. Helbley, T. Carson, W. Seo and I. Iverson, Chem. Commun. **5**, 503 (2006).
- [40] E. Grulke, *Polymer Handbook* (John Wiley and Son, New York, 1989).
- [41] <http://www.surface-tension.de/solid-surface-energy.htm>.
- [42] F. Yeung, J. Ho, Y. Li, F. Xie, O. Tsui, P. Sheng and H. Kwoka, Appl. Phys. Lett. **88**, 051910 (2006).
- [43] I. H. Bechtold, M. P. De Santo, J. J. Bonvent, E. A. Oliveira, R. Barberi and T. Rasing, Liq. Cryst. **30**, 591 (2003).
- [44] D. Bodas and C. Khan-Malek, Microelectronic Engineering **83**, 1277 (2006).
- [45] F. S. Y. Yeung, F. C. Xie, J. T. K. Wan, F. K. Lee, O. K. C., P. Sheng and H. S. Kwok, J. Appl. Phys. **99**, 124506 (2006).

- [46] J. H. Lee, D. Kang, C. M. Clarke and C. Rosenblatt, *J. Appl. Phys.* **105**, 023508 (2009).
- [47] L. Wu, J. Lal, K. A. Simon, E. A. Burton and Y. Y. Luk, *J. Am. Chem. Soc.* **131**, 7430 (2009).
- [48] X. Wang and Q. Zhou, *Liquid Crystalline Polymers* (World Scientific Publishing Co. Pte. Ltd., Singapore, 2004).
- [49] M. Gellert, M. Lipsett and D. Davis, *Proc.Natl.Acad.Sci.U.S.A.* **48**, 2013 (1962).
- [50] S. Neidle and S. Balasubramanian, *Quadruplex Nucleic Acids* (The Royal Society of Chemistry, Thomas Graham House, Science Park, Milton Road, Cambridge CB4 0WF, UK, 2006).
- [51] P. Tougard, J. Chantot and W. Guschlbauer, *Biochim. Biophys. Acta.* **308**, 9 (1973).
- [52] S. Zimmerman, *Lett. Biopolym.* **14**, 889 (1975).
- [53] E. Henderson, C. Hardin, S. Walk, I. Tinoco Jr. and E. Blackburn, *Cell* **51**, 899 (1987).
- [54] S. Arnott, R. Chandrasekaran and C. Marttila, *Biochem.J.* **141**, 537 (1974).
- [55] D. Sen and W. Gilbert, *Nature* **344(6265)**, 410 (1990).
- [56] Q. Xu, H. Deng and W. Braunlin, *Biochemistry* **32**, 13130 (1993).
- [57] A. Wong and G. Wu, *J. Am. Chem. Soc.* **125**, 13895 (2003).
- [58] T. Pinnavaia, C. Marshall, C.L.and Mettler, C. Fisk, H. Miles and E. Becker, *J. Am. Chem. Soc.* **100**, 3625 (1978).
- [59] J. Gu and J. Leczczyński, *J. Phys. Chem. A* **106**, 529 (2002).
- [60] N. Hud, F. Smith, F. Anet and J. Feigon, *Biochemistry* **35**, 15383 (1996).
- [61] S. Bonazzi, M. Copabianco, M. De Morais, A. Garbesi, G. Gottarelli, P. Mariani, M. Bossi, G. Spada and L. Tondelli, *J. Am. Chem. Soc.* **113**, 5809 (1991).
- [62] A. Wong, R. Ida, L. Spindler and G. Wu, *J. Am. Chem. Soc.* **127**, 6990 (2005).

-
- [63] L. De Sio, S. Ferjani, G. Strangi, C. Umeton and R. Bartolino, *Soft Matter* **7**, 3739 (2011).
- [64] K. Y. Dong, G. P. Smith, E. Tsai, M. Moran, D. M. Walba, T. Bellini, I. I. Smalyukh and N. A. Clark, *Liquid Crystals* **39**, 571 (2012).
- [65] W. Saenger, *Principles of Nucleic Acid Structure* (Springer-Verlag, Berlin, 1984).
- [66] G. Gottarelli, S. Lena, S. Masiero, S. Pieraccini and G. Spada, *Chirality* **20**, 471 (2008).
- [67] H. Cleaves, E. Crapster-Pregont, C. Jonsson, C. Jonsson, D. Sverjensky and R. Hazen, *Chemosphere* **83**, 1560 (2011).
- [68] K. Kunstelj, F. Federiconi, L. Spindler and I. Drevensek-Olenik, *Colloids and Surfaces B: Biointerfaces* **59**, 120 (2007).
- [69] K. Loo, N. Degtyareva, J. Park, B. Sengupta, M. Reddish, C. Rogers, A. Bryant and J. Petty, *J. Phys. Chem. B* **114**, 4320 (2010).
- [70] V. Sasisekharan, S. Zimmerman and D. Davies, *J. Mol. Biol.* **92**, 171 (1975).
- [71] J. Dash, A. J. Patil, R. Nath Das, F. L. Dowdall and S. Mann, *Soft Matter* **7**, 8120 (2011).
- [72] G. Proni, G. Gottarelli, P. Mariani and G. Spada, *Chem.Eur.J.* **6**, 3249 (2000).
- [73] A. Bellel, S. Sahli, Z. Ziari, P. Raynaud, Y. Segui and D. Escaich, *Surface & Coatings Technology* **201**, 129 (2006).
- [74] M. Monkade, P. Marinot-Lagarde, G. Durand and C. Granjean, *Journal de Phys.II France* **7**, 1577 (1997).
- [75] M. Gupta, I. Satpathy, A. Roy and R. Pratibha, *J. of Coll. and int.* **352**, 292 (2010).
- [76] Y. Matsuoka, B. Norden and T. Kurucsev, *J. Phys. Chem.* **88**, 971 (1984).
- [77] R. T. West, L. A. Garza, W. R. Winchester and J. A. Walmsley, *Nucleic Acid Research* **22**, 5128 (1994).
- [78] N. A. Lockwood and N. L. Abbott, *Science* **10**, 111 (2005).
-

- [79] I. Langmuir, *J. Am. Chem. Soc.* **39**, 1848 (1917).
- [80] K. Blodgett, *J. Am. Chem. Soc.* **57**, 1007 (1935).
- [81] I. Otto and R. Gust, *Arch. Pharm.* **340**, 117 (2007).
- [82] G. Sava, A. Bergamo and P. J. Dyson, *Dalton Trans.* **40**, 9069 (2011).
- [83] J. A. Drewry and P. T. Gunning, *Coord. Chem. Rev.* **255**, 549 (2011).
- [84] Y. Yoshikawa and H. Yasui, *Curr. Top. Med. Chem.* **12**, 210 (2012).
- [85] Q. Jiang, N. X. J. Zhu, Y. Zhang and Z. Guo, *BioMetals* **22**, 297 (2008).
- [86] D. Pucci, A. Crispini, B. Sanz Mendiguchia, S. Pirillo, M. Ghedini, S. Morelli and L. De Bartolo, *Dalton Trans.* **42**, 9679 (2013).
- [87] T. C. Marsh, J. Vesenka and E. Henderson, *Nucleic Acids Research* **23**, 696 (1995).
- [88] E. A. Venczel and D. Sen, *Biochemistry* **32**, 6220 (1993).
- [89] J. Davis, *Angew. Chem. Int. Ed.* **43**, 668 (2004).
- [90] K. McLuckie, M. Di Antonio, H. Zecchini, J. Xian, C. Caldas, B. Krippendorff, D. Tannahill, C. Lowe and S. Balasubramanian, *Journal of the American Chemical Society* **135**, 9640 (2013).
- [91] E. Lam, D. Beraldi, D. Tannahill and S. Balasubramanian, *Nature Communication* **4**, 1796 (2013).
- [92] I. Otto and R. Gust, *Arch. Pharm.* **340**, 117 (2007).
- [93] G. Sava, A. Bergamo and P. Dyson, *Dalton Trans.* **40**, 9069 (2011).
- [94] B. Mendiguchia, D. Pucci, T. Mastropietro, M. Ghedini and A. Crispini, *Dalton Trans.* **42**, 6768 (2013).
- [95] N. Kim, M. Piatyszek, K. Prowse, C. Harley, M. West, P. Ho, G. Coviello, S. Wright, WE and Weinrich and J. Shay, *Science* **266**, 2011 (1994).
- [96] L. Tortora and O. Lavrentovich, *Proc. Natl. Acad. Sci. U S A* **108**, 5163 (2011).

- [97] J. J. Naidu, Y. J. Bae, K. U. Jeong, S. H. Lee, S. Kang and M. H. Lee, *Bull. Korean Chem. Soc.* **30**, 935 (2009).
- [98] J. Brake, M. Daschner and N. Abbott, *Langmuir* **21**, 2218 (2005).
- [99] R. Walker, D. Gragson and G. Richmond, *Colloids Surf. A* **154**, 175 (1999).
- [100] H. Schindler, *Biochim. Biophys. Acta* **555**, 316 (1979).
- [101] S. Lee, D. Kim and D. Needham, *Langmuir* **17**, 5544 (2001).
- [102] B. Denizot, P. Tchoreloff, J. Proust, F. Puisieux, A. Lindenbaum and M. Dehan, *J. Colloid Interface Sci.* **143**, 120 (1991).
- [103] B. Y and N. Abbott, *Langmuir* **27**, 5719 (2011).
- [104] J. M. Brake, M. K. Daschner, Y. Y. Luk and N. L. Abbott, *Science* **302**, 2049 (2003).
- [105] C. S. Mullin, P. Guyotsionnest and Y. R. Shen, *Phys. Rev. A* **39**, 3745 (1989).
- [106] J. K. Gupta, M. V. Meli, S. Teren and N. L. Abbott, *Phys. Rev. Lett.* **100**, 048301 (2008).
- [107] L. N. Tan, P. J. Bertics and N. L. Abbott, *Langmuir* **27**, 1419 (2011).
- [108] B. Städler, D. Falconnet, I. Pfeiffer, F. Höök and J. Vörös, *Langmuir* **20**, 11348 (2004).
- [109] I. H. Meli, M. V. and Lin and N. L. Abbott, *J. Am. Chem. Soc.* **130**, 4326 (2008).
- [110] J. M. Brake and N. L. Abbott, *Langmuir* **18**, 6101 (2002).
- [111] F. Chiti and C. M. Dobson, *Annu. Rev. Biochem.* **75**, 333 (2006).
- [112] M. R. Chapman, L. S. Robinson, J. S. Pinkner, R. Roth, J. Heuser, M. Hammar, S. Normark and S. J. Hultgren, *Science* **295**, 851 (2002).
- [113] S. K. Maji *et al.*, *Science* **325**, 328 (2009).
- [114] T. P. J. Knowles and M. J. Buehler, *Nat. Nanotechnol.* **6**, 469 (2011).

- [115] J. Loch, A. Polit, A. Gorecki, P. Bonarek, K. Kurpiewska, M. Dziedzicka-Wasylewska and K. Lewinski, *J. Mol. Recognit.* **24**, 341 (2011).
- [116] L. Tan, P. Bertics and N. Abbott, *Langmuir* **27**, 1419 (2011).
- [117] V. Chigrinov, *Electrooptic Effects in Liquid Crystal Materials* (Springer-Verlag, New York, 1993).
- [118] J. Bandekar, *Biochimica et biophysica acta* **1120**, 123 (1992).
- [119] S. Roth, B. S. Murray and E. Dickinson, *J. Agric. Food Chem.* **48**, 1491 (2000).
- [120] E. Dickinson, *Colloid Surf. B* **15**, 161 (1999).
- [121] Y. Fang and D. Dalgleish, *J. of Colloid and Interf. science* **196**, 292 (1997).
- [122] J. Boye, I. Alli, A. Ismail, B. Gibbs and Y. Konishi, *Int. Dairy J.* **5**, 337 (1995).
- [123] X. Qi, C. Holt, D. McNulti, D. Clarke, S. Brownlow and G. Jones, *Biochem. J.* **324**, 341 (1997).
- [124] S. Tcholakova, N. Denkov, D. Sidzhakova and S. Campbell, *Langmuir* **22**, 6042 (2006).
- [125] M. D. De Tercero and N. L. Abbott, *Chem. Eng. Commun* **196**, 234 (2008).
- [126] H. S. Kwok, Y. W. Li and F. S. Yeung, *Mol. Cryst. Liq. Cryst.* **507**, 26 (2009).
- [127] K. Zhang, N. Liu, R. Twieg, B. Auman and P. Bos, *Liq. Cryst.* **35**, 1191 (2008).
- [128] K. Zhang, N. Liu, R. Twieg, B. Auman and P. Bos, *Liq. Cryst.* **35**, 1191 (2008).
- [129] P. Roach, D. Farrar and C. C. Perry, *J. Am. Chem. Soc.* **127**, 8168 (2005).
- [130] E. M. Freer, K. S. Yim, G. G. Fuller and C. J. Radke, *Langmuir* **20**, 10159 (2004).
- [131] A. R. Mackie, A. P. Gunning, L. A. Pugnaroni, E. Dickinson, P. J. Wilde and V. J. Morris, *Langmuir* **19**, 6032 (2003).
- [132] E. Dickinson, *Colloids Surf. B* **15**, 161 (1999).
- [133] W. Norde and J. P. Favier, *Colloids Surf.* **64**, 87 (1992).